Chapter 7
Mitochondrial Respiratory Chain Complexes

Joana S. Sousa, Edoardo D'Imprima, and Janet Vonck

Abstract Mitochondria are the power stations of the eukaryotic cell, using the energy released by the oxidation of glucose and other sugars to produce ATP. Electrons are transferred from NADH, produced in the citric acid cycle in the mitochondrial matrix, to oxygen by a series of large protein complexes in the inner mitochondrial membrane, which create a transmembrane electrochemical gradient by pumping protons across the membrane. The flow of protons back into the matrix via a proton channel in the ATP synthase leads to conformational changes in the nucleotide binding pockets and the formation of ATP. The three proton pumping complexes of the electron transfer chain are NADH-ubiquinone oxidoreductase or complex I, ubiquinone-cytochrome *c* oxidoreductase or complex III, and cytochrome *c* oxidase or complex IV. Succinate dehydrogenase or complex II does not pump protons, but contributes reduced ubiquinone. The structures of complex II, III and IV were determined by x-ray crystallography several decades ago, but complex I and ATP synthase have only recently started to reveal their secrets by advances in x-ray crystallography and cryo-electron microscopy. The complexes I, III and IV occur to a certain extent as supercomplexes in the membrane, the so-called respirasomes. Several hypotheses exist about their function. Recent cryo-electron microscopy structures show the architecture of the respirasome with near-atomic detail. ATP synthase occurs as dimers in the inner mitochondrial membrane, which by their curvature are responsible for the folding of the membrane into cristae and thus for the huge increase in available surface that makes mitochondria the efficient energy plants of the eukaryotic cell.

Keywords ATP synthase · ATP synthesis · Complex I · Complex II · Complex III · Complex IV · Cryo-electron microscopy · Mitochondria · Respirasome · Respiratory chain · X-ray crystallography

J. S. Sousa · E. D'Imprima · J. Vonck (✉)
Department of Structural Biology, Max Planck Institute of Biophysics, Frankfurt am Main, Germany
e-mail: janet.vonck@biophys.mpg.de

J. R. Harris, E. J. Boekema (eds.), *Membrane Protein Complexes: Structure and Function*, Subcellular Biochemistry 87,
https://doi.org/10.1007/978-981-10-7757-9_7

Abbreviations

cryo-EM	cryo-electron microscopy
IMM	inner mitochondrial membrane
IMS	intermembrane space
pmf	proton motive force
RET	reverse electron transfer
ROS	reactive oxygen species
TMH	transmembrane helices

7.1 Introduction

Mitochondria are the power plants of the eukaryotic cell. They produce most of the huge amounts of ATP needed for the functioning of the cell. An athlete can turn over his or her body weight in ATP in a day. A series of large membrane protein complexes in the inner mitochondrial membrane (IMM) is responsible for this remarkable system. The chemical energy in the products of the citric acid cycle is converted into an electrochemical gradient over the IMM by a series of proton pumps. The protons flow back into the mitochondrial matrix via proton channels in the F_1F_o ATP synthase complex and drive a mechanical rotation of the rotor, causing conformational changes in the nucleotide binding pockets of the F_1 subcomplex, thus converting ADP and phosphate to ATP. The respiratory chain complexes are among the largest membrane protein complexes in the cell. They transfer electrons from NADH and succinate to molecular oxygen via a number of redox cofactors including flavins, iron-sulfur clusters, hemes and ions. The proton pumps are NADH:ubiquinone oxidoreductase or complex I, which oxidizes NADH, transfers two electrons to ubiquinone and translocates four protons across the membrane, ubiquinol:cytochrome *c* oxidoreductase (complex III), which transfers electrons from ubiquinone to the peripheral electron carrier cytochrome *c* while translocating 4 protons, and cytochrome *c* oxidase (complex IV), which transfers electrons from cytochrome *c* to molecular oxygen and translocates two protons. In total 10 protons per NADH molecule are translocated across the IMM. Succinate dehydrogenase (complex II), which is part of both the citric acid cycle and the electron transfer chain, contributes additional electrons to ubiquinone that originate from succinate (Fig. 7.1). The mitochondrial respiratory chain derives from endosymbiont α-proteobacteria and all core subunits are highly conserved. However, most mitochondrial complexes have gained large numbers of accessory subunits (Fig. 7.1) with functions that are only now beginning to be understood. In recent years much progress has been made in understanding the structure and function of these complexes, driven by structural information from x-ray crystallography and cryo-electron microscopy (cryo-EM). In addition insight has been gained in their organization in the IMM: complex I, III

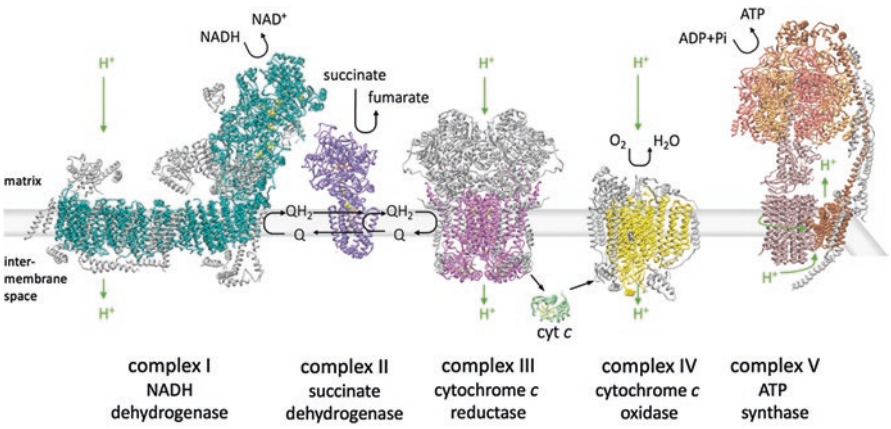

Fig. 7.1 The mitochondrial respiratory chain in the IMM uses the energy in NADH and succinate produced in the citric acid cycle to produce ATP, the energy currency of the cell. Core subunits (colors) also present in bacteria are highly conserved, while the mitochondrial complexes have acquired accessory subunits (grey), often with still unknown functions. Accessory subunits of the ATP synthase bend the membrane and are responsible for the formation of cristae, lined with dimer rows of ATP synthase. Electrons enter the chain from NADH via complex I and from succinate via complex II. Complex I, III and IV pump protons across the IMM, which flow back into the matrix via the ATP synthase, driving the rotor to produce ATP. Proton flow is indicated by green arrows

and IV are found to occur to a large extent as supercomplexes, and the mitochondrial ATP synthase occurs in dimer rows, which are thought to be responsible for the shape of the inner membrane cristae. All these aspects are subject of this chapter.

7.2 Complex I

Complex I (NADH:ubiquinone oxidoreductase) plays a central role in cellular metabolism. By oxidizing NADH to NAD^+ in the mitochondrial matrix, it supplies reducing equivalents to support the tricarboxylic acid cycle (Krebs cycle) and the β-oxidation of fatty acids. Complex I represents the entry point of the electrons in the respiratory chain. In each catalytic cycle two electrons from NADH are used to reduce ubiquinone to ubiquinol, coupled with the vectorial transport of four protons across the IMM. The proton gradient generated contributes ~40% of the proton motive force (pmf) that is used for ATP synthesis and for the import and export of protein and metabolites to and from mitochondria. Complex I is also one of the main sources of reactive oxygen species (ROS) production, which has a huge impact on mitochondria and oxidative stress and may be one of the causes of ageing. Because of its central role in energy production, complex I defects have a noteworthy effect in tissues with a high metabolic rate like brain and heart, especially in early childhood.

7.2.1 Background and Nomenclature

Complex I is one of the largest membrane protein assemblies known and is the largest component of the respiratory chain. It belongs to the protein family of H^+- or Na^+-translocating NADH dehydrogenases (NDH), and more precisely it is a type I NADH dehydrogenase (NDH-I) (Kerscher et al. 2008). The other members of this protein family include type II NAD(P)H dehydrogenase (NDH-II), a non-proton pumping enzyme (Melo et al. 2004), and the sodium pumping NADH-quinone reductase (Na^+-NQR) (Barquera 2014). An analysis of 970 bacterial genomes showed the presence of complex I in the majority of Gram-negative bacteria and mostly in the phylum of Actinobacteria in Gram-positive bacteria (Friedrich and Scheide 2000; Spero et al. 2015).

With one exception (Spero et al. 2015), complex I was not found in 88 archaeal genomes investigated. In eukaryotes, complex I occurs in mitochondria of aerobic (Gabaldon et al. 2005) and anaerobic species (van Hellemond et al. 2003). It is absent in the fungal lineages of *Schizosaccharomyces* and Saccharomycetales, and the cryptomycotan fungus *Rozella* (Gabaldon et al. 2005; Marcet-Houben et al. 2009; James et al. 2013). In fermenting yeasts like *Saccharomyces cerevisiae* that do not contain complex I (Ohnishi et al. 1966), the NADH oxidoreductase activity is performed by the so-called alternative NADH dehydrogenases, a class of flavoenzymes that catalyze the same reaction as complex I but do not couple it to ion translocation over the membrane (Kerscher 2000).

With the only exception of the parasitic plant *Viscum scurruloideum*, which seems to lack complex I (Skippington et al. 2015), in the plant kingdom all mitochondria contain NDH-I (Gabaldon et al. 2005).

Complex I is an L-shaped enzyme composed of two elongated domains also referred to as "arms". The hydrophobic or membrane arm is inserted into the cytoplasmic membrane of bacteria or the IMM and the hydrophilic, peripheral or matrix arm protrudes into the bacterial cytoplasm or the mitochondrial matrix (Clason et al. 2010) (Fig. 7.2). An assembly of 14 core subunits, seven in the membrane arm and seven in the peripheral arm, represent the minimal model of complex I that is sufficient to catalyze the energy transduction and only these subunits are present in most bacteria. Crystal structures of the core subunits were determined first for the bacterial enzymes from *Thermus thermophilus* and *Escherichia coli* (Sazanov and Hinchliffe 2006; Efremov and Sazanov 2011; Baradaran et al. 2013). In eukaryotes the seven core subunits of the membrane arm are encoded by the mitochondrial genome and those of the hydrophilic arm by the nuclear genome.

In addition to the core subunits, mitochondrial complex I contains a large number of accessory subunits (up to ~50% of the total mass of the complex), the phylogenetic analysis of which sheds light on the evolution of complex I (Gabaldon et al. 2005). The best studied eukaryotic systems are complex I from bovine heart (Carroll et al. 2003), the obligate aerobic yeast *Yarrowia lipolytica* (Kerscher et al. 2004) and the fungus *Neurospora crassa* (Videira 1998) (Fig. 7.2). Structural data is avail-

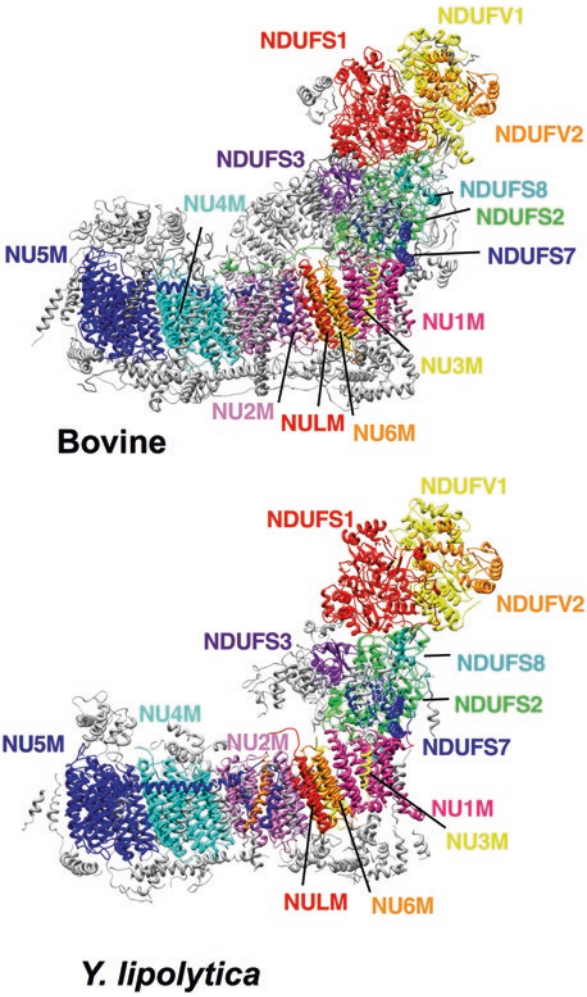

Fig. 7.2 Structure of the mitochondrial complex I core subunits. The homologous bovine (pdb 5lc5) and *Y. lipolytica* (pdb 4wz7) core subunits and labels are colored the same. All accessory subunits are depicted in grey. The human nomenclature was applied

able for mammalian complex I from recent cryo-EM maps (Vinothkumar et al. 2014; Zhu et al. 2016; Fiedorczuk et al. 2016) and for *Y. lipolytica* from crystal structures (Hunte et al. 2010; Zickermann et al. 2015) and a cryo-EM map (D'Imprima et al. 2016).

The well-studied mammalian mitochondrial enzyme from bovine heart, of about 1 MDa molecular weight and with high homology to the human complex I, contains 44 different subunits and, as the SDAP subunit is present in two copies (Vinothkumar et al. 2014), 45 in total.

Since there is no uniform nomenclature, even for the central subunits, Table 7.1 shows the subunits for all commonly studied species. Unless differently indicated, the human nomenclature will be used.

Table 7.1 Subunits of complex I in different species

Homo sapiens	*Bos taurus*	*Y. lipolytica*	*T. thermophilus*	*P. denitrificans*	*E. coli*	comment	module
NDUFS1	75-kDa	NUAM	Nqo3	Nqo3	NuoG	2 [4Fe4S] 1 [2Fe2S]	N
NDUFV1	51-kDa	NUBM	Nqo1	Nqo1	NuoF	FMN; NADH; [4Fe4S]	N
NDUFS2	49-kDa	NUCM	Nqo4	Nqo4	NuoD	Q-binding	Q
NDUFS3	30-kDa	NUGM	Nqo5	Nqo5	NuoC		Q
NDUFV2	29-kDa	NUHM	Nqo2	Nqo2	NuoE	[2Fe2S]	N
NDUFS8	TYKY	NUIM	Nqo9	Nqo9	NuoI	2 [4Fe4S]	Q
NDUFS7	PSST	NUKM	Nqo6	Nqo6	NuoB	Q-binding; [4Fe4S]	Q
NU1M	ND1	NU1M	Nqo8	Nqo8	NuoH	mtDNA[a]	P_P
NU2M	ND2	NU2M	Nqo14	Nqo14	NuoN	mtDNA	P_P
NU3M	ND3	NU3M	Nqo7	Nqo7	NuoA	mtDNA	P_P
NU4M	ND4	NU4M	Nqo13	Nqo13	NuoM	mtDNA	P_D
NU5M	ND5	NU5M	Nqo12	Nqo12	NuoL	mtDNA	P_D
NU6M	ND6	NU6M	Nqo10	Nqo10	NuoJ	mtDNA	P_P
NULM	ND4L	NULM	Nqo11	Nqo11	NuoK	mtDNA	P_P
NDUFA2	B8	NI8M				thioredoxin fold	N
NDUFS4	AQDQ/ 18-kDa	NUYM		pdNUYM			N
NDUFS6	13-kDa	NUMM		pdNUMM		Zn^{2+}	N/Q
NDUFA12	B17.2	N7BM		pdN7BM			N/Q
NDUFA7	B14.5a	NUZM					Q
NDUFA5	B13	NUFM					Q
NDUFA9	39-kDa	NUEM				NADPH	Q
NDUFA6	B14	NB4M				LYR motif	Q
NDUFAB1	SDAP	ACPM1 ACPM2				PP[b] PP[b]	Q P_D
NDUFA1	MWFE	NIMM				1 TMH[c]	P_P
NDUFA3	B9	NI9M				1 TMH	P_P
NDUFA8	PGIV	NUPM				Mia-Cx_9C	P_P
NDUFA11	B14.7	NUJM				4 TMH	P_P
NDUFA13	B16.6	NB6M				1 TMH / GRIM-19	P_P
NDUFS5	PFFD/ 15-kDa	NIPM				Mia-Cx_9C	P_P
NDUFB3	B12	NB2M				1 TMH	P_D
NDUFB4	B15	NB5M				1 TMH	P_D
NDUFB7	B18	NB8M				Mia-Cx_9C	P_D
NDUFB8	ASHI	NIAM				1 TMH	P_D
NDUFB9	B22	NI2M				LYR motif	P_D
NDUFB10	PDSW	NIDM				Cx_yC	P_D
NDUFB11	ESSS	NESM				1 TMH	P_D
NDUFV3	9-kDa						N
NDUFC1	KFYI					1 TMH	P_P
NDUFC2	B14.5b					1 TMH	P_P
NDUFA10	42-kDa						P_P
NDUFB1	MNLL					1 TMH	P_D
NDUFB2	AGGG					1 TMH	P_D
NDUFB5	SDGH					1 TMH	P_D
NDUFB6	B17					1 TMH	P_D
		NUXM				2 TMH	P_P
		NEBM				1 TMH	P_P
		NUNM				1 TMH	P_D
		NUUM				1 TMH	P_D
		ST1				MST[d]	Q
			NQO15			Frataxin family	N
			NQ016			DUF3197 family	Q

Table adapted from Wirth et al. (2016)

The core subunits in the hydrophilic and the membrane arm are shown in blue and red, respectively. The assignment of modules is according to Hunte et al. 2010. Q, quinone reduction module; N, NADH oxidation module; P_P and P_D, proximal and distal proton pumping module, respectively

[a]Mitochondrial DNA; [b]Phosphopantetheine; [c]Transmembrane helix; [d]3-mercaptopyruvate:sulfur transferase

7.2.2 *Mechanism of Complex I*

The first step of the reaction catalyzed by complex I is NADH oxidation by a non-covalently bound flavin-mononucleotide (FMN) at the top of the hydrophilic arm, in the NUDFV1 subunit. The fast electron transfer between C^{4N} of NADH and N^5 of FMN is mediated by a favorable geometry of the nicotinamide ring of NADH, which upon binding forms a stacking interaction with the isoalloxazine ring of FMN (Berrisford and Sazanov 2009). Next electrons are transferred along a chain of seven iron-sulfur (FeS) clusters (Fig. 7.3), spanning a distance of ~90 Å, to ubiquinone in the binding pocket formed by NU1M, NDUFS2 and NDUFS7 at the base of the hydrophilic arm. In the membrane arm, four antiporter-like structural motifs have been identified that are likely to transport one proton each per catalytic cycle. The redox and proton pumping mechanism are not only spatially separated, but they also occur in a remarkably different time-scale: the former ~100 μs and the latter about three orders of magnitude slower (Verkhovskaya et al. 2008; Sharma et al. 2015). The mechanism of coupling between electron transfer and proton translocation is still the least understood aspect of complex I. Currently the two main proposed models are: partially direct redox-driven coupling (Dutton et al. 1998; Ohnishi et al. 2010) and indirect or conformationally

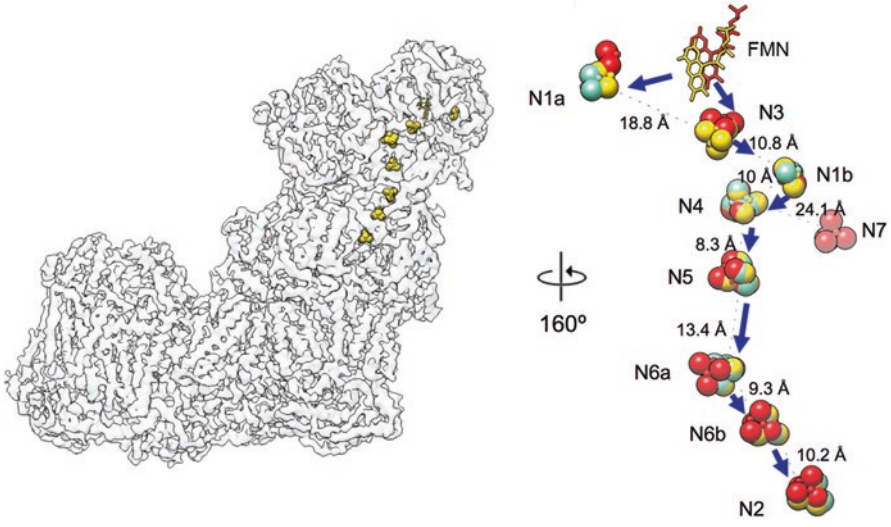

Fig. 7.3 FeS clusters in mammalian, yeast and prokaryote complex I. On the left the coordinates of the ligands of bovine complex I (pdb 5lc5) are docked into the corresponding cryo-EM map (EMD-4032). On the right the coordinates of the FeS clusters of *Y. lipolytica* (pdb 4wz7) (blue) and *T. thermophilus* (pdb 4hea) (pink) were overlapped with the bovine structure (gold). The nomenclature from Baradaran et al. 2013 was used to assign the FeS clusters. Distances were calculated edge-to-edge from the coordinates of pdb 5lc5 except for the distance between clusters N4-N7 for which coordinates from pdb 4hea were used. The blue arrows show the electron flow from the FMN to the cluster N2

driven coupling (Yagi and Matsuno-Yagi 2003; Brandt 2006; Zickermann et al. 2015; Friedrich 2001). The reaction of mitochondrial complex I is fully reversible, and at the expense of the pmf the enzyme can also transfer electrons from ubiquinol upstream for NAD^+ reduction (the so called reverse electron transfer (RET)). This reaction *in vitro* is accompanied by increased production of superoxide, which is rapidly converted to H_2O_2 (Ambrosio et al. 1993; Turrens 2003).

7.2.3 The Dehydrogenase Domain

The hydrophilic arm consists of the dehydrogenase domain (N module), which harbors the cofactors and the subunits involved in the oxidation of NADH and transfer of electrons to quinone, and the quinone-binding domain (Q module).

The N module comprises the core subunits NDUFS1, NDUFV1 and NDUFV2.

Eukaryotes harbor 8 and some bacteria 9 FeS clusters (Fig. 7.3). Binuclear clusters ([2Fe-2S]) contribute to broad absorbance peaks at 420, 470 and 560 nm, tetranuclear clusters ([4Fe-4S]) at 420 nm and FMN at 450 nm (Rasmussen et al. 2001; Euro et al. 2008; Hinchliffe and Sazanov 2005). Extensive studies over the years, particularly from Ohnishi's and Hirst's group using bovine complex I as the main model, allowed to establish the presence of EPR signals from two binuclear (N1a and N1b) and six tetranuclear FeS clusters (Ohnishi 1998; Roessler et al. 2010), making it one of the most complex FeS assemblies known. It has been shown that absorbance in these regions of the spectra decreases upon reduction of complex I (Rasmussen et al. 2001), but it is not possible to de-convolute spectra of individual redox centers, with the exception of the contribution from the high-potential cluster N2 and FMN (~240 mV and 350 mV respectively (Ohnishi 1998)). Due to these limitations a consensus on the assignment of EPR signals to FeS has been reached so far only for the clusters N1a in NDUFV2 and N1b in NDUFS1 (Gnandt et al. 2016; Ohnishi and Nakamaru-Ogiso 2008; Yakovlev et al. 2007). The clusters N3 and N2 are unambiguously assigned to subunits NDUFV1 and NDUFS7, respectively. The position of those clusters is particularly important, since cluster N3 is involved in accepting the electrons from the FMN and cluster N2 interfaces with the quinone (Fig. 7.3). The role of the cluster N1a is still highly debated; it resides at the opposite side of the FMN, separated from the main chain of clusters that connects the NADH oxidation site with the quinone reduction site. It seems to be important for the structure around the flavin site and an interesting hypothesis (Gnandt et al. 2016) proposes that it may serve as a "temporary deposit" of one electron when the most distal cluster N2 is reduced. This might be due to the fact that FeS clusters are one electron carriers and NADH and $FMNH_2$ are two electron donors.

In addition to the eight conserved FeS clusters, in *T. thermophilus* and *E. coli* and some other bacteria there is an additional FeS binding motif in subunit Nqo3 (NuoG), coordinating the tetranuclear cluster N7 (Fig. 7.3) as confirmed by the X-ray structure of the hydrophilic arm of *T. thermophilus* complex I (Sazanov and

Hinchliffe 2006). Since it is too far away from the main FeS chain to be involved in efficient electron tunneling (Page et al. 1999) and not conserved it is unlikely to have an important role in the electron-transfer chain reaction.

7.2.4 The Quinone Binding Module and the A/D Transition

The interface between the membrane and hydrophilic arm is composed of structural elements of the NUM1, NUM3, NDUFS2, NDUFS7 and NDUFS8 subunits.

Different quinones with variable isoprenoid tails lengths are used as electron acceptors in different species. The mitochondrial enzyme uses ubiquinone, whereas the prokaryotic enzyme uses either menaquinone or ubiquinone. This cofactor is currently considered the key point at which the redox potential is coupled with the proton pumping in the membrane arm. Despite the recent high-resolution structural data from yeast (Zickermann et al. 2015), bovine (Zhu et al. 2016) and ovine (Fiedorczuk et al. 2016) complex I, the conformational changes that take place at the level of the Q module are difficult to interpret and the mechanism of coupling is still elusive. For example, the loops β1-β2 in the core subunit NDUFS2, which are thought to be critical for ubiquinone binding, can be in different conformations (Baradaran et al. 2013; Fiedorczuk et al. 2016; Zickermann et al. 2015; Zhu et al. 2016).

A very interesting characteristic of mitochondrial complex I is the fact that it can adopt two different states, the so called active (A) and de-active or dormant (D) state. The existence of two distinct catalytic forms of the enzyme was shown *in vitro* (Kotlyar and Vinogradov 1990; Roberts and Hirst 2012), in cultured cells and in mouse and rat tissue under ischemic conditions (Galkin et al. 2009; Chouchani et al. 2013). The A and D forms, first characterized for the mammalian enzyme (Kotlyar and Vinogradov 1990), are also evident in other vertebrates and certain yeasts, but have not been detected so far in prokaryotes (*Rhodobacter capsulatus*, *Paracoccus denitrificans*, or *E. coli*) (Maklashina et al. 2003; Grivennikova et al. 2003). Respiratory complex I in A and D state displays structural rearrangements in the Q module and remarkably different catalytic activity. During steady state aerobic respiration, the A form is predominant. It catalyzes the fast physiological NADH:ubiquinone oxidoreductase reaction with a linear rate over time and it is insensitive to cysteine-modifying reagents such as nitrosothiols, peroxynitrite or ROS. Conversely the D state is characterized by a lower activity and an initial lag phase, which was reported already in 1964 (Minakami et al. 1964). The lag phase can be prolonged in the presence of divalent cations or alkaline pH (Babot et al. 2014). If oxygen is absent the A-form spontaneously converts to the D-form, which can be re-activated in the case of re-oxygenation (given substrate ubiquinone availability). In recent years several groups reported strong evidence that the sensitivity of complex I to redox modifications is different for the A and D forms (Galkin and Moncada 2007; Gorenkova et al. 2013; Babot et al. 2014; Drose et al. 2014). Particularly in the D form the access of the ubiquinone head group to the terminal

FeS cluster N2 is somehow restricted due to conformational changes of the subunits that build the ubiquinone binding site, lowering the activity of the complex, in a similar way as rotenone (a potent inhibitor of complex I) when complex I is in the physiological A state, in the end preventing the formation of superoxide. The most intriguing hypothesis to explain the physiological role of the A/D transition in the view of recent biochemical data (reviewed in Drose et al. 2016) and the most detailed structural studies (Baradaran et al. 2013; Zickermann et al. 2015; Zhu et al. 2016; Fiedorczuk et al. 2016) proposes that the temporary and reversible deactivation of respiratory complex I *in situ* may prevent an "oxidative burst" mediated by ROS in the early stage of reperfusion when the oxygen level increases dramatically and the metabolic intermediates are not yet balanced (Chouchani et al. 2013). This would happen because upon re-oxygenation complex I initiates a strong sudden redox activity with high production rates of hydrogen peroxide, which may be prevented by locking the complex in a low activity state: the D state.

These discoveries highlight the importance of the A/D transition during oxidative stress and its potential biomedical relevance in translational medicine. In the light of these new findings the respiratory complex I becomes an attractive drug target for a chemical compound that can selectively affect the A/D state of the enzyme in order to treat ischemia-reperfusion (I/R) injury caused by an excess of production of ROS in myocardial infarction and stroke (Chouchani et al. 2014).

7.2.5 The Membrane Arm

The membrane arm contains the proton pumping module, which is constituted by the seven core subunits NU1M, NU2M, NU3M, NU6M, NULM, NU4M and NU5M. Within this module four antiporter-like motifs have been identified that are thought to transport one proton each per catalytic cycle. The subunits NU2M, NU5M and NU4M each represent one proton transfer unit (Efremov and Sazanov 2011) and a fourth unit is built by subunits NU1M, NULM and NU6M (Baradaran et al. 2013) (Fig. 7.2).

Each antiporter-like subunit contains ten transmembrane helices (TMH) organized in two symmetry-related sets of five, each constituting a half-channel. The antiporter-like subunits are encoded by mitochondrial DNA and are conserved from bacteria to mammals. Although the proton extrusion pathways seem to be conserved between bacterial and mitochondrial complex I, there are some differences in the proton uptake routes (Zickermann et al. 2015; Baradaran et al. 2013; Efremov and Sazanov 2011). Experimental evidence that these antiporter-like subunits are functional is not abundant, but it has been shown that deletion of the gene for NDUFB7 results in the loss of the entire P_D module, but generates complex I that still pumps two protons per cycle, i.e. at 50% stoichiometry (Drose et al. 2011). Furthermore, it is still unclear how the pumping cycle operates: if the pumping units work in sync or whether proton translocation is a two-step process that mirrors the two-step reduction of ubiquinone.

The hydrophobic arm contains a long horizontal -helix that runs along the concave side of the membrane arm on the matrix side (Fig. 7.2). This helix belongs to the core subunit NU5M and bridges the P_D and P_P modules. It has a variable length in different species, from ~60 Å in *Y. lipolytica* to ~110 Å in *E. coli*; the C-terminus of subunit NU5M is anchored to the NU2M subunit by two TMH in *Y. lipolytica* complex I, but only one TMH in the bacterial and bovine complex I (Zickermann et al. 2015; Efremov et al. 2010; Vinothkumar et al. 2014) (Fig. 7.2). The function of this -helix (HL-helix) is highly debated; first it was proposed to be a proton coupling element acting as a "piston" to transmit energy for proton pumping (Efremov et al. 2010), but several studies on the bacterial system do not support this hypothesis (Belevich et al. 2011; Steimle et al. 2015). Another hypothesis proposes that the HL helix with its anchoring is required for "clamping" the two proton pumping modules, providing structural stability (Wirth et al. 2016; Zhu et al. 2016).

Another characteristic of the membrane arm is the presence of charged and polar residues in the middle of the membrane, spanning from the quinone-binding site near the peripheral arm to the last membrane core subunit NU5M. These residues are mostly found in the discontinuous TMH and are surrounded by several water molecules (Baradaran et al. 2013; Zickermann et al. 2015). They seem to form a hydrophilic central region inside the membrane arm that is likely to play an important role in the proton pumping mechanism.

7.2.6 Accessory Subunits of Complex I

Apart from the conserved 14 core subunits, mitochondrial complex I contains a large number of accessory or supernumerary subunits. They form a "cage" around the core subunits, in many species doubling the molecular weight of the complex (Fig. 7.4). The number of subunits which compose complex I ranges from 14 in proteobacteria (Weidner et al. 1993) to 45 in mammals (Carroll et al. 2006) and 49 in plants (Peters et al. 2013). In addition, a number of assembly factors have also been characterized (Merz and Westermann 2009; Carilla-Latorre et al. 2010; Bych et al. 2008; Lightowlers and Chrzanowska-Lightowlers 2013; Andrews et al. 2013). However, it should be noted that the distinction between assembly factors and accessory subunits is only based on whether the protein is retained in the mature complex I or not, independent of a role in the assembly process. Moreover, many accessory subunits/assembly factors may not survive purification of the complex, depending on the protocol used and the species under investigation. The ambiguity in the terminology used to address the accessory subunits reflects the fact that up to date very little is known about their function.

Most of the current knowledge about accessory subunits has been recently reviewed (Elurbe and Huynen 2016). All 31 accessory subunits in the mammalian complex were traced and localized (Zhu et al. 2016; Fiedorczuk et al. 2016), but the

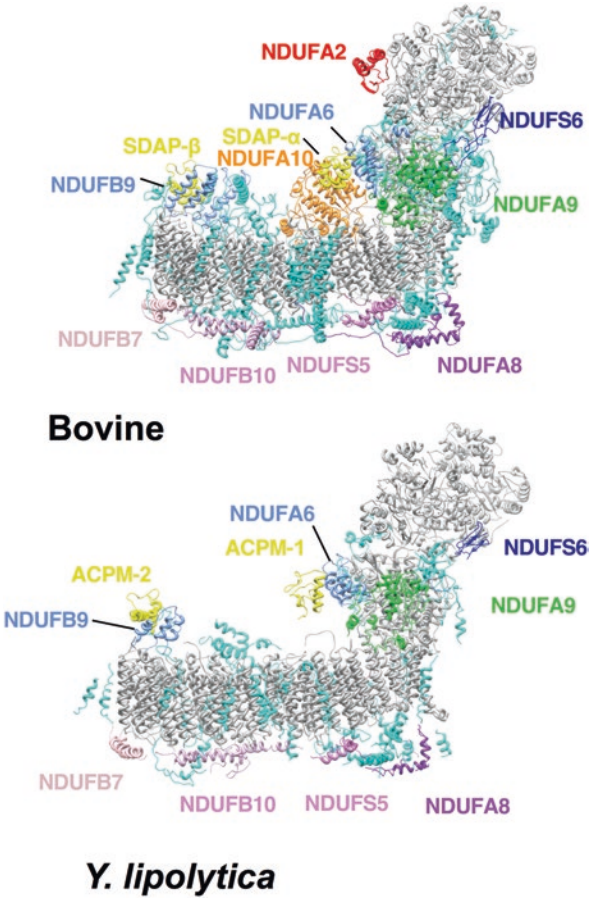

Fig. 7.4 Structure of the mitochondrial complex I accessory subunits. The homologous accessory subunits of bovine (pdb 5lc5) and *Y. lipolytica* (pdb 4wz7) complex I which were assigned so far are colored the same. NDUFA2, mutations of which seem to be linked to Parkinson disease, is colored in red (Morais et al. 2014). NDUFA10 (which is not present in *Y. lipolytica*) is highlighted in orange. NDUFAB1 (yellow) is present in two copies in bovine and *Y. lipolytica*. They are named SDAP-α and SDAP-β and ACPM-1 and ACPM-2, respectively. NDUFA8, NDUFS5, NDUFB7 and NDUFB10, members of the twin Cys-X_9-Cys family (Longen et al. 2009), are located at the intermembrane space (IMS) side of complex I and are shown in different shades of pink. All other accessory subunits are depicted in cyan and the core subunits in grey

assignment of the *Y. lipolytica* subunits is still incomplete (Zickermann et al. 2015; D'Imprima et al. 2016) (Fig. 7.4). During evolution complex I accessory subunits co-evolved in many different ways, either maintaining, modifying or losing their original function. The only accessory subunits that appear to be unique for metazoa are NDUFA10, NDUFB6, NDUFV3, NDUFC1 and NDUFB1.

Accessory subunits for which some biochemical information is available include NDUFAB1, which has retained its original function. It is homologous to the acyl-carrier proteins from bacteria, chloroplast and mitochondria that are involved in fatty acid synthesis (Chan and Vogel 2010). In *Y. lipolytica* and bovine systems they are known as ACPM and SDAP, respectively. In mitochondria they often come in isoforms and they are implicated in the synthesis of the lipoic acid cofactor of α-ketoacid dehydrogenases (Hiltunen et al. 2010). Despite the fact that they have been reported to carry a covalently attached pantetheine-4′-phosphate group (Runswick et al. 1991) and the recent cryo-EM map of bovine complex I displays densities consistent with such a ligand, no activity has been reported (Zhu et al. 2016). Moreover, NDUFAB1 is the only subunit of complex I that is also present in fermenting yeasts lacking complex I like *S. cerevisiae*. Interestingly, in *Y. lipolytica* NDUFAB1 is present as two isoforms, ACPM1 and ACPM2, that exhibit different properties although they have a very similar sequence (Dobrynin et al. 2010). The phosphopantetheine binding serine in ACPM1 is required for *Y. lipolytica* viability, whereas the one in ACPM2 is only required for complex I activity (Dobrynin et al. 2010). In the bovine system NDUFAB1 is present as two identical copies of the SDAP protein (Fig. 7.4).

In both high-resolution structures of eukaryotic complex I, the NDUFAB1 accessory subunits are docked to the complex by two members of the LYR (leucine/tyrosine/arginine) motif protein family: NDUFA6 and NDUFB9. The mitochondrial LYR proteins are shown to be involved in the FeS protein biogenesis (Angerer 2015), raising the possibility that LYR family proteins may be involved in transferring the FeS clusters from the iron-sulfur cluster assembly enzyme IscU to recipient proteins (Maio et al. 2014).

The subunit NDUFA10 is homologous to deoxyribonucleoside kinases. It is regarded as specific for metazoa and was found only in some branches of higher eukaryotes, including mammals (Brandt 2006). It seems to be loosely bound to complex I and resides on the matrix side of the NU2M core subunit (Vinothkumar et al. 2014). Zhu et al. (2016) reported that in the structure the active site appears accessible and the key nucleoside kinase residues seem to be present, although no activity has been reported. NDUFA2 has a thioredoxin fold and in mammals and plants it has two cysteines that in the oxidized form of the protein may form a disulfide bond (Brockmann et al. 2004). It is not known whether this disulfide bond has a specific function and this is not conserved in fungi and some lower eukaryotes e.g. *C. elegans* (Brockmann et al. 2004). Since this protein was found to be phosphorylated by PINK1, a connection with Parkinson disease has been postulated (Morais et al. 2014).

An accessory subunit that seems to have been recruited at the early stages of eukaryotic evolution (Gabaldon et al. 2005) is NDUFA9. It is attached to the core subunits NDUFS7 and NDUFS3 in the hydrophilic arm. This protein belongs to the protein family of NAD-dependent short chain dehydrogenases/reductases (Fearnley and Walker 1992) and displays a NAD(P)-binding Rossmann fold with a parallel seven-stranded β-sheet. It was found to bind NADPH (Abdrakhmanova et al. 2006) and a density assigned as NADPH was observed in the recent cryo-EM

structures (Zhu et al. 2016; Fiedorczuk et al. 2016). Fiedorczuk et al. hypothesize that it may function as a redox sensor.

NDUFS6 resides in the hydrophilic arm at the interface between the NADH domain and the rest of the complex and it has been thoroughly characterized in *Y. lipolytica* (Kmita et al. 2015). Its C-terminal domain harbors a zinc-binding site formed by three cysteines and a histidine (Vinothkumar et al. 2014). This motif in the *Y. lipolytica* ortholog NUMM has been shown to bind a Zn atom and deletion of the whole gene or residues coordinating the Zn atom causes stalling of the final stage of complex I assembly (Kmita et al. 2015). The position of the Zn atom has also been confirmed in the mammalian enzyme (Zhu et al. 2016; Fiedorczuk et al. 2016).

Accessory subunits NDUFS5, NDUFB7, NDUFA8 and NDUFB10 are members of the twin Cys-X_9-Cys family (Longen et al. 2009) and they are located at the intermembrane face of complex I (Zhu et al. 2016) (Fig. 7.4). The former three proteins display CHCH domains (pairs of helices linked by two disulfide bonds) (Szklarczyk et al. 2011) and are substrate for the Mia40 oxidative-folding pathway (Banci et al. 2009).

Although the main and more frequent complex I deficiencies are related to malfunctions of core subunits, so far already 17 accessory subunits have been linked to complex I related diseases (Rodenburg 2016). It has been proposed that they may work as a protective case against ROS (Requejo et al. 2010), "insulating" the redox cofactors and thereby preventing electron transfer to molecular oxygen (Hirst 2011). However, this hypothesis does not agree with the data of O_2 reduction which are similar in eukaryotes and bacteria (Esterhazy et al. 2008) and it does not explain how the prokaryotic enzyme survives without all those accessory subunits.

7.2.7 *Complex I Link to Sulfur Metabolism in* Y. lipolytica

Knowledge about the function and catalytic activity of the accessory subunits of complex I is still lacking in most cases. Recently a function was proposed for an accessory subunit of *Y. lipolytica* complex I: ST1 (D'Imprima et al. 2016). The consistent presence of an extra ~34 kDa subunit in *Y. lipolytica* complex I preparations was reported in 2005 and this protein was identified as a member of the sulfur transferase protein family (E.C. 2.8.1) (Abdrakhmanova et al. 2005). Sulfur transferases are present in organisms of all phyla and transfer sulfur-containing groups, reviewed thoroughly in Bordo and Bork 2002. Although the members of this protein family differ largely at the sequence level, their tertiary structure seems to be highly conserved and resembles that of bovine rhodanese, the most studied and best characterized sulfur transferase (Ploegman et al. 1978). Depending on their substrate the sulfur transferase family can be divided in two subclasses; these are thiosulfate:sulfur transferases (TST; E.C. 2.8.1.1) and 3-mercaptopyruvate:sulfur transferases (MST; E.C. 2.8.1.2). Usually the CRXGX[R/T] sequence in the active loop of TSTs enzymes is used as a marker to distinguish them from MSTs, which contain CG[S/T] GVT (Bordo and Bork 2002). Since the amino acid sequence of *Y. lipolytica* ST1

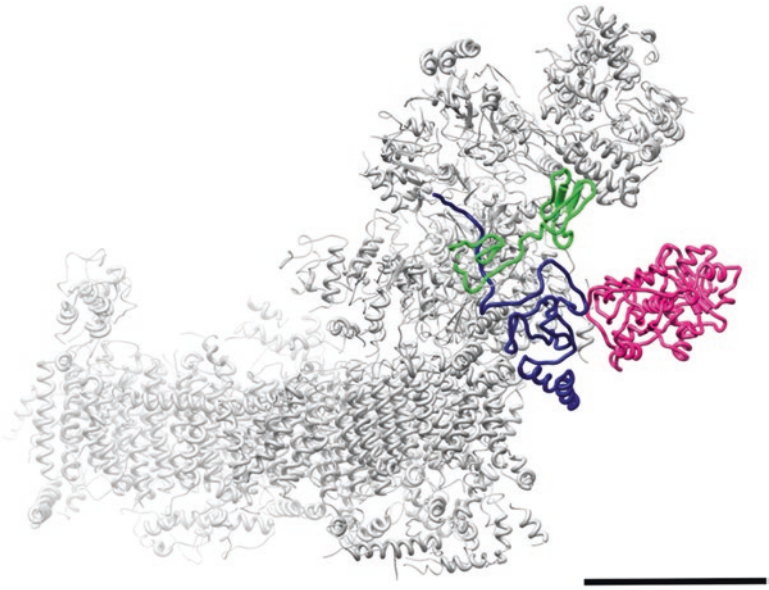

Fig. 7.5 The accessory subunit ST1 in complex I from *Y. lipolytica*. The x-ray structure (pdb 4wz7) is displayed as grey ribbon and the homology model of ST1 (D'Imprima et al. 2016) in pink. The accessory subunits B8 and 13-kDa from bovine (pdb 5lc5) (homologues of N7BM and NUMM in *Y. lipolytica*) which form the interface are shown in green and blue, respectively. Scale bar: 50 Å

contains the sequence CGSGVT, the accessory subunit ST1 can be classified as an MST enzyme.

A cryo-EM map shows that ST1 is located on the side of the hydrophilic arm in the vicinity of the core subunit NDUFS2 (D'Imprima et al. 2016). Based on a comparison with the fully annotated structure of bovine complex I (Zhu et al. 2016), it can be concluded that the interface of ST1 with complex I is provided by the accessory subunits NDUFS6 and NDUFA12 (Fig. 7.5). This is in agreement with biochemical data showing that *Y. lipolytica* complex I mutants lacking the accessory subunits NUMM and N7BM (orthologues of NDUFS6 and NDUFS6, respectively) completely lack ST1 (Kmita et al. 2015). MST activity was measured in both purified *Y. lipolytica* complex I and for the ST1 protein heterologously expressed in *E. coli* (D'Imprima et al. 2016). No MST activity was detected in complex I preparations after being supplied by NADH or NADPH; moreover, no H_2S formation was found in the presence of 3-MP and DTT in a ST1 deletion strain (Abdrakhmanova et al. 2005). These results prove that the observed sulfur transferase activity of the *Y. lipolytica* complex I preparation can be assigned to the accessory subunit ST1.

H_2S is a potent and effective gasotransmitter that can have beneficial physiological implications or highly toxic effects, depending on the tissue and on the concentration in which it is released (see Wang 2012 for an exhaustive review).

A rapid catabolism that prevents the H_2S cellular concentration to reach toxic levels might be achieved by directly linking ST1 H_2S formation to a pathway for H_2S consumption. An ideal candidate could be sulfide quinone reductase (SQR), a flavoprotein that supplies electrons into the respiratory chain via ubiquinone, which represents the main route of H_2S detoxification in mitochondria (Yong and Searcy 2001). D'Imprima et al. propose that a not yet identified SQR in the mitochondrial membrane of *Y. lipolytica* may interact with ST1 bound to complex I, which thus provides a structural scaffold that connects the ubiquinone reduction with the biogenesis of H_2S and its nearly instantaneous detoxification. It is tempting to speculate that *Y. lipolytica* uses this enzymatic pathway to provide electrons from H_2S rather than NADH during stressful situations or in a very polluted environment, where this non-fermentative yeast was first discovered.

7.3 Complex II

Complex II or succinate dehydrogenase, also named succinate-coenzyme Q reductase or mitochondrial succinate:ubiquinone oxidoreductase (mitochondrial SQR) (EC 1.3.5.1) is the only respiratory chain complex that does not pump protons across the IMM. It is part of the citric acid cycle, where it catalyzes the oxidation of succinate to fumarate, coupled to the reduction of ubiquinone to ubiquinol. Ubiquinol is a substrate for complex III and thus complex II provides a second direct link between the citric acid cycle and the respiratory chain, apart from NADH that enters the respiratory chain at the level of complex I. Complex II is homologous to quinol:fumarate reductase (QFR), which performs the reverse reaction and is found in anaerobic cells respiring with fumarate as terminal electron acceptor (Hägerhäll 1997). Unlike the other respiratory chain complexes, which have additional subunits in eukaryotes, complex II has the same composition in mitochondria and prokaryotes. It consists of two hydrophilic proteins, a flavoprotein (Fp) containing an FAD cofactor and an iron-sulfur protein (Ip) with three FeS clusters, and a membrane anchoring domain, in mitochondria consisting of the two transmembrane proteins, CybL and CybS, with one heme. The membrane domain is less conserved than the catalytic subunits and can consist of one or two proteins with one, two or no heme groups (Hägerhäll 1997).

Crystal structures were first determined from prokaryotic QFR (Iverson et al. 1999; Lancaster et al. 1999) and complex II (Yankovskaya et al. 2003). The structure of the 124-kDa porcine mitochondrial complex II was determined in 2005 (pdb 1zoy) (Sun et al. 2005), followed by the very similar avine complex (Huang et al. 2006). The 68-kDa Fp protein has a Rossmann fold and contains the FAD cofactor, the electron acceptor for succinate, in an extended conformation (Fig. 7.6). As was already known for many years (Kearney 1960; Walker and Singer 1970) the FAD is covalently bound to a histidine side chain. The 29-kDa Ip protein contains three iron-sulfur clusters, a [2Fe-2S], [4Fe-4S] and [3Fe-4S], and forms the core of the complex, connecting with Fp on one side and with the membrane anchor on the other side. The two membrane-anchor proteins, CybL (15 kDa) and CybS (11 kDa),

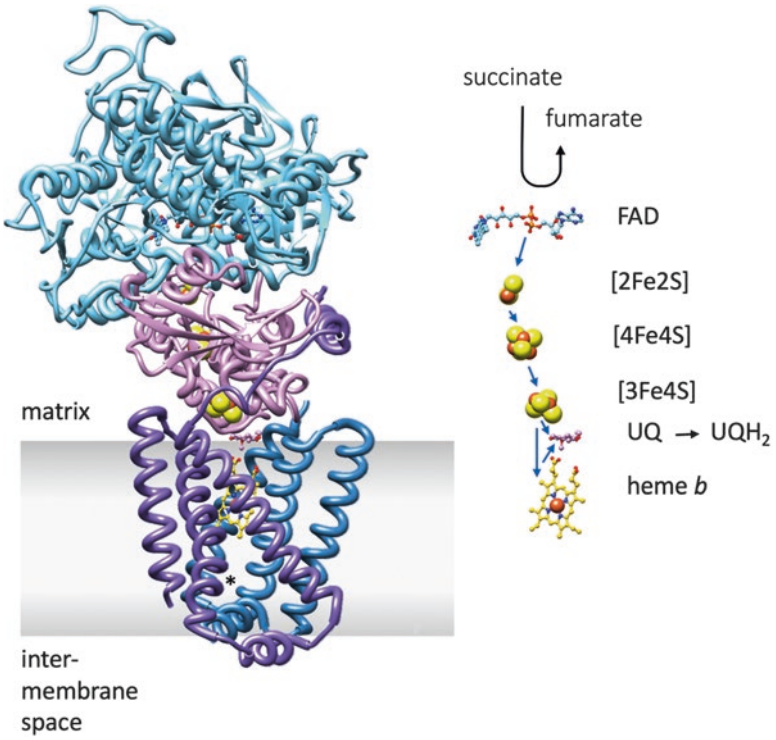

Fig. 7.6 Structure of complex II (porcine heart, pdb 1zoy) (Sun et al. 2005). The FAD binding protein (Fp) is shown in light blue; iron-sulfur protein (Ip) in pink; the transmembrane proteins CybL and CybS in purple and dark blue, respectively. The putative membrane region is shaded in gray. The Qd site is indicated by an asterisk. On the right side, the prosthetic groups constituting the electron transfer pathway are shown together with ubiquinone. The electron transfer flow to the Qp site is indicated by blue arrows

each have three TMH and a heme *b* is coordinated between them. The heme iron is coordinated by the imidazole of two histidines, one from each subunit. The succinate and ubiquinone binding sites in the structure were probed with inhibitors. A 3.5-Å crystal structure (1zp0) (Sun et al. 2005) shows 3-nitropropionate (NPA), a succinate analog and a strong inhibitor for the succinate-oxidation enzymatic activity of complex II, in the expected position near the FMN group of FAD. TTFA (2-thenoyltrifluoroacetone) is an inhibitor for the ubiquinone reduction of complex II by occupying its ubiquinone-binding sites. Two TTFA molecules were found in the crystal structure, one in the proximity of the [3Fe-4S] cluster on the matrix side (Qp) and one at the distal side of the transmembrane anchor near the IMS (Qd) (Fig. 7.6). These sites confirm biochemical evidence for two ubiquinone-binding sites in mitochondrial complex II (Hägerhäll 1997). Comparison with the prokaryotic structures and sequence analysis confirm the position of the matrix binding site, with contributing residues from both transmembrane subunits and the Ip (Sun

et al. 2005). While the Fp and Ip subunits are highly conserved from prokaryotes to mitochondria, the membrane anchor is more divergent with sequence identities <20%, implying a different function of this region, and the distal ubiquinone-binding site appears to be specific for mitochondria (Sun et al. 2005).

7.4 Complex III

Complex III, also known as cytochrome bc_1, is the second enzyme in the mitochondrial respiratory chain, to which the distinct substrate-dependent branches of the chain converge. This complex couples the electron transfer from QH_2 to cytochrome *c* with the translocation of protons across the IMM (Trumpower and Gennis 1994).

7.4.1 Structure of Complex III

Close to 50 crystal structures of the eukaryotic bc_1 complex have been produced in the last 20 years. The first complete structure was obtained in 1998 for the bovine complex (Iwata et al. 1998). The structures include native and inhibitor bound states of the enzyme from beef, chicken and yeast and were invaluable for progress in the field. Complex III is a symmetrical dimer, with three core subunits that are highly conserved from bacteria to mammals (Yang and Trumpower 1986). Additionally, up to eight supernumerary subunits can be present in the mitochondrial complex, for a total of 11 subunits per monomer in the mammalian enzyme (Schägger et al. 1986) (Fig. 7.7). The conserved, catalytically active subunits are cytochrome *b* (cyt *b*), with two *b*-type hemes (b_L and b_H), cytochrome c_1 (cyt c_1), with one *c*-type heme (c_1), and the Rieske iron-sulfur protein (ISP) that encloses a high-potential [2Fe-2S] cluster (Yang and Trumpower 1986). Cyt *b* is the only mitochondrial-encoded subunit from complex III and it harbors two distinct quinone-binding sites located on opposite sides of the membrane (Xia et al. 1997). The Q_o site, located on the positive side, serves quinol oxidation, while at the Q_i site quinone (or semiquinone, $SQ^{\bullet-}$) is reduced. This integral membrane protein forms the center of the complex, to which both cyt c_1 and ISP anchor through a single TMH (Xia et al. 1997). The soluble domains of the cyt c_1 and ISP subunits accommodate the respective cofactors and are located in the IMS (Xia et al. 1997). Cytochrome *c* interacts with the bc_1 complex through the soluble domain of cyt c_1 (Lange and Hunte 2002).

The supernumerary subunits do not participate in electron transfer and proton pumping and are most likely required for assembly, stability, modulation and regulation of the complex. These subunits are Core 1, Core 2, ISP presequence and subunits 6 to 10 (Iwata et al. 1998). Core 1 and Core 2 are the two largest subunits of the complex and were initially proposed to occupy a central position in the structure (Silman et al. 1967), though later studies proved their peripheral structural and

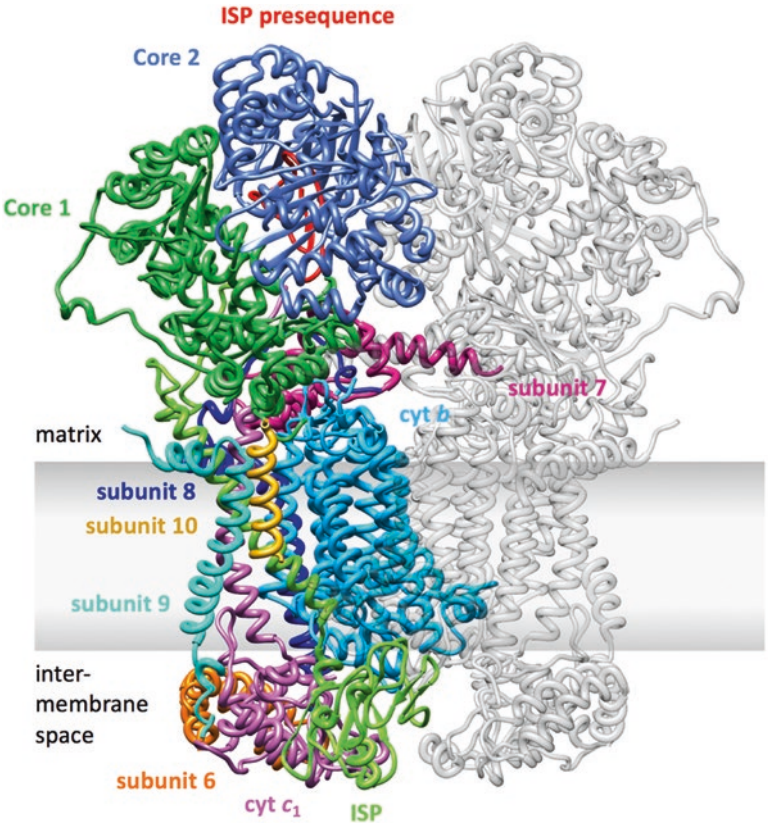

Fig. 7.7 Structure of complex III (bovine heart, pdb 1bgy) (Iwata et al. 1998). Subunits are color-coded in one monomer, the second monomer is presented in grey. The putative membrane region is shaded in gray

functional role. These subunits are located in the mitochondrial matrix and are homologous to the matrix processing peptidase (MPP). Accordingly, the Core proteins have been suggested to be responsible for the cleavage of the ISP signal peptide. This hypothesis is supported by the presence of the ISP presequence in the mature complex from vertebrates as a stoichiometric subunit, within the cavity formed by Core 1 and Core 2 (Iwata et al. 1998), and also by measurements of proteolytic activity for the bovine proteins (Deng et al. 1998; Deng et al. 2001). However, a clear demonstration of this processing protease activity for maturation of the complex has not been achieved (Berry et al. 2013). Subunit 6 interacts with cyt c_1 and has been suggested to conserve the environment of the heme and aid cytochrome *c* binding (Nakai et al. 1993; Yang and Trumpower 1994). In the matrix, subunit 7 is at the interface with the membrane and contacts the Core 2 subunit of the opposite monomer (Xia et al. 1997; Iwata et al. 1998). The remaining supernu-

merary subunits 8, 9 and 10 have a single TMH each and surround the conserved membrane domain (Xia et al. 1997; Iwata et al. 1998).

Complex III is an obligate dimer and although rapid electron equilibration between the b_L hemes (Castellani et al. 2010; Lanciano et al. 2011) and conformational communication between Q_o and Q_i sites have been proven (Covian and Trumpower 2006), it is still controversial whether the monomers function cooperatively or independently (Khalfaoui-Hassani et al. 2012; Hong et al. 2012). One notable feature of the cytochrome bc_1 dimer is the topology of the ISP. Each ISP subunit spans the two monomers, with its TMH associated with one monomer while the soluble domain with the [2Fe-2S] cluster transfers electrons from quinol to cytochrome *c* in the other monomer. Complex III biogenesis has been extensively studied in yeast, allowing a comprehensive description of this multistep process (Zara et al. 2009; Conte et al. 2015). Recent studies have shown that the dimerization occurs early in the assembly pathway and irrespective of expression of the ISP (Conte et al. 2015). The first intermediate forms by association of subunits 7 and 8 to cyt *b*. Subcomplexes containing cyt c_1, Core 1 and Core 2 are then added to the early core, followed by subunits 6 and 9 for generation of the late core subcomplex, which exists as an immature dimer. Lastly, the late core is activated by incorporation of ISP and subunit 10 (Zara et al. 2009; Conte et al. 2015). Several nuclear-encoded enzymes aid the formation and assembly of complex III, with some of these integrating the intermediate structures.

7.4.2 Mechanism of Complex III

The reaction catalyzed by cytochrome bc_1 proceeds according to the modified Q-cycle mechanism, based on Peter Mitchell's original proposal (Mitchell 1972, 1976) (Fig. 7.8). Upon binding of quinol at the Q_o site, one electron is transferred to the oxidized [2Fe-2S] cluster of the ISP that subsequently reduces heme c_1 (high potential chain). The reduced cyt c_1 finally transfers the electron to the soluble carrier cytochrome *c*. The unstable $SQ^{\bullet-}$ radical generated at the Q_o site donates the second electron to the low potential chain, consisting of hemes b_L and b_H from cyt *b*. At the Q_i site, a quinone molecule is reduced to $SQ^{\bullet-}$ by the high potential heme b_H. To complete the Q-cycle, a second quinol is oxidized at the Q_o site for reduction of a second cytochrome *c* molecule and reduction of the stabilized $SQ^{\bullet-}$ to quinol at the Q_i site. The topological separation of the Q_o and Q_i sites allows the vectorial transport of protons across the membrane, with the uptake of two H^+ at the negative side for quinol production and the release of four H^+ at the positive side (two per quinol molecule that is oxidized). The mechanism used for the electron bifurcation observed at the Q_o site is however still unknown.

The unique features of the ISP are also key for the catalytic mechanism of complex III. The soluble domain of the ISP has been shown to occupy different positions in the several crystal structures of the complex, where the distances between the [2Fe-2S] cluster and the Q_o site or heme c_1 are incompatible with efficient elec-

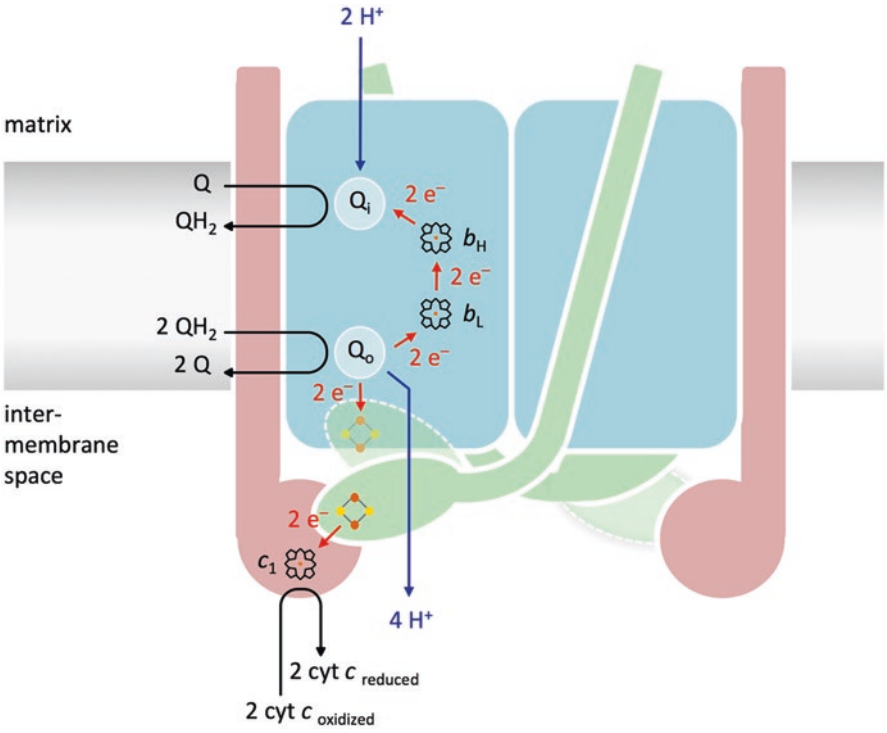

Fig. 7.8 Cytochrome bc_1 Q-cycle mechanism. Cytochrome *b*, cytochrome c_1 and ISP are depicted in blue, pink and green, respectively. The soluble domain of the ISP is represented in two different conformations, corresponding to the *b* and *c* positions. Blue arrows indicate the uptake and release of protons, while red arrows illustrate transfer of electrons. Q, quinone. QH_2, quinol. The membrane is depicted in gray

tron transfer (Page et al. 1999). The observed differences result from the distinct conformations adopted by this domain; it has been shown that for the electron transfer between the Q_o site and heme c_1 to take place, the soluble domain of the ISP must undergo significant conformational changes (Darrouzet et al. 2000). The movement between the *b* position (close to the Q_o site) and the *c* position (close to cyt c_1) allows the complex to optimize the distances between the cofactors for a productive electron transfer (Iwata et al. 1998).

As stated earlier, complex III is an obligate dimer. However, studies of a heterodimeric cytochrome bc_1 from *Paracoccus denitrificans* with an inactivating mutation in one of the Q_o sites revealed the same activity levels as the wild-type enzyme (Castellani et al. 2010). These results imply that under normal steady-state conditions only one Q_o site is active at a given time, confirming that the complex operates according to the half-of-the-sites reactivity model. This model postulates also that the activation switch between monomers should be random. The half-of-the-sites mechanism should reduce the leakage of electrons to oxygen and, therefore, the formation of ROS. Additionally, it was shown that an asymmetric binding to the

Q_i sites allows both Q_o sites to be active simultaneously. This explains the increased activity observed in presence of low concentrations of antimycin A, an inhibitor of the Q_i site (Castellani et al. 2010).

Complex III contributes significantly to the production of ROS in the cell (McLennan and Degli Esposti 2000). In contrast to complex I that generates superoxide exclusively in the matrix, complex III releases ROS in the IMS and possibly in the matrix as well (St-Pierre et al. 2002; Muller et al. 2004). In addition to the damaging effects of mitochondrial ROS, evidence for a regulatory role of ROS produced by the bc_1 complex has been reported. In particular, it has been proposed that complex III-derived ROS contribute to the cellular adaptive response to hypoxia and related cardioprotective ischemic preconditioning (Chandel 2010), adipocyte differentiation (Tormos et al. 2011) and apoptosis (Soberanes et al. 2009). Treatments with myxothiazol or stigmatellin, Q_o site inhibitors, reduce or abolish ROS production, while inhibition by antimycin A, at the Q_i site, produces a drastic increase in these species (Bleier and Drose 2013). These observations prove that production of ROS by complex III occurs primarily at the Q_o site. The rate of ROS generation is also closely linked to the membrane potential (Rottenberg et al. 2009) and the redox state of the Q-pool (Drose and Brandt 2008). Two putative mechanisms can explain the generation of ROS by the $SQ^{\bullet-}$ radicals at the Q_o site: a *semiforward* electron transfer or a *semireverse* electron transfer (Bleier and Drose 2013; Lanciano et al. 2013). In the *semiforward* model, the leakage of electrons is thought to accrue from an increased accumulation or stabilization of the $SQ^{\bullet-}$ at the Q_o site, compared to the normal turnover in the native enzyme. This reaction may become significant at inhibition by antimycin A, for a highly reduced Q-pool, high membrane potential or specific mutations of the Q_o site. Concurrently, the *semireverse* model advances that the production of ROS results from a reverse electron transfer from the reduced heme b_L to $SQ^{\bullet-}$ and subsequently oxygen. Results supporting either mechanism have been reported (Sarewicz et al. 2010; Quinlan et al. 2011).

Mutations of complex III are not among the most frequent causes of mitochondrial diseases, but they are still linked to a large number of pathologies. Most mitochondrial disorders associated with complex III dysfunction result from mutations of the cytochrome *b* subunit or of the assembly factor BCS1L (Meunier et al. 2013), which is required for translocation and incorporation of the ISP on cytochrome bc_1.

7.5 Complex IV

Cytochrome *c* oxidase (complex IV) is the terminal oxidase in the mitochondrial respiratory chain and reduces O_2 to H_2O while pumping protons across the IMM. This member of the heme-copper oxidases family is probably the best understood enzyme from the three mitochondrial proton pumping respiratory complexes, made possible by the 2.8 Å x-ray structures of the bovine and bacterial enzyme published in 1995 and 1996 (Tsukihara et al. 1995; Iwata et al. 1995; Tsukihara et al. 1996) that stimulated experimental studies with a wide range of techniques.

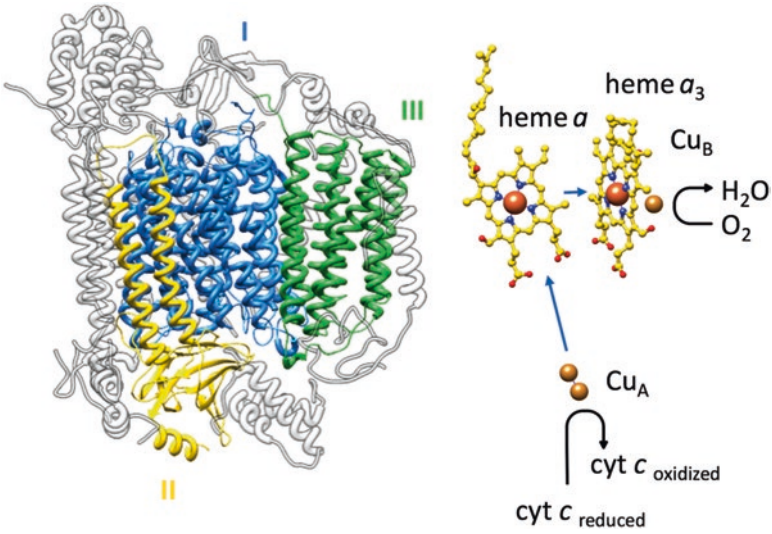

Fig. 7.9 Structure of complex IV (bovine heart, pdb 1occ) (Tsukihara et al. 1996). Core subunits are color-coded and accessory subunits are shown in grey. Right: redox metal centers that participate in the electron transfer from cytochrome *c* to dioxygen. The electron transfer flow is indicated by blue arrows

7.5.1 Core Subunits of Complex IV

Complex IV is composed of 14 different subunits in mammals and birds, from which only the three mitochondrial-encoded subunits I, II and III are present in the simpler bacterial enzyme (Fig. 7.9). Subunit I is a membrane embedded subunit, with 12 TMH and three of the four cofactors, heme *a*, heme a_3 and Cu_B. The fourth catalytic site, Cu_A, is located in subunit II, which is anchored by two TMH and has a soluble domain in the IMS, to which cytochrome *c* binds. Subunit III with seven TMH stabilizes the other two core proteins and acts as an initial proton acceptor in one of the transfer pathways (Varanasi and Hosler 2012; Alnajjar et al. 2014).

7.5.2 The Catalytic Cycle of Complex IV

As stated earlier, cytochrome *c* oxidase contains four redox-active metal centers: Cu_A, heme *a* (Fe_a) and a binuclear center composed of heme a_3 (Fe_{a3}) and Cu_B (Fig. 7.9). In each catalytic cycle, four reduced cytochrome *c* molecules donate sequentially one electron to Cu_A, which is transferred through Fe_a to the active site. Concurrently to each electron transfer to the Fe_{a3}/Cu_B binuclear center, the uptake of two protons occurs; in total eight protons are taken from the matrix, from which half

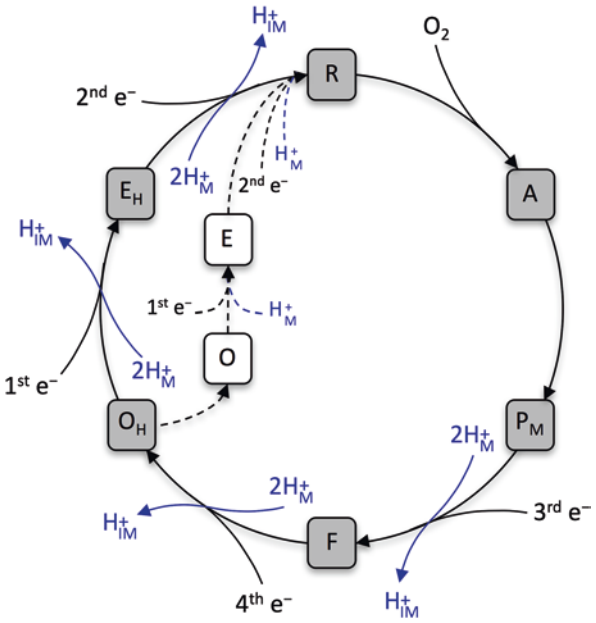

Fig. 7.10 Catalytic cycle of cytochrome *c* oxidase. Dashed arrows indicate the transitions between reductive phase intermediates not coupled to proton pumping. Blue arrows represent the uptake and release of protons on the matrix and IMS side, respectively

are used for water formation in the binuclear center and the other four are pumped across the membrane into the IMS (Wikström 1977).

Numerous reaction intermediates with specific redox and protonation states of Fe_{a3} and Cu_B have been identified, which contributed to the formulation of a detailed model of the catalytic cycle (Konstantinov 2012; Popovic 2013; Sharma and Wikström 2016; Yoshikawa and Shimada 2015). This can be divided in two phases: the reductive phase and the oxidative phase (Fig. 7.10). In the reductive phase, oxidized complex IV (*O_H state*) receives sequentially two electrons from two molecules of cytochrome *c*; the first electron, together with a proton from the matrix, produces the one-electron reduced intermediate (*E_H-state*), while the second electron and proton produce the reduced state (*R-state*). During the reductive phase a hydroxide ion in the binuclear center remaining from the previous cycle is protonated and released as water. The *R-state* has two electrons in the binuclear center (mixed-valence state) and in anaerobic conditions two more electrons, bound to heme *a* and Cu_A (fully-reduced state).

In the oxidative reaction phase, four electrons are transferred to O_2 for its reduction to H_2O. This phase starts with O_2 binding to cytochrome *c* oxidase in the *R-state*. The reduced binuclear site rapidly reacts with O_2 for formation of the oxygen adduct intermediate (*A-state*). The simultaneous transfer of four electrons to the molecule of O_2 converts the *A-state* to the peroxy intermediate (*P_M-state*). Three of these electrons are donated by the binuclear center (two from Fe_{a3} and one from Cu_B), while an amino acid residue in the vicinity of the active site provides the fourth electron. This residue is thought to be Tyr244, which is covalently bound to one of the histidine ligands of Cu_B. The conversion of the *P_M-state* to the ferryl-oxo

intermediate (*F-state*) requires the entry of a third electron into the enzyme, provided by the third cytochrome *c* molecule, and the uptake of a proton from the matrix. In the *F-state* a water molecule is formed. Delivery of the fourth electron by cytochrome *c* and a proton from the matrix produces the fully-oxidized high-energy state of the enzyme (O_H*-state*). The formation of the O_H*-state* marks the transition to the reductive phase of a new cycle.

It is important to note that the structure of cytochrome *c* oxidase and, in particular, the nonsequential four electron reduction of the bound O_2 molecule are crucial for the negligible production of ROS by this complex (Muramoto et al. 2010).

7.5.3 Proton Pumping by Complex IV

The following transitions in the catalytic cycle are accompanied by pumping of one proton across the membrane: $P_M \rightarrow F$, $F \rightarrow O_H$, $O_H \rightarrow E_H$ and $E_H \rightarrow R$. The fully-oxidized low-energy state (*O-state*), which may form in the absence of an electron donor by relaxation of the O_H*-state*, and the subsequent one-electron reduced state (*E-state*) are not capable of proton pumping upon reduction and most likely are not natural states during the turnover of complex IV (Belevich et al. 2006).

It has been proposed that the transfer of the protons in the interior of complex IV for water formation and proton pumping occurs through a hydrogen bond network or by mobile water molecules in the hydronium state. Three proton transfer pathways have been described for the mitochondrial enzyme: D-, K- and H-channel (Wikström et al. 2015). Several studies have identified the D-channel as the pathway for the four protons that are pumped into the IMS during the catalytic cycle and also for the uptake of one or two of the chemical protons used at the binuclear center for water formation (Konstantinov et al. 1997; Brzezinski and Adelroth 1998). The D-channel includes ten water molecules and ends approximately in the middle of the membrane at a glutamic acid residue. The K-channel extends from a glutamic acid residue near the conserved lysine on the matrix side of subunit II to the conserved tyrosine close to the binuclear center. Only a few water molecules have been shown to be present in the channel, which is lined by numerous hydrophobic residues of subunit I. This pathway is responsible for the uptake of one or two chemical protons during the reductive phase (Konstantinov et al. 1997; Brzezinski and Adelroth 1998). High-resolution structures of the enzyme from bovine heart mitochondria revealed a third pathway called H-channel, which crosses the membrane all the way from the matrix to the IMS (Tsukihara et al. 1995). This channel consists of water-filled cavities and is lined by several polar residues and passes far from the catalytic site of complex IV. The enzyme from bovine heart with several mutations in the H-channel presented normal turnover activity, but no proton translocation (Tsukihara et al. 2003; Shimokata et al. 2007). In bacteria, with few exceptions the residues that compose the H-channel are conserved. However, site-directed mutations of this channel in the bacterial complex showed no effects in either turnover activity or proton pumping (Lee et al. 2000; Salje et al. 2005). In an attempt to

reconcile this results, the H-channel has been suggested not to be involved in proton pumping, but instead to work as a dielectric channel for minimization of the thermodynamic cost of moving electrons from the membrane surface into the nonpolar membrane domain where heme *a* is located (Rich and Marechal 2013).

7.5.4 Accessory Subunits of Complex IV

The accessory subunits of cytochrome *c* oxidase strongly depress the activity of the core subunits and have a fundamental role in the regulation of the complex. Subunit IV is the largest of the supernumerary subunits (Fig. 7.11) and binds ATP, being responsible for the allosteric ATP-inhibition of complex IV at high cytosolic ATP/ADP-ratios (Arnold and Kadenbach 1997). This inhibition is dependent on the phosphorylation of subunit I and its disruption leads to an increase of the membrane potential and ROS production in mitochondria, associated with apoptosis and degenerative diseases. Subunit Va and Vb are both located exclusively in the matrix. The former was shown to abolish the allosteric ATP-inhibition upon binding to the thyroid hormone T2 (3,5-diiofothyronine) in the enzyme from bovine heart (Arnold et al. 1998b). Subunit Vb contains a Zn site with a classic zinc finger motif and it has been suggested to play a role in the assembly of the complex (Galati et al. 2009). This subunit also interacts with the regulatory subunit of the cAMP-dependent protein kinase A for a cAMP-dependent inhibition of complex IV (Yang et al. 1998). Subunit VIa has one TMH and a small soluble domain in the IMS and has been implicated in stimulation of thermogenesis for maintenance of the body temperature

Fig. 7.11 Structure of bovine complex IV accessory subunits (pdb 1occ) (Tsukihara et al. 1996). Accessory subunits are color-coded and core subunits are shown in grey

in response to different stimuli in muscle and other tissues (Anthony et al. 1993; Lee and Kadenbach 2001). The only subunit located exclusively in the IMS is subunit VIb, which has been proposed to participate in cytochrome *c* binding and that, together with subunit VIa, stabilizes the dimeric state in which the protein was crystallized. Both subunits VIIa and VIIb have a single TMH and small extramembrane domains in the matrix and IMS, respectively. The first one was shown to form protein-protein contacts with complex III in the respirasome (Sousa et al. 2016; Gu et al. 2016; Letts et al. 2016), while the latter has been proposed to be essential for complex IV assembly and activity (Indrieri et al. 2012). Also subunit VIIc is involved in the formation of the respirasome by interaction with complex I (Sousa et al. 2016; Gu et al. 2016; Letts et al. 2016). No specific function has been proposed for subunits VIc and VIII, each with one TMH.

The most recently identified subunit of complex IV was initially thought to belong to complex I and named NDUFA4 (Carroll et al. 2003; Carroll et al. 2006). This subunit is encoded in the nucleus and is loosely attached to the rest of the enzyme, and its assignment was controversial (Hirst et al. 2003). However, NDUFA4 was shown to interact with subunits of complex IV and to be an essential subunit for its biogenesis (Balsa et al. 2012; Pitceathly et al. 2013). Recently a new cytochrome *c* subunit was identified in *Saccharomyces cerevisiae* named Cox26; however, this subunit is not conserved in higher eukaryotes (Levchenko et al. 2016).

Cytochrome *c* oxidase occurs in different isoforms. Subunits VIa, VIIa and VIII were first shown to have distinct isoforms in heart and liver mitochondria. The isoforms VIa-H, VIIa-H, VIII-H and VIa-L, VIIa-L, VIII-L are predominant in skeletal muscle cells and all other tissues, respectively (Schlerf et al. 1988). Isoforms of subunits VIa and VIIa were also shown to have specific expression patterns during development (Ewart et al. 1991; Bonne et al. 1993; Parsons et al. 1996). A third isoform of subunit VIII (VIII-3) was identified, for which the level of specificity is still not known (Huttemann et al. 2003b). Subunit IV has a lung-specific isoform (IV-2) (Huttemann et al. 2001) and subunit VIb (and possibly VIIb) a testes-specific isoform (VIb-2; VIIb-2) (Huttemann et al. 2003a). The expression of these tissue-specific and developmental-specific isoforms introduces an extra level of regulation of complex IV activity.

7.5.5 Complex IV Deficiencies

Numerous pathologies have been reported after a perturbation of complex IV assembly or function (Rak et al. 2016). Few of these reports are associated to mutations of nuclear-encoded subunits of complex IV, as is the case for other respiratory complexes. Mutations of the mitochondrial-encoded subunits I, II and III are linked to a large number of different phenotypes and have been often observed, but even more frequently complex IV deficiencies have their origin in mutations of specific assembly factors. The diversity of phenotypes has been accredited to the degree of heteroplasmy in the case of subunits I, II and III and to the existence of several of the nuclear-encoded subunits in distinct isoforms.

7.6 Supramolecular Organization of the Respiratory Chain Complexes

The organization of the respiratory complexes in the mitochondrial membrane has been extensively debated for decades. Originally, it was proposed that the components of the respiratory chain were packed in the membrane, forming high order structures that allowed efficient electron transfer (Chance and Williams 1955). This solid-state model was however quickly discredited and gave place to the fluid or random collision model. The new paradigm was that each complex exists as a single entity that freely diffuses in the membrane and electron transfer occurs during random collisions (Hackenbrock et al. 1986). The existence of stable supercomplexes of complexes III and IV in some prokaryotes was considered specific for these species (Iwasaki et al. 1995). Only at the beginning of the twenty-first century, through solubilization with mild detergents like digitonin and analysis by blue-native polyacrylamide gel electrophoresis, supercomplexes were shown to be present in eukaryotes (Schägger and Pfeiffer 2000). Negative stain electron microscopy (EM) studies showed that these supercomplexes had a defined structure, including I_1III_2 complexes from plants (Dudkina et al. 2005a), I_1III_2 and $I_1III_2IV_1$ from bovine heart (Schäfer et al. 2006), and III_2IV_2 and III_2IV_1 complexes from *S. cerevisiae* (which lacks complex I) (Heinemeyer et al. 2007). These results introduced the currently established plasticity model, according to which the respiratory complexes exist free in the membrane but also as large supramolecular structures (Acin-Pérez et al. 2008). Since their first isolation, numerous stoichiometric supercomplexes formed by complexes I, III and IV have been identified, while the association of complex II in such structures was hypothesized in only a few cases (Acin-Pérez et al. 2008; Schönfeld et al. 2010). Studies with bovine heart mitochondria suggest that all complex I is associated in supercomplexes, while approximately 30% of complex III and more than 85% of complex IV exists as free enzymes (Schägger and Pfeiffer 2001).

7.6.1 The Respirasome

Special interest has been devoted to the study of the respirasome ($I_1III_2IV_1$), which contains all the enzymes required for the electron transfer from NADH to molecular oxygen and is conserved in all higher eukaryotes. It is the most abundant supercomplex in bovine heart mitochondria (Schägger and Pfeiffer 2000, 2001; Schäfer et al. 2006) and has higher activity than the species lacking complex IV (Schäfer et al. 2006). Its three-dimensional structure has been studied by EM and after initial structures from 33–18 Å where the relative orientation of the complexes could be seen (Schäfer et al. 2007; Althoff et al. 2011; Dudkina et al. 2011) structures with sub-nanometer resolution were recently produced for several mammalian species (Gu et al. 2016; Letts et al. 2016; Sousa et al. 2016). The overall arrangement of the complexes is conserved in all respirasome structures; the complex III dimer lies on

the inner side of the complex I membrane arc, while complex IV is located at the distal end of the membrane arm of complex I and adjacent to complex III (Fig. 7.12). The three complexes are associated by several direct protein-protein interactions that mostly involve accessory subunits. The contacts between complex I and complex III are the most extensive within the respirasome, with subunits B22 (NDUFB9) and B14.7 (NDUFA11) of complex I interacting with Core 1 and subunit 8 of complex III, respectively. Additionally, Core 1, and also subunit 10, of complex III associate with subunit VIIa of complex IV. Only one core subunit among the three complexes is involved in the stabilization of the supercomplex; this subunit is ND5 (NU5M) from complex I, which binds subunit VIIc of complex IV. Lipid-mediated interactions are equally important for supercomplex stability. In particular, cardiolipin, which exists almost exclusively in the IMM, has been shown to be required for formation of supercomplexes (Mileykovskaya and Dowhan 2014).

The assembly process of the supercomplexes, and more significantly of the respirasome, is still unknown. Two conflicting models have been proposed based on studies performed in higher eukaryotes. According to the first model, the respirasome is formed by association of the mature individual complexes (Acin-Pérez et al. 2008; Guerrero-Castillo et al. 2016). Conversely, evidence for the formation of the respirasome by a progressive integration of single subunits or intermediate assemblies has been also reported (Moreno-Lastres et al. 2012). In the latter case, it was suggested that in addition to the direct assembly in supercomplexes, biogenesis of complexes III and IV might occur independently, while mature complex I is exclusively assembled in the respirasome. At this moment, only one protein has been unquestionably identified as a supercomplex assembly factor; SCAFI is required for the association of complex IV into supercomplexes but does not affect the assembly or stability of the individual complex (Lapuente-Brun et al. 2013; Cogliati et al. 2016).

7.6.2 Functions of the Respirasome

Advantages of the organization of the respiratory chain in supercomplexes have been hotly debated, with the possibilities ranging from structural to kinetic and other functional roles. From a structural perspective, supercomplexes have been proposed to be required for proper expression of complex I, by contributing to its assembly or stabilization. This hypothesis gained force with the identification of several combined deficiencies in patients with mitochondrial disorders, where impaired expression of complex III induces the secondary loss of complex I (Bruno et al. 2003; Lamantea et al. 2002). Similar effects were observed in mammalian cells with complex IV deficiencies (D'Aurelio et al. 2006; Vempati et al. 2009; Diaz et al. 2006). Recent reports suggested that the degradation of complex I in the absence of complexes III or IV might be due to the accumulation of reduced quinone and consequent ROS production through RET (Guarás et al. 2016).

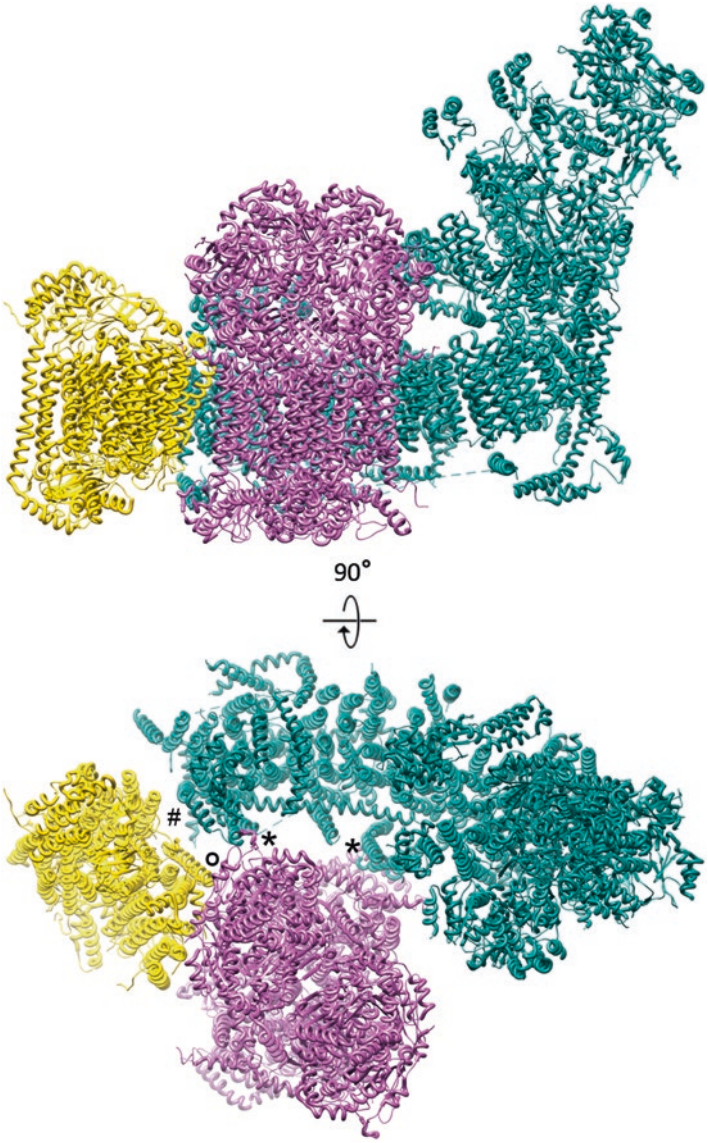

Fig. 7.12 Structure of respirasome (bovine heart, pdb 5luf) (Sousa et al. 2016). View perpendicular to the membrane (top) and from the matrix (bottom). Complex I is shown in dark cyan, complex III in pink and complex IV in yellow. *: contacts between subunits of complex I and III; **#**: I and IV; **O**: III and IV as described in the text

However, several studies showed also that inhibition of complex III or IV activity is insufficient to prompt complete degradation of complex I (Acin-Pérez et al. 2004; Guarás et al. 2016), suggesting that physical interaction with other respiratory complexes is most likely important for maintaining complex I levels.

Another possible function of the respiratory supercomplexes relates to ROS production. By enhancing the ratio of free to superassembled complex I, the production of ROS was also increased (Maranzana et al. 2013), showing that the supramolecular organization of the respiratory chain reduces the leakage of electrons from complex I. Similar observations were reported upon destabilization of supercomplexes from *Saccharomyces cerevisiae* that contain only complexes III and IV, which imply that also ROS production by complex III might be reduced (Chen et al. 2012; Vukotic et al. 2012).

Finally, one of the most discussed advantages of supercomplexes has been the possibility of enhanced catalysis and efficiency of the electron transfer due to substrate channeling (Fig. 7.13). Substrate channeling is the direct transfer of an intermediate between the active sites of two enzymes that catalyze consecutive reactions. In the case of the respirasome, channeling of both quinone and cytochrome *c* were hypothesized. Contradictory results regarding channeling of cytochrome *c* between complex III and complex IV hinder a conclusion in this case. However, channeling of quinone from complex I to complex III within the respirasome has found support in numerous reports. Studies by flux control analysis found that both enzymes are rate-limiting for NADH oxidation, suggesting a relevant functional association (Bianchi et al. 2004; Lapuente-Brun et al. 2013). In case of channeling, a partition of the quinone pool would also be observed, with dedicated populations for succinate and NADH-dependent respiration. This compartmentalization explains for example why a reduction of complex III levels can impair succinate-dependent electron transfer, while NADH oxidation is maintained, due to the association of all the available complex III to complex I (Lapuente-Brun et al. 2013). Further arguments in favor of quinone channeling have been provided by the architecture of the respirasome. Early structures of this supercomplex revealed that the quinone-binding sites of complex I and the central monomer of complex III are aligned and within a short diffusion distance (Althoff et al. 2011). Recently, a functional asymmetry of the complex III dimer was observed in one structure of the bovine superassembly, where the central monomer preferentially catalyzes cytochrome *c* reduction (Sousa et al. 2016). The non-involvement of the outer monomer in the transfer of electrons from ubiquinol to the soluble carrier could be explained by the larger distance between the quinone-binding sites, which is incompatible with substrate channeling. Despite all the evidence supporting a kinetic advantage associated with respirasome formation, no consensus has been reached until now.

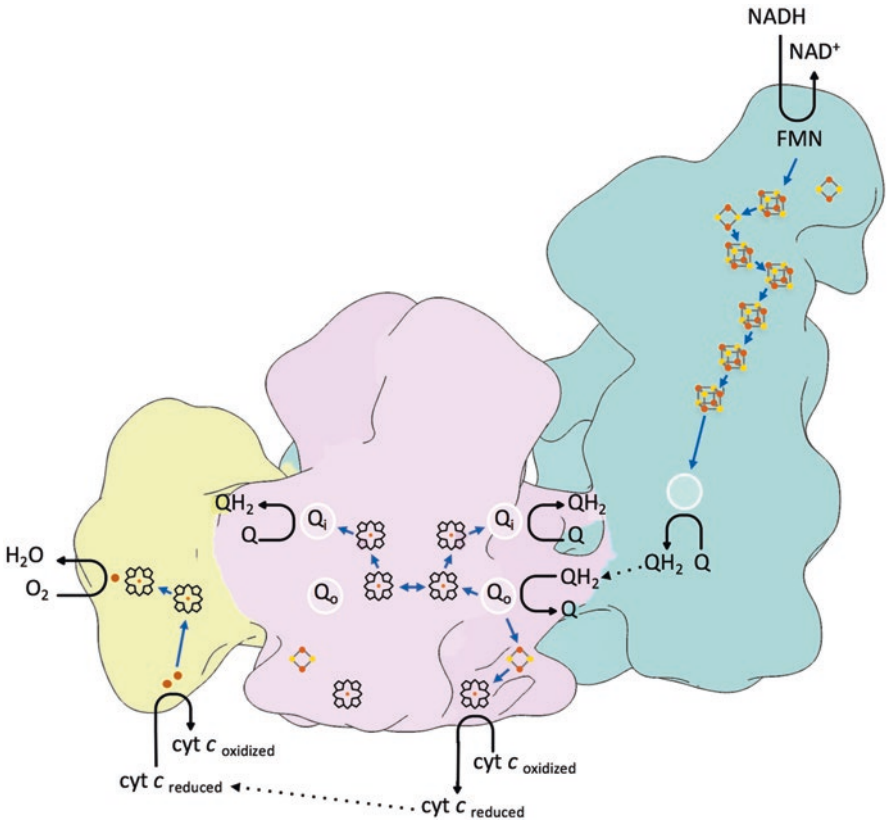

Fig. 7.13 Electron and substrate transfer in the respirasome according to the channeling model. Rapid electron equilibration between b_L hemes allows quinone reduction in either monomer of complex III. Quinone oxidation occurs preferentially at the central monomer of complex III. Complex I, III and IV are depicted in blue, pink and yellow, respectively. Quinone-binding sites are represented by circles. Blue arrows indicate transfer of electrons and dotted arrows diffusion of substrates. Reactions are indicated by black arrows

7.6.3 Plasticity of the Supramolecular Organization in the IMM

The ratio between free complexes and supercomplexes in the IMM is highly regulated, varying among cell types and in response to physiological stimuli. Disorganization of the cristae during apoptotic remodeling of the mitochondrial architecture leads to impaired assembly of supercomplexes, while the narrowing of cristae observed during starvation conditions favors supercomplex formation (Cogliati et al. 2013). Also the lipid composition of the IMM is critical in the

supercomplex dynamics; whereas cardiolipin is required for the formation of supercomplexes, depletion of other lipids such as phosphatidylethanolamine stabilizes these structures (Bottinger et al. 2012). The dynamics of supercomplexes is further regulated by the transmembrane electrochemical potential, with the formation of superassemblies being favored at lower values (Quarato et al. 2011). Additionally, the acidification of the mitochondrial matrix, as induced during hypoxia, can promote the dissociation of respirasomes (Ramirez-Aguilar et al. 2011). Post-translational modifications have been also conjectured to influence supercomplex formation, however no correlation has yet been established.

The plasticity of the respiratory chain organization might be imperative for metabolic regulation. For instance, glucose feeds more electrons into the respiratory chain through NADH and therefore through complex I and the respirasome, whereas fatty acid oxidation largely contributes electrons through an FAD-linked pathway that is favored by free complexes (Lenaz and Genova 2016). A change in the equilibrium between free complexes and supercomplexes might be used for adaptation to substrate availability, ensuring their efficient oxidation. The plasticity observed might also modulate the production of ROS and therefore cellular activity, since these are known to act as signaling molecules (Whelan and Zuckerbraun 2013).

7.7 ATP Synthase

The proton gradient created by the respiratory chain drives a membrane-embedded rotor, the F_o part of the F_1F_o ATP synthase, and ATP is generated by conformational changes in the three nucleotide-binding pockets of the F_1 head by the binding change mechanism (Boyer 1993; Abrahams et al. 1994; Boyer 1997). The ATP synthase is a combination of two molecular machines and can act as an ion-gradient driven ATP synthase or as an ion pump powered by ATP hydrolysis. The binding change mechanism was first proposed by Paul Boyer (reviewed in (Boyer 1997)) and later confirmed by x-ray structures of the bovine F_1 in John Walker's laboratory (Abrahams et al. 1994). Rotation of the γ subunit was shown directly (Noji et al. 1997) by fixing a $\alpha_3\beta_3\gamma$ complex to a glass surface through the β subunit with a fluorescent actin filament attached to γ. After adding ATP, the rotation could be observed under a microscope. Also the direction of rotation for hydrolysis (counterclockwise as viewed from the membrane domain) was unambiguously determined by this experiment. ATP synthase consists of eight or nine different subunits in bacteria which are conserved across most species including mitochondria and chloroplasts, while mitochondrial ATP synthase has acquired more subunits (Table 7.2).

Table 7.2 Subunits of ATP synthase in different species

E. coli	Chloroplasts	Mammals	Yeasts	*Polytomella*	Location and function
α3	α3	α3	α3	α3	F_1 head
β3	β3	β3	β3	β3	F_1 head/catalytic subunit
γ	γ	γ	γ	γ	Central stalk/rotor
ε	ε	δ	δ	δ	Central stalk/rotor
		ε	ε	ε	Central stalk/rotor
δ	δ	OSCP	OSCP	OSCP	Peripheral stalk
–	–	*d*	*d*	–	Peripheral stalk
–	–	F6	*h*	–	Peripheral stalk
b	*b*	*b*	4	–	F_o/peripheral stalk
b	*b*’	A6L	8	–	F_o/peripheral stalk[a]
a	*a*	*a*	6	*a*	F_o/stator/proton channel
*c*12	*c*14	*c*8	9/*c*10	*c*10	F_o/rotor/proton channel
–	–	f	f	–	F_o/stator/dimerization
–	–	–	*i*	–	F_o/stator
–	–	*e*	*e*	–	F_o/dimerization
–	–	*g*	*g*	–	F_o/dimerization
–	–	–	*k*	–	F_o/dimerization
–	–	IF1	IF1	–	ATPase inhibitor
–	–	–	–	ASA1–9	Peripheral stalk[b]

[a]The relation between the *b* subunit and 8/A6L was established by Hahn et al. (2016)
[b]*Polytomella* and *Chlamydomonas* have an elaborate peripheral stalk consisting of 9 different subunits without known relatives (van Lis et al. 2003; van Lis et al. 2007)

7.7.1 Composition and Subunits

7.7.1.1 F_1 Head

The soluble or F_1 part is the catalytic head, consisting of an alternating arrangement of three α and three β subunits, arranged around the γ subunit, which is part of the rotor (Fig. 7.14). The α and β subunits are homologous and have the same fold, but only the β subunit is catalytic. The α subunits permanently contain a nucleotide without a known function, while the nucleotide-binding pockets of the β subunits are in turn in an open, loose and tight state upon rotation of the asymmetric γ subunit, which forms a long α helix coiled coil. Numerous crystal structures of F_1 in the ground state or ADP-inhibited state (reviewed in (Walker 2013)) show that two of the three nucleotide-binding sites in the β subunit have a similar conformation and contain either ADP and AMP-PNP (a non-hydrolysable ATP analogue), two ADP, or two AMP-PNP. The third site has a very different conformation and is almost always empty. The three sites interconvert upon rotation of the γ subunit.

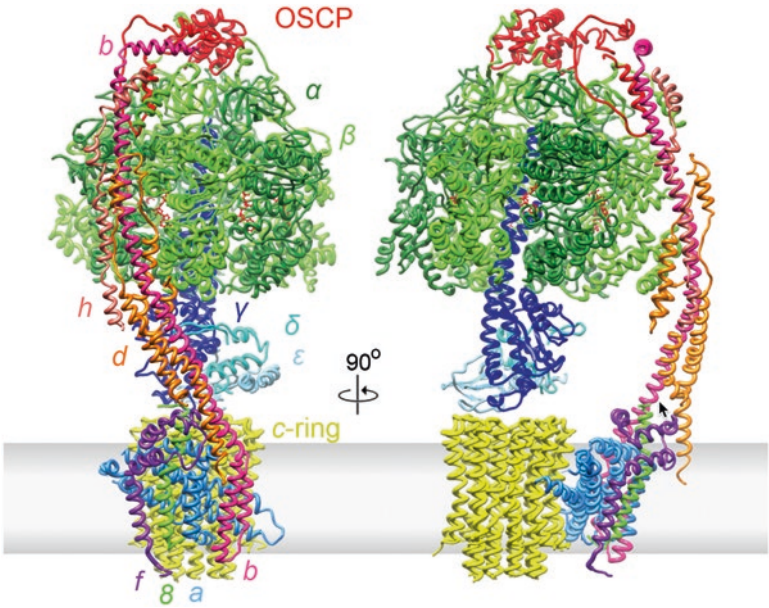

Fig. 7.14 Subunit composition of mitochondrial ATP synthase from *Yarrowia lipolytica* (Hahn et al. 2016). View from the dimer interface (left) and from the side (right)

7.7.1.2 The Rotor

The rotor shaft is a coiled coil formed by the long N-terminal and C-terminal helices of the γ subunit. The central part of γ is attached to a membrane-embedded ring of *c*-subunits, together with the δ subunit (ε in bacteria) and in mitochondria another small protein, confusingly called ε (Fig. 7.14). The *c*-subunits are helix hairpins with a conserved negatively charged amino acid (in most species a glutamate, but an aspartate in *E. coli*) in the middle of the outer helix. This residue is expected to be protonated, so neutral, when in contact with the lipid environment of the membrane, but deprotonated and charged in the hydrophilic contact site with the stator. The number of subunits in the rotor ring was long an issue of debate, until structural data (Stock et al. 1999; Seelert et al. 2000; Stahlberg et al. 2001) showed that the number varies between species. By now, in bacterial ATP synthases rings have been found with 9 to 15 subunits (Stahlberg et al. 2001; Pogoryelov et al. 2005; Meier et al. 2006; Fritz et al. 2008; Pogoryelov et al. 2009; Matthies et al. 2009; Morales-Rios et al. 2015; Preiss et al. 2015), chloroplasts have 14 (Seelert et al. 2000; Seelert et al. 2009), while mammalian mitochondrial ATP synthase has 8 subunits (Watt et al. 2010) and those in yeasts (Stock et al. 1999; Hahn et al. 2016) and green algae (Allegretti et al. 2015) have 10. A rotor ring of *n* *c*-subunits yields 3 ATP per *n* translocated ions, so the stoichiometry has bioenergetic implications. The primary structure of the *c*-subunit determines the stoichiometry, and a region at the top of the

inner helix appears to be the major contributor. A conserved sequence GxGxGxG enables a close packing of the helices in the c_{11}-ring of *Ilyobacter tartaricus* (Vonck et al. 2002), the first ring for which the x-ray structure was solved (Meier et al. 2005). The glycines are exchanged to alanine or serine in some species (Liu et al. 2011), for example to AxAxAxA in the alkaliphilic soil bacterium *Bacillus pseudofirmus* OF4, resulting in a reduced curvature and thus a larger ring with 13 subunits (Preiss et al. 2010). Mutations in this motif can alter the stoichiometry (Pogoryelov et al. 2012; Preiss et al. 2013), and mutants of *B. pseudofirmus* OF4 with a smaller c_{12}-ring grew slower than the wt $c_{13,}$ showing a direct connection between the ion-to-ATP ratio and cell physiology (Preiss et al. 2013).

7.7.1.3 Rotation Mechanism and the *a* Subunit

Before the structure of the *c*-ring was known, rotation of the ring was already hypothesized to occur by a "Brownian ratchet" mechanism, where the ring carries out random Brownian motions and only neutral (protonated) glutamates can enter the lipid phase, thus imposing directionality on the rotation of the ring (Junge et al. 1997; Vik and Antonio 1994). In this model, two half-channels allow access to the protonation site from either side of the membrane and the direction of rotation (and thus ATP synthesis or hydrolysis) depends on the electrochemical gradient. The first structures of the rotor ring (Meier et al. 2005; Murata et al. 2005) supported this model, and evidence for the postulated half-channels accessible from the two sides of the membrane also emerged (Angevine and Fillingame 2003; Fillingame and Steed 2014). However, the structure of the stator, the *a* subunit, remained elusive. The *a* subunit was predicted to have 5–7 TMH, with a consensus tending to 5 (Vik and Dao 1992; Cain and Simoni 1986), but the helix boundaries were uncertain and differed considerably between models. The highest sequence similarity is found at the C-terminus, which contains a completely conserved and essential arginine residue as well as several other conserved polar residues. Several residues in this region could be exchanged (Cain and Simoni 1988; Hatch et al. 1995) or crosslinked to the *c*-subunits (Jiang and Fillingame 1998; Moore and Fillingame 2008), leading to a model where the C-terminus contains two TMH facing the *c*-ring as part of a four-helix bundle (Schwem and Fillingame 2006). Attempts to purify the *a* subunit were often unsuccessful, although a preparation in a chloroform-methanol-water mixture gave promising results for NMR measurements (Dmitriev et al. 2004) and a two-dimensional crystal of a bacterial F_o subcomplex appeared to show the four-helix bundle (Hakulinen et al. 2012). Attempts to crystallize the whole ATP synthase always yielded a structure lacking the stator (Stock et al. 1999; Pagadala et al. 2011; Giraud et al. 2012; Hahn et al. 2016). The introduction of direct electron detectors finally led to cryo-EM maps of intact ATP synthase complexes with sufficient resolution to solve the *a* subunit enigma. The first structure was the unusually stable mitochondrial dimer from the chlorophyll-less green alga *Polytomella* (Allegretti et al. 2015), soon followed by a monomeric bovine complex (Zhou et al. 2015) and the dimer of the yeast *Y. lipolytica* (Hahn et al. 2016). Apart from these

mitochondrial complexes, also a cryo-EM map of a vacuolar ATPase (Zhao et al. 2015) and its membrane domain (Mazhab-Jafari et al. 2016) were determined, as well as the first x-ray structure of an almost complete ATP synthase, from *Paracoccus denitrificans* (Morales-Rios et al. 2015). The ATP synthase structures all showed the same architecture of the *a* subunit: the predicted four-helix bundle with the two C-terminal helices facing the *c*-ring, but unexpectedly, the bundle is almost horizontal in the membrane. The distantly related V-ATPase also displays two helices facing the rotor at the same angle, showing the ancient and essential nature of this feature. All structures are at intermediate resolution where side chains are not yet visible, so the interpretation is not unambiguous. However, the known interaction of the C-terminal part of the *a* subunit with the *c*-ring places this region in the helix hairpin next to the ring and the availability of thousands of sequences and the observed high structural homology between available structures place restraints on possible models (Fig. 7.15). For example, although the two C-terminal helices are the most conserved parts of the structure, the loop between them has a variable length. The presence of two conserved, interchangeable pairs (His-Glu and Arg-Gln) (Cain and Simoni 1988; Hatch et al. 1995) with a member on each helix fixes the relative orientation (Allegretti et al. 2015). A model for the bovine *a* subunit was built using constraints from analysis of evolutionary covariance in the sequences (Zhou et al. 2015). From the bovine and yeast structures (Zhou et al. 2015; Hahn et al. 2016) almost the entire *a* subunit was assigned, and the models are very similar. The structure consists of six helices: a vertical TMH with the N-terminus in the IMS, an amphipathic helix on the matrix surface, and two helix hairpins forming a bundle at a high angle in the membrane (Fig. 7.16). These features are conserved in bacterial, mitochondrial and chloroplast *a* subunit sequences (Fig. 7.15) and can also be recognized in partially unassigned features of the *Polytomella* cryo-EM map (EMD-2852) (Allegretti et al. 2015) and the bacterial x-ray structure (pdb 5dn6) (Morales-Rios et al. 2015), as well as in the structure of monomeric ATP synthase from the yeast *Pichia angusta* (Vinothkumar et al. 2016).

The two C-terminal helices (5 and 6) are highly conserved in all F_iF_o ATP synthases and are characterized by a series of charged or polar residues in a hydrophobic environment. The helices form a hairpin at an angle of ~20° to the membrane plane, with a loop near the IMS surface and the termini on the matrix side. The length of the loop is not conserved (Fig. 7.15), but the region is highly hydrophobic, in agreement with its location in the membrane interior, and includes one or several proline residues in most species, which probably contribute to breaking of the helices and/or forming a bend. The proton entrance on the IMS side is near the helix5-6 loop. The helix closest to the IMS, in most structures interpreted as helix 5, curves around the *c*-ring (Fig. 7.16). Conserved hydrophilic residues in this region on helix 5 and 6 line an aqueous cavity on the matrix side, where the protons will be released from the *c*-ring after almost a complete rotation of the ring. The conserved arginine of subunit *a* is located between the two proton channels and its charged side chain would prevent passage of a protonated, uncharged glutamate on the *c*-ring and thus ensure unidirectional rotation of the rotor. The resulting direction (counterclockwise as seen from the matrix for ATP synthesis) fits the observation (Noji et al. 1997).

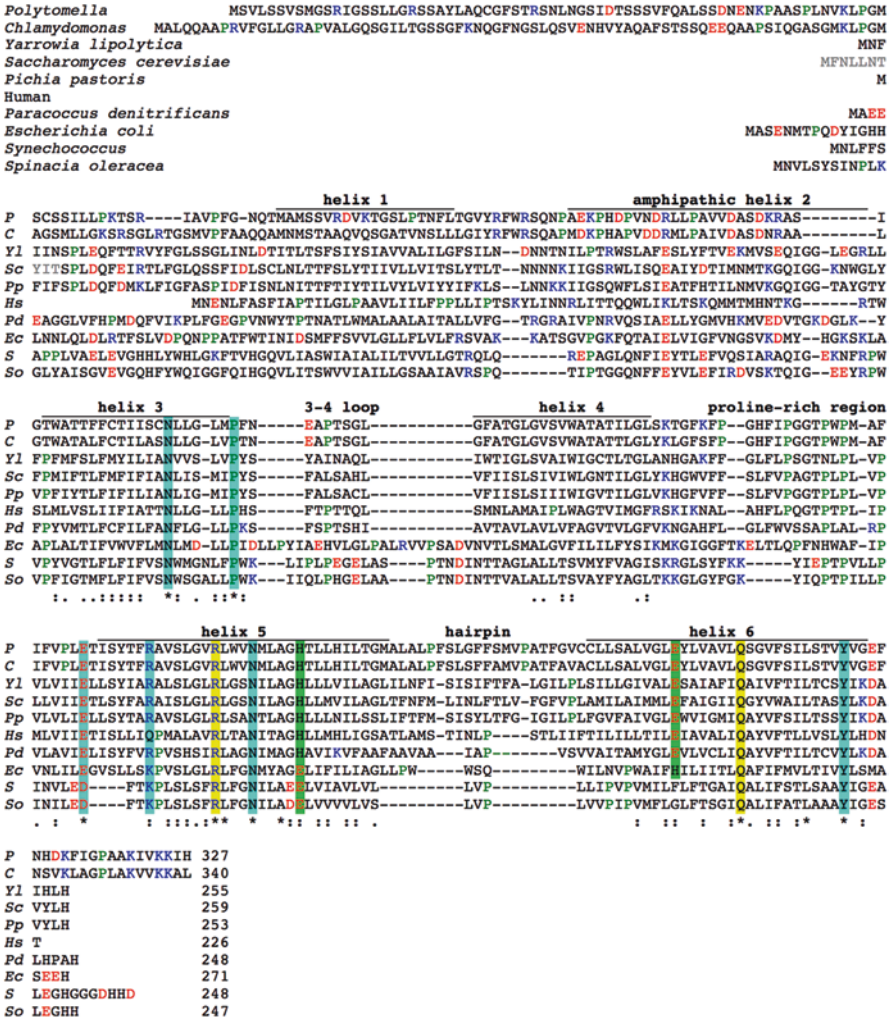

Fig. 7.15 Sequence alignment of the *a* subunit. Shown are mitochondrial ATP synthase (*Polytomella* and *Chlamydomonas*; the yeasts *Y. lipolytica*, *S. cerevisiae* and *P. pastoris*; human); the bacteria *P. denitrificans* (an α-proteobacterium related to the ancestor of mitochondria), *E. coli* and *Synechococcus* (a cyanobacterium related to the ancestor of chloroplasts), and chloroplast ATP synthase from spinach. Positively charged residues are shown in blue, negative ones in red font, prolines in green. Highly conserved residues are highlighted in cyan, and two pairs of interchangeable residues in yellow (including the essential arginine) and green. The approximate helix boundaries and other conserved features are indicated above the alignment. The cleaved N-terminal presequence in *S. cerevisiae* is shown in grey font

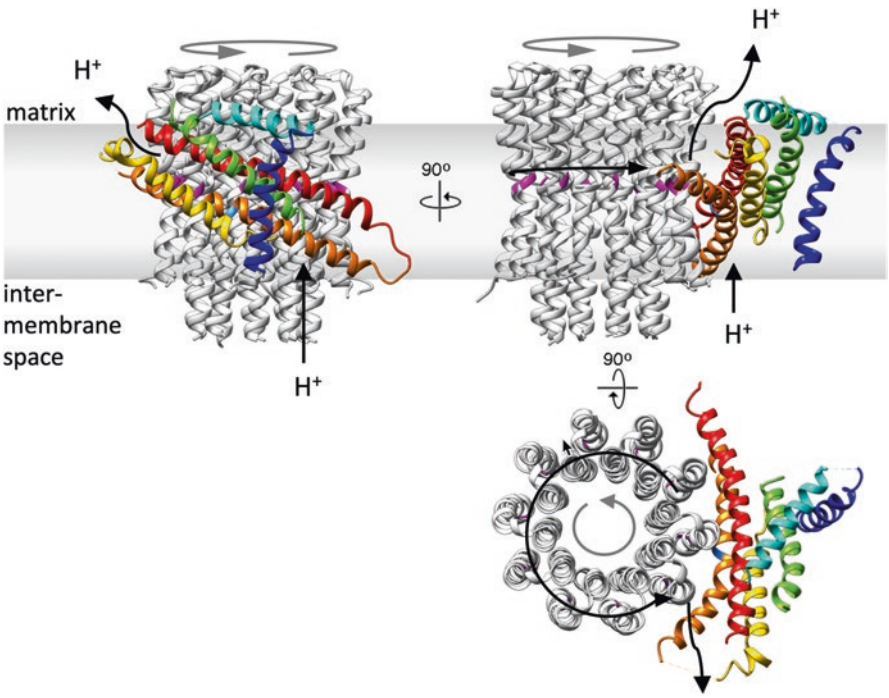

Fig. 7.16 The *a* subunit and *c*-ring form the proton translocation channel in ATP synthase. Shown is the model from the yeast *Y. lipolytica* (Hahn et al. 2016). Grey, c_{10}-ring; color, *a* subunit. Blue, helix 1; cyan, amphipathic helix 2; green and yellow, helix 3 and 4 forming a horizontal helix hairpin; orange and red, helix 5 and 6 forming the second helix hairpin, which is adjacent to the *c*-ring. The conserved arginine on helix 5 is shown in cyan and the glutamates on the *c*-ring in magenta. Black arrows indicate proton flow and grey arrows ring rotation during ATP synthesis. Left, view from the dimer interface; right, view along the *a/c* interface; bottom, view from the matrix

7.7.1.4 The Peripheral Stalk

The central stalk (the γ subunit), confirmed as the rotor in the F_1 x-ray structure (Abrahams et al. 1994) was visible in early EM images (Gogol et al. 1987) connecting F_1 and F_o. However, the complete architecture of the complex and especially the membrane-bound F_o part and its connection to F_1 was still not clear. Biochemical evidence implicated unassigned subunits in a second stalk as part of a stator to counteract rotation of the head (Collinson et al. 1996; Ogilvie et al. 1997), which was confirmed by cryo-EM (Wilkens and Capaldi 1998). Such a feature was also seen in bacterial V-type ATPase (Boekema et al. 1997), which later turned out to have two peripheral stalks (Boekema et al. 1999; Bernal and Stock 2004; Vonck et al. 2009; Lau and Rubinstein 2010, 2012). In bacteria, the peripheral stalk is made up of the δ subunit, the equivalent of OSCP in mitochondria, on top of the head, and two *b* subunits, either two copies of the same protein or one each of homologous *b* and *b*'

proteins. The *b* subunits are predicted to be mainly α-helical with an N-terminal transmembrane domain, and the two subunits are thought to form a dimer. The N-terminal TMH of *b* from *E. coli* was solved by NMR (Dmitriev et al. 1999).

While the bacterial structure is conserved in chloroplast ATP synthase, the mitochondrial complex has a more elaborate peripheral stalk, consisting in the mammalian enzyme of the soluble OSCP, *b*, *d* and F_6 subunits and membrane subunits A6L and *f*. The yeast protein has a similar composition (Table 7.2). Crystal structures of subcomplexes of the soluble part of the bovine ATP synthase (Kane Dickson et al. 2006; Rees et al. 2009) showed that the mitochondrial peripheral stalk is mainly α-helical. Cryo-EM structures of the complete bovine (Rubinstein et al. 2003; Baker et al. 2012) and yeast (Lau et al. 2008) ATP synthase indicated a distinct curvature of the stalk, different from the crystal structure, apparently caused by its anchoring in the membrane domain (Baker et al. 2012). The stator seems to have an essential role not only in keeping the F_1 head stationary during rotation of the rotor but also in positioning the *a* subunit correctly relative to the *c*-ring. The cryo-EM structure of the dimer from the yeast *Yarrowia lipolytica* showed the architecture of the complete stator (Fig. 7.12). Behind the horizontal helix bundle of the *a* subunit run six TMH, which were interpreted as belonging to subunit *i*, *f, 8, a,* and the first and second TMH of *b* (Hahn et al. 2016). Subunit *8* appears to be the equivalent of the second bacterial *b* subunit, although the matrix C-terminal part of subunit *8* is truncated to different extents in the mitochondrial enzyme (Hahn et al. 2016). The *f* subunit and the first TMH of *b* are specific for mitochondria and do not occur in bacteria. The *f* subunit has an extension in the IMS and seems to make the main dimer contact (Hahn et al. 2016).

7.7.2 ATP Synthase Dimerization and Crista Morphology

Submitochondrial particles of 70–80 Å diameter were recognized in early electron microscopic images in regular patterns on the cristae and correctly shown to be facing the matrix (Parsons 1963; Stoeckenius 1963). These features were initially named “elementary particles” and assumed to contain the complete respiratory chain (Fernández-Morán 1962), but later shown to be the F_1 ATPase (Kagawa and Racker 1966). First indications for a higher-order structure of the ATP synthase came from rapid-freeze deep-etch techniques on the cristae of *Paramecium* (Allen et al. 1989), where double rows of F_1 in a helical array around the tubular cristae were found. The occurrence of double rather than single rows suggested that the building blocks are dimers of ATP synthase. Dimers of ATP synthases were later found on Blue-Native-PA gels after solubilization of mitochondrial membranes with mild detergents, in all phyla: yeasts (Arnold et al. 1998a), fungi (Krause et al.

2004b), mammals (Schägger and Pfeiffer 2000; Krause et al. 2005; Cortes-Hernandez et al. 2007; Dencher et al. 2007), and higher plants (Eubel et al. 2003; Krause et al. 2004a). The corresponding bands were eluted from the gels and examined by EM, providing direct evidence for ATP synthase dimers in many species (Minauro-Sanmiguel et al. 2005; Dudkina et al. 2005b; Dudkina et al. 2006; Thomas et al. 2008; Cano-Estrada et al. 2010). The dimers were associated via their membrane domains, which included angles of 40–90°, strongly suggesting that the dimers were responsible for bending the IMM and dictating cristae morphology (Dudkina et al. 2005b; Minauro-Sanmiguel et al. 2005; Dudkina et al. 2006). Direct evidence for this came from cryo-electron tomography of submitochondrial particles of several species (Strauss et al. 2008; Dudkina et al. 2010; Davies et al. 2011; Davies et al. 2012), where dimer rows of ATP synthase were seen on all highly curved crista edges.

7.7.3 Dimer-Specific Subunits of ATP Synthase

The small membrane-associated proteins *e, g* and *k* were identified as dimer-specific subunits in yeast (Arnold et al. 1998a). These mitochondrial subunits are not necessary for ATPase or ATP synthase activity, but deletion of the genes for *e* or *g* resulted in mitochondria that lacked ATP synthase dimers and had abnormal morphology with the inner membranes forming onion-like multilayered structures (Paumard et al. 2002; Giraud et al. 2002). The location of the *e* and *g* subunits in the ATP synthase complex was determined by comparing low resolution EM maps of yeast core ATP synthase and bovine ATP synthase with *e* and *g* attached (Lau et al. 2008; Baker et al. 2012) and is at the periphery of the F_o domain.

The cryo-EM maps of mammalian (Zhou et al. 2015) and yeast (Hahn et al. 2016) ATP synthase both show a similar feature in this region: a funnel-shaped density in the membrane with a helix-like protrusion in the IMS. Subunit *e* is predicted to have an N-terminal TMH containing an essential GxxxG motif, suggesting a role in helix-helix interaction (Arselin et al. 2003), and a hydrophilic C-terminus located in the IMS, that would account for the observed helix protrusion (Fig. 7.17). Subunit *g* has an N-terminal matrix domain and a predicted C-terminal TMH also containing a conserved GxxxG motif. GxxxG motifs are often found to be important for mediating the interaction of TMH (Senes et al. 2004). Subunits *e* and *g* may thus form a tight heterodimer in the membrane. The helices in such a tight dimer would not be resolved at a resolution lower than ~6 Å, and may be forming the funnel-shaped density in the cryo-EM maps. The density is located near the *b* subunit, in support of the observation that the *g*-subunit can be crosslinked to the N-terminus of *b* in the matrix and that deleting the first TMH of *b* results in the loss of *g* and dissociation of the dimer (Soubannier et al. 2002).

The cryo-EM map of the *Yarrowia* ATP synthase dimer (Hahn et al. 2016) surprisingly showed that the *e* and *g* subunits are located at the outside of the F_o dimer, not as expected in the center where they would mediate dimer formation (Vonck and Schäfer 2009). Interestingly, the bovine ATP synthase monomer including *e* and *g*

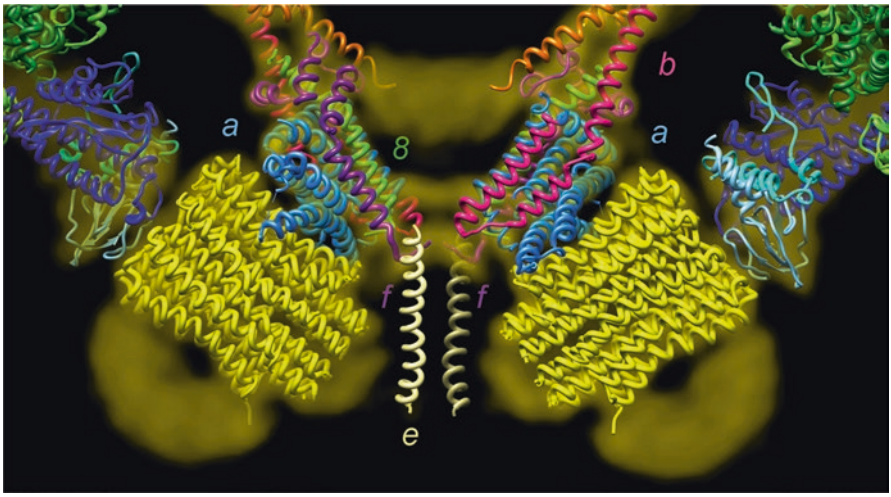

Fig. 7.17 The dimer interface of the *Y. lipolytica* ATP synthase model with a slab of the cryo-EM map superimposed (Hahn et al. 2016). The dimer contact is on the IMS side only. The khaki helix extending in the IMS is probably the C-terminus of subunit *e.* Detergent is visible on the matrix side of the dimer interface and around the *c*-rings

has a bent detergent belt, suggesting that the role of the *eg* heterodimer is in bending the membrane (Baker et al. 2012). A monomer of the *Yarrowia* enzyme, lacking these subunits, has a straight detergent belt (Hahn et al. 2016) (Fig. 7.18), confirming this role. The sequence of both the *e* and *g* subunit contains several conserved charged or polar residues around the GxxxG motif in the putative TMH, which might be involved in specific interactions with the membrane components. The bending of the membrane probably orients the monomers in such a way that the dimerization subunits can establish dimer contacts (Fig. 7.17).

7.7.4 Assembly of ATP Synthase

Although bacterial ATP synthases have been expressed cell-free (Matthies et al. 2011) or heterologously (Zhang et al. 2014) and were fully assembled and active, mitochondrial ATP synthase assembly is highly regulated and depends on specific chaperones. The assembly of $\alpha_3\beta_3$ requires Atp11p and Atp12p, which bind specifically to β and α, respectively and prevent aggregate formation (Ludlam et al. 2009). Although most subunits are encoded in the nucleus, in most species the F_o subunits *a, c* and subunit 8 are mitochondrially encoded. In yeast, at least three proteins are required for F_o assembly, Atp10p, Atp23p and Atp25p. The first two are involved in incorporation of the *a* subunit into the complex (Tzagoloff et al. 2004; Osman et al. 2007; Zeng et al. 2007). Atp23p cleaves the N-terminal presequence (10 residues in *S. cerevisiae*, Fig. 7.15); however, there is an Atp23p homolog in human

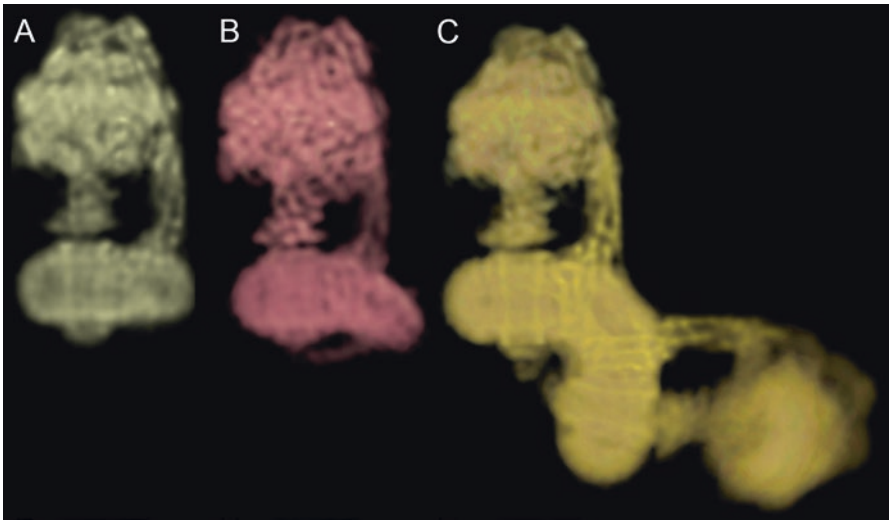

Fig. 7.18 Subunit *e* and *g* bend the IMM. (**a**): Monomeric ATP synthase of *Y. lipolytica*, where subunit *e* and *g* were lost during purification The detergent belt forms a straight ring around F_o (Hahn et al. 2016). (**b**): Monomeric bovine ATP synthase (EMD-3165) (Zhou et al. 2015). Subunits *e* and *g* were retained during purification. The detergent belt is bent. (**c**): Dimeric ATP synthase of *Y. lipolytica* has a bent detergent belt. Subunits *e* and *g* were retained during purification in the mild detergent digitonin (Hahn et al. 2016)

mitochondria, where the *a* subunit does not have an extension (Osman et al. 2007; Zeng et al. 2007); the additional function of Atp23p is unknown. Atp25p is thought to be required for the assembly of the rotor ring (Zeng et al. 2008). Assembly of ATP synthase appears to be modular, with one subcomplex consisting of F_1 with the *c*-ring and another the mitochondrial encoded *a* subunit and subunit 8, transiently interacting with Atp10p, together with at least some peripheral stalk subunits (Rak et al. 2011). Recently a complex was identified, consisting of the IMM subunits Ina17 and Ina22, that plays a role in peripheral stalk assembly (Lytovchenko et al. 2014), and thus the coupling of the two motors and completion of the complex.

7.7.5 Evolution of Rotary ATPases

ATP synthase is an ancient machine that was already present in the last universal common ancestor (LUCA) (Weiss et al. 2016). The bacterial and archaeal versions share the basic architecture, and homology of the catalytic head and of the ion-translocating subunits is still easily recognizable. Both the bacterial and archaeal ATP synthase are still functional in eukaryotes. The bacterial version is found in both energy producing organelles, the chloroplast and mitochondrion, while the archaeal enzyme yielded the vacuolar (V-type) ATPase, an ATP-driven proton pump involved in vacuolar pH homeostasis. Whereas the chloroplast enzyme is similar to

the bacterial ancestor, the V-type ATPase and the mitochondrial enzyme have gained new subunits, most with a regulatory function, but in the case of the mitochondrial enzyme also a structural role in affecting membrane morphology. While the functional units of the ATP synthase, namely the $\alpha_3\beta_3$ head, the γ subunit, the *c*-ring and the *a* subunit have remained remarkably similar, the differences between bacterial and mitochondrial ATP synthase involve the peripheral stalk, in a way that does not affect the ATP synthase function of the complex. Whereas in the bacterial enzyme the peripheral stalk consists of only the δ subunit and two copies of *b*, the mammalian and fungal lineage have added several other subunits to the soluble part of the stalk as well as the membrane domain. While the advantage of the more robust soluble part is not yet clear, it is interesting to note that the accessory membrane subunits, *f*, *e,* and *g,* are involved in membrane bending and dimer formation, leading to the folding of the IMM into cristae. The resulting huge gain in IMM surface area is responsible for the large respiratory capacity of the mitochondria and thus an adequate ATP supply to meet the high energy demands of eukaryotic cells. So gain of a new role by ATP synthase appears to have had a huge impact on eukaryotic evolution. Many questions remain about ATP synthase dimerization however. In green algae such as *Chlamydomonas* and *Polytomella* the whole peripheral stalk has been replaced by unrelated proteins, forming a very stable dimer (Allegretti et al. 2015) with a different dimer angle than that in mammals and fungi. So far the structure of the 9 ASA (ATP synthase associated) subunits and a possible relation to the mammalian dimerization subunits is not known.

7.8 Concluding Remarks

The mitochondrial respiratory chain has a central role in energy metabolism and decades of work have been devoted to elucidating its structure and function. Crystallization of these large membrane protein complexes has been a major challenge and the elucidation of many structures by x-ray crystallography since the 1980s have brought huge breakthroughs. The recent revolution in cryo-EM has greatly advanced our knowledge of the mitochondrial respiratory chain for all still incompletely understood complexes, from complex I (Vinothkumar et al. 2014; Zhu et al. 2016; Fiedorczuk et al. 2016; D'Imprima et al. 2016) to the respirasome (Letts et al. 2016; Gu et al. 2016; Sousa et al. 2016) to ATP synthase (Allegretti et al. 2015; Zhou et al. 2015; Hahn et al. 2016). However, many questions remain regarding not only the detailed structure, but especially the mechanism of the complexes. The mode of action of complex I and coupling of ubiquinone reduction to proton translocation, the function of the respirasome, and the atomic structure of F_o and the proton path through the *a* subunit are still not understood. It is to be expected that further progress in cryo-EM instrumentation and image processing techniques will lead to better structures of the mitochondrial respiratory chain complexes in different conformational states and a full understanding of the function of this amazing machinery.

References

Abdrakhmanova A, Dobrynin K, Zwicker K, Kerscher S, Brandt U (2005) Functional sulfurtransferase is associated with mitochondrial complex I from *Yarrowia lipolytica*, but is not required for assembly of its iron–sulfur clusters. FEBS Lett 579(30):6781–6785. https://doi.org/10.1016/j.febslet.2005.11.008

Abdrakhmanova A, Zwicker K, Kerscher S, Zickermann V, Brandt U (2006) Tight binding of NADPH to the 39-kDa subunit of complex I is not required for catalytic activity but stabilizes the multiprotein complex. Biochim Biophys Acta 1757:1676–1682. https://doi.org/10.1016/j.bbabio.2006.09.003

Abrahams JP, Leslie AG, Lutter R, Walker JE (1994) Structure at 2.8 Å resolution of F_1 ATPase from bovine heart mitochondria. Nature 370:621–628

Acin-Pérez R, Bayona-Bafaluy MP, Fernández-Silva P, Moreno-Loshuertos R, Pérez-Martos A, Bruno C, Moraes CT, Enríquez JA (2004) Respiratory complex III is required to maintain complex I in mammalian mitochondria. Mol Cell 13:805–815

Acin-Pérez R, Fernández-Silva P, Peleato ML, Pérez-Martos A, Enriquez JA (2008) Respiratory active mitochondrial supercomplexes. Mol Cell 32:529–539

Allegretti M, Klusch N, Mills DJ, Vonck J, Davies KM, Kühlbrandt W (2015) Horizontal membrane-intrinsic α-helices in the stator *a*-subunit of an F-type ATP synthase. Nature 521:237–240

Allen RD, Schroeder CC, Fok AK (1989) An investigation of mitochondrial inner membranes by rapid-freeze deep-etch techniques. J Cell Biol 108(6):2233–2240

Alnajjar KS, Hosler J, Prochaska L (2014) Role of the N-terminus of subunit III in proton uptake in cytochrome *c* oxidase of *Rhodobacter sphaeroides*. Biochemistry 53(3):496–504. https://doi.org/10.1021/bi401535q

Althoff T, Mills DJ, Popot J-L, Kühlbrandt W (2011) Assembly of electron transport chain components in bovine mitochondrial supercomplex $I_1III_2IV_1$. EMBO J 30:4662–4664

Ambrosio G, Zweier JL, Duilio C, Kuppusamy P, Santoro G, Elia PP, Tritto I, Cirillo P, Condorelli M, Chiariello M et al (1993) Evidence that mitochondrial respiration is a source of potentially toxic oxygen free radicals in intact rabbit hearts subjected to ischemia and reflow. J Biol Chem 268(25):18532–18541

Andrews B, Carroll J, Ding S, Fearnley IM, Walker JE (2013) Assembly factors for the membrane arm of human complex I. Proc Natl Acad Sci U S A 110(47):18934–18939. https://doi.org/10.1073/pnas.1319247110

Angerer H (2015) Eukaryotic LYR proteins interact with mitochondrial protein complexes. Biology (Basel) 4(1):133–150. https://doi.org/10.3390/biology4010133

Angevine CA, Fillingame RH (2003) Aqueous access channels in subunit *a* of rotary ATP synthase. J Biol Chem 278:6066–6074. https://doi.org/10.1074/jbc.M210199200

Anthony G, Reimann A, Kadenbach B (1993) Tissue-specific regulation of bovine heart cytochrome *c* oxidase activity by ADP via interaction with subunit VIa. Proc Natl Acad Sci U S A 90(5):1652–1656. https://doi.org/10.1073/pnas.90.5.1652

Arnold S, Kadenbach B (1997) Cell respiration is controlled by ATP, an allosteric inhibitor of cytochrome-c oxidase. Eur J Biochem 249:350–354

Arnold I, Pfeiffer K, Neupert W, Stuart RA, Schägger H (1998a) Yeast mitochondrial F_1F_0-ATP synthase exists as a dimer: identification of three dimer-specific subunits. EMBO J 17(24):7170–7178

Arnold S, Goglia F, Kadenbach B (1998b) 3,5-diiodothyronine binds to subunit Va of cytochrome-c oxidase and abolishes the allosteric inhibition of respiration by ATP. Eur J Biochem 252(2):325–330. https://doi.org/10.1046/j.1432-1327.1998.2520325.x

Arselin G, Giraud M-F, Dautant A, Vaillier J, Brethes D, Coulary-Salin B, Schaeffer J, Velours J (2003) The GxxxG motif of the transmembrane domain of subunit e is involved in the dimerization/oligomerization of the yeast ATP synthase complex in the mitochondrial membrane. Eur J Biochem 270:1875–1884

Babot M, Birch A, Labarbuta P, Galkin A (2014) Characterisation of the active/de-active transition of mitochondrial complex I. Biochim Biophys Acta 1837(7):1083–1092. https://doi.org/10.1016/j.bbabio.2014.02.018

Baker LA, Watt IN, Runswick MJ, Walker JE, Rubinstein JL (2012) Arrangement of subunits in intact mammalian mitochondrial ATP synthase determined by cryo-EM. Proc Natl Acad Sci U S A 00:1–2

Balsa E, Marco R, Perales-Clemente E, Szklarczyk R, Calvo E, Landázuri MO, Enríquez JA (2012) NDUFA4 is a subunit of complex IV of the mammalian electron transport chain. Cell Metab 16(3):378–386. https://doi.org/10.1016/j.cmet.2012.07.015

Banci L, Bertini I, Cefaro C, Ciofi-Baffoni S, Gallo A, Martinelli M, Sideris DP, Katrakili N, Tokatlidis K (2009) MIA40 is an oxidoreductase that catalyzes oxidative protein folding in mitochondria. Nat Struct Mol Biol 16(2):198–206. https://doi.org/10.1038/nsmb.1553

Baradaran R, Berrisford JM, Minhas GS, Sazanov LA (2013) Crystal structure of the entire respiratory complex I. Nature 494(7438):443–448. https://doi.org/10.1038/nature11871

Barquera B (2014) The sodium pumping NADH:quinone oxidoreductase (Na^+-NQR), a unique redox-driven ion pump. J Bioenerg Biomembr 46(4):289–298. https://doi.org/10.1007/s10863-014-9565-9

Belevich I, Verkhovsky MI, Wikström M (2006) Proton-coupled electron transfer drives the proton pump of cytochrome c oxidase. Nature 440(7085):829–832. https://doi.org/10.1038/nature04619

Belevich G, Knuuti J, Verkhovsky MI, Wikström M, Verkhovskaya M (2011) Probing the mechanistic role of the long α-helix in subunit L of respiratory complex I from Escherichia coli by site-directed mutagenesis. Mol Microbiol 82(5):1086–1095. https://doi.org/10.1111/j.1365-2958.2011.07883.x

Bernal RA, Stock D (2004) Three-dimensional structure of the intact *Thermus thermophilus* H^+-ATPase/synthase by electron microscopy. Structure 12:1789–1798

Berrisford JM, Sazanov LA (2009) Structural basis for the mechanism of respiratory complex I. J Biol Chem 284(43):29773–29783. https://doi.org/10.1074/jbc.M109.032144

Berry EA, De Bari H, Huang L-S (2013) Unanswered questions about the structure of cytochrome bc1 complexes. Biochim Biophys Acta Bioenerg 1827(11):1258–1277

Bianchi C, Genova ML, Parenti Castelli G, Lenaz G (2004) The mitochondrial respiratory chain is partially organized in a supercomplex assembly: kinetic evidence using flux control analysis. J Biol Chem 279(35):36562–36569

Bleier L, Drose S (2013) Superoxide generation by complex III: from mechanistic rationales to functional consequences. BBA-Bioenergetics 1827(11–12):1320–1331. https://doi.org/10.1016/j.bbabio.2012.12.002

Boekema EJ, Ubbink-Kok T, Lolkema JS, Brisson A, Konings WN (1997) Visualization of a peripheral stalk in V-type ATPase: evidence for the stator structure essential to rotational catalysis. Proc Natl Acad Sci U S A 94:14291–14293

Boekema EJ, van Breemen JFL, Brisson A, Ubbink-Kok T, Konings WN, Lolkema JS (1999) Connecting stalks in V-type ATPase. Nature 401:37–38

Bonne G, Seibel P, Possekel S, Marsac C, Kadenbach B (1993) Expression of human cytochrome-c-oxidase subunits during fetal development. Eur J Biochem 217(3):1099–1107. https://doi.org/10.1111/j.1432-1033.1993.tb18342.x

Bordo D, Bork P (2002) The rhodanese/Cdc25 phosphatase superfamily. Sequence-structure-function relations. EMBO Rep 3(8):741–746. https://doi.org/10.1093/embo-reports/kvf150

Bottinger L, Horvath SE, Kleinschroth T, Hunte C, Daum G, Pfanner N, Becker T (2012) Phosphatidylethanolamine and cardiolipin differentially affect the stability of mitochondrial respiratory chain supercomplexes. J Mol Biol 423(5):677–686. https://doi.org/10.1016/j.jmb.2012.09.001

Boyer PD (1993) The binding change mechanism for ATP synthase – some probabilities and possibilities. Biochim Biophys Acta 1140:215–250

Boyer PD (1997) The ATP synthase: a splendid molecular machine. Annu Rev Biochem 66:717–749

Brandt U (2006) Energy converting NADH:quinone oxidoreductase (complex I). Annu Rev Biochem 75:69–92. https://doi.org/10.1146/annurev.biochem.75.103004.142539

Brockmann C, Diehl A, Rehbein K, Strauss H, Schmieder P, Korn B, Kühne R, Oschkinat H (2004) The oxidized subunit B8 from human complex I adopts a thioredoxin fold. Structure 12(9):1645–1654. https://doi.org/10.1016/j.str.2004.06.021

Bruno C, Santorelli FM, Assereto S, Tonoli E, Tessa A, Traverso M, Scapolan S, Bado M, Tedeschi S, Minetti C (2003) Progressive exercise intolerance associated with a new muscle-restricted nonsense mutation (G142X) in the mitochondrial cytochrome b gene. Muscle Nerve 28(4):508–511. https://doi.org/10.1002/mus.10429

Brzezinski P, Adelroth P (1998) Pathways of proton transfer in cytochrome c oxidase. J Bioenerg Biomembr 30(1):99–107. https://doi.org/10.1023/A:1020567729941

Bych K, Kerscher S, Netz DJ, Pierik AJ, Zwicker K, Huynen MA, Lill R, Brandt U, Balk J (2008) The iron-sulphur protein Ind1 is required for effective complex I assembly. EMBO J 27(12):1736–1746. https://doi.org/10.1038/emboj.2008.98

Cain BD, Simoni RD (1986) Impaired proton conductivity resulting from mutations in the *a* subunit of F_1F_o ATPase in *Escherichia coli*. J Biol Chem 261:10043–10050

Cain BD, Simoni RD (1988) Interaction between Glu-219 and His-245 within the *a* subunit of F_1F_o ATPase in *Escherichia coli*. J Biol Chem 263:6602–6612

Cano-Estrada A, Vázquez-Acevedo M, Villavicencio-Queijeiro A, Figueroa-Martínez F, Miranda-Astudillo H, Cordeiro Y, Mignaco JA, Foguel D, Cardol P, Lapaille M, Remacle C, Wilkens S, González-Halphen D (2010) Subunit–subunit interactions and overall topology of the dimeric mitochondrial ATP synthase of Polytomella sp. Biochim Biophys Acta 1797(8):1439–1448. https://doi.org/10.1016/j.bbabio.2010.02.024

Carilla-Latorre S, Gallardo ME, Annesley SJ, Calvo-Garrido J, Grana O, Accari SL, Smith PK, Valencia A, Garesse R, Fisher PR, Escalante R (2010) MidA is a putative methyltransferase that is required for mitochondrial complex I function. J Cell Sci 123(Pt 10):1674–1683. https://doi.org/10.1242/jcs.066076

Carroll J, Fearnley IM, Shannon RJ, Hirst J, Walker JE (2003) Analysis of the subunit composition of complex I from bovine heart mitochondria. Mol Cell Proteomics 2(2):117–126. https://doi.org/10.1074/mcp.M300014-MCP200

Carroll J, Fearnley IM, Skehel JM, Shannon RJ, Hirst J, Walker JE (2006) Bovine complex I is a complex of 45 different subunits. J Biol Chem 281:32724–32727

Castellani M, Covian R, Kleinschroth T, Anderka O, Ludwig B, Trumpower BL (2010) Direct demonstration of half-of-the-sites reactivity in the dimeric cytochrome bc1 complex: enzyme with one inactive monomer is fully active but unable to activate the second ubiquinol oxidation site in response to ligand binding at the ubiquinone reduction site. J Biol Chem 285(1):502–510. https://doi.org/10.1074/jbc.M109.072959

Chan DI, Vogel HJ (2010) Current understanding of fatty acid biosynthesis and the acyl carrier protein. Biochem J 430(1):1–19. https://doi.org/10.1042/BJ20100462

Chance B, Williams GR (1955) A method for the localization of sites for oxidative phosphorylation. Nature 176:250–254

Chandel NS (2010) Mitochondrial regulation of oxygen sensing. Adv Exp Med Biol 661:339–354. https://doi.org/10.1007/978-1-60761-500-2_22

Chen YC, Taylor EB, Dephoure N, Heo JM, Tonhato A, Papandreou I, Nath N, Denko NC, Gygi SP, Rutter J (2012) Identification of a protein mediating respiratory supercomplex stability. Cell Metab 15(3):348–360. https://doi.org/10.1016/j.cmet.2012.02.006

Chouchani ET, Methner C, Nadtochiy SM, Logan A, Pell VR, Ding S, James AM, Cocheme HM, Reinhold J, Lilley KS, Partridge L, Fearnley IM, Robinson AJ, Hartley RC, Smith RA, Krieg T, Brookes PS, Murphy MP (2013) Cardioprotection by S-nitrosation of a cysteine switch on mitochondrial complex I. Nat Med 19(6):753–759. https://doi.org/10.1038/nm.3212

Chouchani ET, Pell VR, Gaude E, Aksentijevic D, Sundier SY, Robb EL, Logan A, Nadtochiy SM, Ord EN, Smith AC, Eyassu F, Shirley R, CH H, Dare AJ, James AM, Rogatti S, Hartley RC, Eaton S, Costa AS, Brookes PS, Davidson SM, Duchen MR, Saeb-Parsy K, Shattock MJ,

Robinson AJ, Work LM, Frezza C, Krieg T, Murphy MP (2014) Ischaemic accumulation of succinate controls reperfusion injury through mitochondrial ROS. Nature 515(7527):431–435. https://doi.org/10.1038/nature13909

Clason T, Ruiz T, Schägger H, Peng G, Zickermann V, Brandt U, Michel H, Radermacher M (2010) The structure of eukaryotic and prokaryotic complex I. J Struct Biol 169(1):81–88

Cogliati S, Frezza C, Soriano ME, Varanita T, Quintana-Cabrera R, Corrado M, Cipolat S, Costa V, Casarin A, Gomes LC, Perales-Clemente E, Salviati L, Fernandez-Silva P, Enriquez JA, Scorrano L (2013) Mitochondrial cristae shape determines respiratory chain supercomplexes assembly and respiratory efficiency. Cell 155(1):160–171. https://doi.org/10.1016/j.cell.2013.08.032

Cogliati S, Calvo E, Loureiro M, Guaras AM, Nieto-Arellano R, Garcia-Poyatos C, Ezkurdia I, Mercader N, Vázquez J, Enriquez JA (2016) Mechanism of super-assembly of respiratory complexes III and IV. Nature 539(7630):579–582

Collinson IR, Skehel JM, Fearnley IM, Runswick MJ, Walker JE (1996) The F_1F_o-ATPase complex from bovine heart mitochondria: the molar ratio of the subunits in the stalk region linking the F_1 and F_o domains. Biochemistry 34:12640–12646

Conte A, Papa B, Ferramosca A, Zara V (2015) The dimerization of the yeast cytochrome bc(1) complex is an early event and is independent of Rip1. Biochim Biophys Acta 1853(5):987–995. https://doi.org/10.1016/j.bbamcr.2015.02.006

Cortes-Hernandez P, Vázquez-Memije ME, Garcia JJ (2007) *ATP6* homoplasmic mutations inhibit and destabilize the human F_1F_0-ATP synthase without preventing enzyme assembly and oligomerization. J Biol Chem 282:1051–1058

Covian R, Trumpower BL (2006) Regulatory interactions between ubiquinol oxidation and ubiquinone reduction sites in the dimeric cytochrome bc(1) complex. J Biol Chem 281(41):30925–30932. https://doi.org/10.1074/jbc.M604694200

D'Aurelio M, Gajewski CD, Lenaz G, Manfredi G (2006) Respiratory chain supercomplexes set the threshold for respiration defects in human mtDNA mutant cybrids. Hum Mol Genet 15(13):2157–2169. https://doi.org/10.1093/hmg/ddl141

D'Imprima E, Mills DJ, Parey K, Brandt U, Kühlbrandt W, Zickermann V, Vonck J (2016) Cryo-EM structure of respiratory complex I reveals a link to mitochondrial sulfur metabolism. Biochim Biophys Acta 1857:1935–1942

Darrouzet E, Valkova-Valchanova M, Moser CC, Dutton PL, Daldal F (2000) Uncovering the [2Fe2S] domain movement in cytochrome bc1 and its implications for energy conversion. Proc Natl Acad Sci U S A 97(9):4567–4572

Davies KM, Strauss M, Daum B, Kief JH, Osiewacz HD, Rycovska A, Zickermann V, Kühlbrandt W (2011) Macromolecular organization of ATP synthase and complex I in whole mitochondria. Proc Natl Acad Sci U S A 108:14121–14126

Davies KM, Anselmi C, Wittig I, Faraldo-Gómez JD, Kühlbrandt W (2012) Structure of the yeast F_1F_o-ATP synthase dimer and its role in shaping the mitochondrial cristae. Proc Natl Acad Sci U S A 109(34):13602–13607

Dencher NA, Frenzel M, Reifschneider NH, Sugawa M, Krause F (2007) Proteome alterations in rat mitochondria caused by aging. Ann N Y Acad Sci 1100:291–298

Deng K, Zhang L, Kachurin AM, Yu L, Xia D, Kim H, Deisenhofer J, Yu C-A (1998) Activation of a matrix processing peptidase from the crystalline cytochrome bc complex of bovine heart mitochondria. J Biol Chem 273(33):20752–20757

Deng K, Shenoy SK, Tso S-C, Yu L, Yu C-A (2001) Reconstitution of mitochondrial processing peptidase from the core proteins (subunits I and II) of bovine heart mitochondrial cytochrome bc complex. J Biol Chem 276(9):6499–6505

Diaz F, Fukui H, Garcia S, Moraes CT (2006) Cytochrome *c* oxidase is required for the assembly/stability of respiratory complex I in mouse fibroblasts. Mol Cell Biol 26:4872–4881

Dmitriev O, Jones PC, Jiang W, Fillingame RH (1999) Structure of the membrane domain of subunit *b* of the *Escherichia coli* F_0F_1 ATP synthase. J Biol Chem 274(22):15598–15604

Dmitriev OY, Altendorf K, Fillingame RH (2004) Subunit a of the E. coli ATP synthase: reconstitution and high resolution NMR with protein purified in a mixed polarity solvent. FEBS Lett 556:35–38

Dobrynin K, Abdrakhmanova A, Richers S, Hunte C, Kerscher S, Brandt U (2010) Characterization of two different acyl carrier proteins in complex I from *Yarrowia lipolytica*. Biochim Biophys Acta 1797(2):152–159. https://doi.org/10.1016/j.bbabio.2009.09.007

Drose S, Brandt U (2008) The mechanism of mitochondrial superoxide production by the cytochrome bc complex. J Biol Chem 283(31):21649–21654. https://doi.org/10.1074/jbc.M803236200

Drose S, Krack S, Sokolova L, Zwicker K, Barth HD, Morgner N, Heide H, Steger M, Nubel E, Zickermann V, Kerscher S, Brutschy B, Radermacher M, Brandt U (2011) Functional dissection of the proton pumping modules of mitochondrial complex I. PLoS Biol 9(8):e1001128. https://doi.org/10.1371/journal.pbio.1001128

Drose S, Brandt U, Wittig I (2014) Mitochondrial respiratory chain complexes as sources and targets of thiol-based redox-regulation. Biochim Biophys Acta 1844(8):1344–1354. https://doi.org/10.1016/j.bbapap.2014.02.006

Drose S, Stepanova A, Galkin A (2016) Ischemic A/D transition of mitochondrial complex I and its role in ROS generation. Biochim Biophys Acta 1857(7):946–957. https://doi.org/10.1016/j.bbabio.2015.12.013

Dudkina NV, Eubel H, Keegstra W, Boekema EJ, Braun HP (2005a) Structure of a mitochondrial supercomplex formed by respiratory-chain complexes I and III. Proc Natl Acad Sci U S A 102:3225–3229

Dudkina NV, Heinemeyer J, Keegstra W, Boekema EJ, Braun HP (2005b) Structure of dimeric ATP synthase from mitochondria: an angular association of monomers induces the strong curvature of the inner membrane. FEBS Lett 579(25):5769–5772

Dudkina NV, Sunderhaus S, Braun HP, Boekema EJ (2006) Characterization of dimeric ATP synthase and cristae membrane ultrastructure from *Saccharomyces* and *Polytomella* mitochondria. FEBS Lett 580(14):3427–3432

Dudkina NV, Oostergetel GT, Lewejohann D, Braun H-P, Boekema EJ (2010) Row-like organization of ATP synthase in intact mitochondria determined by cryo-electron tomography. Biochim Biophys Acta 1797(2):272–277

Dudkina NV, Kudryashev M, Stahlberg H, Boekema EJ (2011) Interaction of complexes I, III, and IV within the bovine respirasome by single particle cryoelectron tomography. Proc Natl Acad Sci U S A 108(37):15196–15200

Dutton PL, Moser CC, Sled VD, Daldal F, Ohnishi T (1998) A reductant-induced oxidation mechanism for complex I. Biochim Biophys Acta 1364(2):245–257

Efremov RG, Sazanov LA (2011) Structure of the membrane domain of respiratory complex I. Nature 476(7361):414–420. https://doi.org/10.1038/nature10330

Efremov RG, Baradaran R, Sazanov LA (2010) The architecture of respiratory complex I. Nature 465:441–447

Elurbe DM, Huynen MA (2016) The origin of the supernumerary subunits and assembly factors of complex I: a treasure trove of pathway evolution. Biochim Biophys Acta 1857(7):971–979. https://doi.org/10.1016/j.bbabio.2016.03.027

Esterhazy D, King MS, Yakovlev G, Hirst J (2008) Production of reactive oxygen species by complex I (NADH:ubiquinone oxidoreductase) from *Escherichia coli* and comparison to the enzyme from mitochondria. Biochemistry 47(12):3964–3971. https://doi.org/10.1021/bi702243b

Eubel H, Jänsch L, Braun HP (2003) New insights into the respiratory chain of plant mitochondria. Supercomplexes and a unique composition of complex II. Plant Physiol 133:274–286

Euro L, Bloch DA, Wikström M, Verkhovsky MI, Verkhovskaya M (2008) Electrostatic interactions between FeS clusters in NADH:ubiquinone oxidoreductase (complex I) from Escherichia coli. Biochemistry 47(10):3185–3193. https://doi.org/10.1021/bi702063t

Ewart GD, Zhang YZ, Capaldi RA (1991) Switching of bovine cytochrome-c-oxidase subunit VIa isoforms in skeletal-muscle during development. FEBS Lett 292(1–2):79–84. https://doi.org/10.1016/0014-5793(91)80839-U

Fearnley IM, Walker JE (1992) Conservation of sequences of subunits of mitochondrial complex I and their relationships with other proteins. Biochim Biophys Acta 1140(2):105–134

Fernández-Morán H (1962) Low-temperature electron microscopy and X-ray diffraction studies of lipoprotein components in lamellar systems. Circulation 26:1039–1065

Fiedorczuk K, Letts JA, Degliesposti G, Kaszuba K, Skehel M, Sazanov LA (2016) Atomic structure of the entire mammalian mitochondrial complex I. Nature 538:406–410. https://doi.org/10.1038/nature19794

Fillingame RH, Steed PR (2014) Half channels mediating H^+ transport and the mechanism of gating in the F_o sector of *Escherichia coli* F_1F_o ATP synthase. Biochim Biophys Acta 1837:1063–1068

Friedrich T (2001) Complex I: a chimaera of a redox and conformation-driven proton pump? J Bioenerg Biomembr 33(3):169–177

Friedrich T, Scheide D (2000) The respiratory complex I of bacteria, archaea and eukarya and its module common with membrane-bound multisubunit hydrogenases. FEBS Lett 479(1–2):1–5

Fritz M, Klyszejko AL, Morgner N, Vonck J, Brutschy B, Muller DJ, Meier T, Müller V (2008) An intermediate step in the evolution of ATPases – a hybrid F_o-V_o rotor in a bacterial Na^+ F_1F_o ATP synthase. FEBS J 275(9):1999–2007

Gabaldon T, Rainey D, Huynen MA (2005) Tracing the evolution of a large protein complex in the eukaryotes, NADH:ubiquinone oxidoreductase (Complex I). J Mol Biol 348(4):857–870. https://doi.org/10.1016/j.jmb.2005.02.067

Galati D, Srinivasan S, Raza H, Prabu SK, Hardy M, Chandran K, Lopez M, Kalyanaraman B, Avadhani NG (2009) Role of nuclear-encoded subunit Vb in the assembly and stability of cytochrome c oxidase complex: implications in mitochondrial dysfunction and ROS production. Biochem J 420:439–449. https://doi.org/10.1042/Bj20090214

Galkin A, Moncada S (2007) S-nitrosation of mitochondrial complex I depends on its structural conformation. J Biol Chem 282(52):37448–37453. https://doi.org/10.1074/jbc.M707543200

Galkin A, Abramov AY, Frakich N, Duchen MR, Moncada S (2009) Lack of oxygen deactivates mitochondrial complex I: implications for ischemic injury? J Biol Chem 284(52):36055–36061. https://doi.org/10.1074/jbc.M109.054346

Giraud M-F, Paumard P, Soubannier V, Vaillier J, Arselin G, Salin B, Schaeffer J, Brethes D, di Rago J-P, Velours J (2002) Is there a relationship between the supramolecular organization of the mitochondrial ATP synthase and the formation of cristae? Biochim Biophys Acta 1555:174–180

Giraud M-F, Paumard P, Sanchez C, Brèthes D, Velours J, Dautant A (2012) Rotor architecture in the yeast and bovine F_1-c-ring complexes of F-ATP synthase. J Struct Biol 177(2):490–497. https://doi.org/10.1016/j.jsb.2011.10.015

Gnandt E, Dorner K, Strampraad MF, de Vries S, Friedrich T (2016) The multitude of iron-sulfur clusters in respiratory complex I. Biochim Biophys Acta 1857(8):1068–1072

Gogol EP, Lücken U, Capaldi RA (1987) The stalk connecting the F_1 and F_0 domains of ATP synthase visualized by electron microscopy of unstained specimens. FEBS Lett 219:274–278

Gorenkova N, Robinson E, Grieve DJ, Galkin A (2013) Conformational change of mitochondrial complex I increases ROS sensitivity during ischemia. Antioxid Redox Signal 19(13):1459–1468. https://doi.org/10.1089/ars.2012.4698

Grivennikova VG, Serebryanaya DV, Isakova EP, Belozerskaya TA, Vinogradov AD (2003) The transition between active and de-activated forms of NADH:ubiquinone oxidoreductase (Complex I) in the mitochondrial membrane of *Neurospora crassa*. Biochem J 369(Pt 3):619–626. https://doi.org/10.1042/BJ20021165

Gu J, Wu M, Guo R, Yan K, Lei J, Gao N, Yang M (2016) The architecture of the mammalian respirasome. Nature 537:639–643. https://doi.org/10.1038/nature19359

Guarás A, Perales-Clemente E, Calvo E, Acín-Pérez R, Loureiro-Lopez M, Pujol C, Martínez-Carrascoso I, Nunez E, García-Marqués F, Rodríguez-Hernández MA, Cortés A, Diaz F,

Pérez-Martos A, Moraes CT, Fernández-Silva P, Trifunovic A, Navas P, Vazquez J, Enríquez JA (2016) The CoQH /CoQ ratio serves as a sensor of respiratory chain efficiency. Cell Rep 15(1):197–209. https://doi.org/10.1016/j.celrep.2016.03.009

Guerrero-Castillo S, Baertling F, Kownatzki D, Wessels HJ, Arnold S, Brandt U, Nijtmans L (2016) The assembly pathway of mitochondrial respiratory chain complex I. Cell Metab. https://doi.org/10.1016/j.cmet.2016.09.002. (in press)

Hackenbrock CR, Chazotte B, Gupte SS (1986) The random collision model and a critical assessment of diffusion and collision in mitochondrial electron transport. J Bioenerg Biomembr 18:331–368

Hägerhäll C (1997) Succinate: quinone oxidoreductases. Variations on a conserved theme. Biochim Biophys Acta 1320:107–141

Hahn A, Parey K, Bublitz M, Mills DJ, Zickermann V, Vonck J, Kühlbrandt W, Meier T (2016) Structure of a complete ATP synthase dimer reveals the molecular basis of inner mitochondrial membrane morphology. Mol Cell 63:445–456. https://doi.org/10.1016/j.molcel.2016.05.037

Hakulinen JK, Klyszejko AL, Hoffmann J, Eckhardt-Strelau L, Brutschy B, Vonck J, Meier T (2012) A structural study on the architecture of the bacterial ATP synthase F_o motor. Proc Natl Acad Sci U S A 109:E2050–E2056

Hatch LP, Cox GB, Howitt SM (1995) The essential arginine residue at position 210 in the *a* subunit of the *Escherichia coli* ATP synthase can be transferred to position 252 with partial retention of activity. J Biol Chem 270(49):29407–29412

Heinemeyer J, Braun HP, Boekema EJ, Kouril R (2007) A structural model of the cytochrome c reductase/oxidase supercomplex from yeast mitochondria. J Biol Chem 282(16):12240–12248

Hiltunen JK, Autio KJ, Schonauer MS, Kursu VA, Dieckmann CL, Kastaniotis AJ (2010) Mitochondrial fatty acid synthesis and respiration. Biochim Biophys Acta 1797(6–7):1195–1202. https://doi.org/10.1016/j.bbabio.2010.03.006

Hinchliffe P, Sazanov LA (2005) Organization of iron-sulfur clusters in respiratory complex I. Science 309:771–774

Hirst J (2011) Why does mitochondrial complex I have so many subunits? Biochem J 437(2):e1–e3. https://doi.org/10.1042/BJ20110918

Hirst J, Carroll J, Fearnley IM, Shannon RJ, Walker JE (2003) The nuclear encoded subunits of complex I from bovine heart mitochondria. Biochimica et Biophysica Acta-Bioenergetics 1604(3):135–150. https://doi.org/10.1016/S0005-2728(03)00059-8

Hong S, Victoria D, Crofts AR (2012) Inter-monomer electron transfer is too slow to compete with monomeric turnover in bc 1 complex. Biochimica et Biophysica Acta (BBA)-Bioenergetics 1817(7):1053–1062

Huang LS, Sun G, Cobessi D, Wang AC, Shen JT, Tung EY, Anderson VE, Berry EA (2006) 3-nitropropionic acid is a suicide inhibitor of mitochondrial respiration that, upon oxidation by complex II, forms a covalent adduct with a catalytic base arginine in the active site of the enzyme. J Biol Chem 281(9):5965–5972. https://doi.org/10.1074/jbc.M511270200

Hunte C, Zickermann V, Brandt U (2010) Functional modules and structural basis of conformational coupling in mitochondrial complex I. Science 329:448–451. https://doi.org/10.1126/science.1191046

Huttemann M, Kadenbach B, Grossman LI (2001) Mammalian subunit IV isoforms of cytochrome c oxidase. Gene 267(1):111–123. https://doi.org/10.1016/S0378-1119(01)00385-7

Huttemann M, Jaradat S, Grossman LI (2003a) Cytochrome c oxidase of mammals contains a testes-specific isoform of subunit VIb – the counterpart to testes-specific cytochrome c? Mol Reprod Dev 66(1):8–16. https://doi.org/10.1002/mrd.10327

Huttemann M, Schmidt TR, Grossman LI (2003b) A third isoform of cytochrome c oxidase subunit VIII is present in mammals. Gene 312:95–102. https://doi.org/10.1016/S0378-1119(03)00604-8

Indrieri A, van Randen VA, Tiranti V, Morleo M, Iaconis D, Tammaro R, D'Amato I, Conte I, Maystadt I, Demuth S, Zvulunov A, Kutsche K, Zeviani M, Franco B (2012) Mutations in COX7B cause microphthalmia with linear skin lesions, an unconventional mitochondrial disease. Am J Hum Genet 91(5):942–949. https://doi.org/10.1016/j.ajhg.2012.09.016

Iverson TM, Luna-Chavez C, Cecchini G, Rees DC (1999) Structure of the *Escherichia coli* fumarate reductase respiratory complex. Science 284:1961–1966

Iwasaki T, Matsuura K, Oshima T (1995) Resolution of the aerobic respiratory system of the thermoacidophilic archaeon, *Sulfolobus* sp. strain 7. I. The archaeal terminal oxidase supercomplex is a functional fusion of respiratory complexes III and IV with no *c*-type cytochromes. J Biol Chem 270(52):30881–30892

Iwata S, Ostermeier C, Ludwig B, Michel H (1995) Structure at 2.8 Å resolution of cytochrome c oxidase from Paracoccus denitrificans. Nature 376(6542):660–669. https://doi.org/10.1038/376660a0

Iwata S, Lee JW, Okada K, Lee JK, Iwata M, Rasmussen B, Link TA, Ramaswamy S, Jap BK (1998) Complete structure of the 11-subunit mitochondrial cytochrome bc_1 complex. Science 281:64–71

James TY, Pelin A, Bonen L, Ahrendt S, Sain D, Corradi N, Stajich JE (2013) Shared signatures of parasitism and phylogenomics unite Cryptomycota and microsporidia. Curr Biol 23(16):1548–1553. https://doi.org/10.1016/j.cub.2013.06.057

Jiang W, Fillingame RH (1998) Interacting helical faces of subunits *a* and *c* in the F_1F_0 ATP synthase of *Escherichia coli* defined by disulfide cross-linking. Proc Natl Acad Sci U S A 95:6607–6612

Junge W, Lill H, Engelbrecht S (1997) ATP synthase: an electrochemical transducer with rotatory mechanics. Trends Biochem Sci 22:420–423

Kagawa Y, Racker E (1966) Partial resolution of the enzymes catalyzing oxidative phosphorylation. X. Correlation of morphology and function in submitochondrial particles. J Biol Chem 341(10):2475–2482

Kane Dickson V, Silvester JA, Fearnley IM, Leslie AGW, Walker JE (2006) On the structure of the stator of the mitochondrial ATP synthase. EMBO J 25(12):2911–2918

Kearney EB (1960) Studies on succinic dehydrogenase. XII. Flavin component of the mammalian enzyme. J Biol Chem 235:865–877

Kerscher SJ (2000) Diversity and origin of alternative NADH:ubiquinone oxidoreductases. Biochim Biophys Acta 1459(2–3):274–283

Kerscher S, Grgic L, Garofano A, Brandt U (2004) Application of the yeast *Yarrowia lipolytica* as a model to analyse human pathogenic mutations in mitochondrial complex I (NADH:ubiquinone oxidoreductase). Biochim Biophys Acta 1659:197–205. https://doi.org/10.1016/j.bbabio.2004.07.006

Kerscher S, Drose S, Zickermann V, Brandt U (2008) The three families of respiratory NADH dehydrogenases. Results Probl Cell Differ 45:185–222. https://doi.org/10.1007/400_2007_028

Khalfaoui-Hassani B, Lanciano P, Lee DW, Darrouzet E, Daldal F (2012) Recent advances in cytochrome bc(1): inter monomer electronic communication? FEBS Lett 586:617–621. https://doi.org/10.1016/j.febslet.2011.08.032

Kmita K, Wirth C, Warnau J, Guerrero-Castillo S, Hunte C, Hummer G, Kaila VRI, Zwicker K, Brandt U, Zickermann V (2015) Accessory NUMM (NDUFS6) subunit harbors a Zn-binding site and is essential for biogenesis of mitochondrial complex I. Proc Natl Acad Sci U S A 112(18):5685–5690. https://doi.org/10.1073/pnas.1424353112

Konstantinov AA (2012) Cytochrome c oxidase: intermediates of the catalytic cycle and their energy-coupled interconversion. FEBS Lett 586(5):630–639. https://doi.org/10.1016/j.febslet.2011.08.037

Konstantinov AA, Siletsky S, Mitchell D, Kaulen A, Gennis RB (1997) The roles of the two proton input channels in cytochrome c oxidase from Rhodobacter sphaeroides probed by the effects of site-directed mutations on time-resolved electrogenic intraprotein proton transfer. Proc Natl Acad Sci U S A 94(17):9085–9090. https://doi.org/10.1073/pnas.94.17.9085

Kotlyar AB, Vinogradov AD (1990) Slow active/inactive transition of the mitochondrial NADH-ubiquinone reductase. Biochim Biophys Acta 1019(2):151–158

Krause F, Reifschneider NH, Vocke D, Seelert H, Rexroth S, Dencher NA (2004a) "Respirasome"-like supercomplexes in green leaf mitochondria of spinach. J Biol Chem 279(46):48369–48375

Krause F, Scheckhuber CQ, Werner A, Rexroth S, Reifschneider NH, Dencher NA, Osiewacz HD (2004b) Supramolecular organization of cytochrome *c* oxidase- and alternative oxidase-

dependent respiratory chains in the filamentous fungus *Podospora anserina*. J Biol Chem 279(25):26453–26461
Krause F, Reifschneider NH, Goto S, Dencher NA (2005) Active oligomeric ATP synthases in mammalian mitochondria. Biochem Biophys Res Commun 329:583–590
Lamantea E, Carrara F, Mariotti C, Morandi L, Tiranti V, Zeviani M (2002) A novel nonsense mutation (Q352X) in the mitochondrial cytochrome b gene associated with a combined deficiency of complexes I and III. Neuromuscul Disord 12(1):49–52
Lancaster CR, Kröger A, Auer M, Michel H (1999) Structure of fumarate reductase from Wolinella succinogenes at 2.2 Å resolution. Nature 402:377–385
Lanciano P, Lee D-W, Yang H, Darrouzet E, Daldal F (2011) Intermonomer electron transfer between the low-potential b hemes of cytochrome bc. Biochemistry 50(10):1651–1663. https://doi.org/10.1021/bi101736v
Lanciano P, Khalfaoui-Hassani B, Selamoglu N, Ghelli A, Rugolo M, Daldal F (2013) Molecular mechanisms of superoxide production by complex III: a bacterial versus human mitochondrial comparative case study. BBA-Bioenergetics 1827(11–12):1332–1339. https://doi.org/10.1016/j.bbabio.2013.03.009
Lange C, Hunte C (2002) Crystal structure of the yeast cytochrome bc_1 complex with its bound substrate cytochrome *c*. Proc Natl Acad Sci U S A 99(5):2800–2805
Lapuente-Brun E, Moreno-Loshuertos R, Acín-Pérez R, Latorre-Pellicer A, Colás C, Balsa E, Perales-Clemente E, Quirós PM, Calvo E, Rodríguez-Hernández MA, Navas P, Cruz R, Carracedo A, López-Otin C, Pérez-Martos A, Fernández-Silva P, Fernandez-Vizarra E, Enríquez JA (2013) Supercomplex assembly determines electron flux in the mitochondrial electron transport chain. Science 340(6140):1567–1570. https://doi.org/10.1126/science.1230381
Lau WCY, Rubinstein JL (2010) Structure of intact *Thermus thermophilus* V-ATPase by cryo-EM reveals organization of the membrane-bound V_O motor. Proc Natl Acad Sci U S A 107(4):1367–1372. https://doi.org/10.1073/pnas.0911085107
Lau WCY, Rubinstein JL (2012) Subnanometre-resolution structure of the intact *Thermus thermophilus* H^+-driven ATP synthase. Nature 481(7380):214–218. https://doi.org/10.1038/nature10699
Lau WCY, Baker LA, Rubinstein JL (2008) Cryo-EM structure of the yeast ATP synthase. J Mol Biol 382(5):1256–1264
Lee I, Kadenbach B (2001) Palmitate decreases proton pumping of liver-type cytochrome c oxidase. Eur J Biochem 268(24):6329–6334. https://doi.org/10.1046/j.0014-2956.2001.02602.x
Lee HM, Das TK, Rousseau DL, Mills D, Ferguson-Miller S, Gennis RB (2000) Mutations in the putative H-channel in the cytochrome c oxidase from Rhodobacter sphaeroides show that this channel is not important for proton conduction but reveal modulation of the properties of heme a. Biochemistry 39(11):2989–2996. https://doi.org/10.1021/bi9924821
Lenaz G, Genova ML (2016) Respiratory cytochrome supercomplexes. In: Cytochrome complexes: evolution, structures, energy transduction, and signaling. Springer, Dordrecht, pp 585–628
Letts JA, Fiedorczuk K, Sazanov LA (2016) The architecture of respiratory supercomplexes. Nature 537:644–648. https://doi.org/10.1038/nature19774
Levchenko M, Wuttke J-M, Römpler K, Schmidt B, Neifer K, Juris L, Wissel M, Rehling P, Deckers M (2016) Cox26 is a novel stoichiometric subunit of the yeast cytochrome c oxidase. Biochim Biophys Acta Mol Cell Res 1863(7):1624–1632
Lightowlers RN, Chrzanowska-Lightowlers ZM (2013) Human pentatricopeptide proteins: only a few and what do they do? RNA Biol 10(9):1433–1438. https://doi.org/10.4161/rna.24770
Liu J, Fackelmayer OJ, Hicks DB, Preiss L, Meier T, Sobie EA, Krulwich TA (2011) Mutations in a helix-1 motif of the ATP synthase c-subunit of *Bacillus pseudofirmus* OF4 cause functional deficits and changes in the c-ring stability and mobility on sodium dodecyl sulfate–polyacrylamide gel. Biochemistry 50(24):54897–55506
Longen S, Bien M, Bihlmaier K, Kloeppel C, Kauff F, Hammermeister M, Westermann B, Herrmann JM, Riemer J (2009) Systematic analysis of the twin Cx C protein family. J Mol Biol 393(2):356–368. https://doi.org/10.1016/j.jmb.2009.08.041

Ludlam A, Brunzelle J, Pribyl T, Xu X, Gatti DL, Ackerman SH (2009) Chaperones of F_1-ATPase. J Biol Chem 284:17138–17146

Lytovchenko O, Naumenko N, Oeljeklaus S, Schmidt B, von der Malsburg K, Deckers M, Warscheid B, van der Laan M, Rehling P (2014) The INA complex facilitates assembly of the peripheral stalk of the mitochondrial F_1F_o-ATP synthase. EMBO J 33(15):1624–1638

Maio N, Singh A, Uhrigshardt H, Saxena N, Tong WH, Rouault TA (2014) Cochaperone binding to LYR motifs confers specificity of iron sulfur cluster delivery. Cell Metab 19(3):445–457. https://doi.org/10.1016/j.cmet.2014.01.015

Maklashina E, Kotlyar AB, Cecchini G (2003) Active/de-active transition of respiratory complex I in bacteria, fungi, and animals. Biochim Biophys Acta 1606(1–3):95–103

Maranzana E, Barbero G, Falasca AI, Lenaz G, Genova ML (2013) Mitochondrial respiratory supercomplex association limits production of reactive oxygen species from complex I. Antioxid Redox Sign 19(13):1469–1480. https://doi.org/10.1089/ars.2012.4845

Marcet-Houben M, Marceddu G, Gabaldon T (2009) Phylogenomics of the oxidative phosphorylation in fungi reveals extensive gene duplication followed by functional divergence. BMC Evol Biol 9:295. https://doi.org/10.1186/1471-2148-9-295

Matthies D, Preiß L, Klyszejko AL, Muller DJ, Cook GM, Vonck J, Meier T (2009) The c_{13} ring from a thermoalkaliphilic ATP synthase reveals an extended diameter due to a special structural region. J Mol Biol 388:611–618

Matthies D, Haberstock S, Joos F, Dötsch V, Vonck J, Bernhard F, Meier T (2011) Cell-free expression and assembly of ATP synthase. J Mol Biol 413(3):593–603

Mazhab-Jafari MT, Rohou A, Schmidt C, Bueler SA, Benlekbir S, Robinson CV, Rubinstein JL (2016) Atomic model for the membrane-embedded V_o motor of a eukaryotic V-ATPase. Nature 539:118–122. https://doi.org/10.1038/nature19828

McLennan HR, Degli Esposti M (2000) The contribution of mitochondrial respiratory complexes to the production of reactive oxygen species. J Bioenerg Biomembr 32(2):153–162. https://doi.org/10.1023/A:1005507913372

Meier T, Polzer P, Diederichs K, Welte W, Dimroth P (2005) Structure of the rotor ring of F-type Na^+-ATPase from *Ilyobacter tartaricus*. Science 308:659–662

Meier T, Ferguson SA, Cook GM, Dimroth P, Vonck J (2006) Structural investigations of the membrane-embedded rotor ring of the F-ATPase from *Clostridium paradoxum*. J Bacteriol 188(22):7759–7764

Melo AM, Bandeiras TM, Teixeira M (2004) New insights into type II NAD(P)H:quinone oxidoreductases. Microbiol Mol Biol Rev 68(4):603–616. https://doi.org/10.1128/MMBR.68.4.603-616.2004

Merz S, Westermann B (2009) Genome-wide deletion mutant analysis reveals genes required for respiratory growth, mitochondrial genome maintenance and mitochondrial protein synthesis in Saccharomyces cerevisiae. Genome Biol 10(9):R95. https://doi.org/10.1186/gb-2009-10-9-r95

Meunier B, Fisher N, Ransac S, Mazat JP, Brasseur G (2013) Respiratory complex III dysfunction in humans and the use of yeast as a model organism to study mitochondrial myopathy and associated diseases. Biochim Biophys Acta 1827(11–12):1346–1361. https://doi.org/10.1016/j.bbabio.2012.11.015

Mileykovskaya E, Dowhan W (2014) Cardiolipin-dependent formation of mitochondrial respiratory supercomplexes. Chem Phys Lipids 179:42–48. https://doi.org/10.1016/j.chemphyslip.2013.10.012

Minakami S, Schindler FJ, Estabrook RW (1964) Hydrogen transfer between reduced diphosphopyridine nucleotide dehydrogenase and the respiratory chain. I. Effect of sulfhydryl inhibitors and phospholipase. J Biol Chem 239:2042–2048

Minauro-Sanmiguel F, Wilkens S, Garcia JJ (2005) Structure of dimeric mitochondrial ATP synthase: novel F_0 bridging features and the structural basis of mitochondrial cristae biogenesis. Proc Natl Acad Sci U S A 102(35):12356–12358

Mitchell P (1972) Chemiosmotic coupling in energy transduction – logical development of biochemical knowledge. J Bioenerg 3(1-2):5–24. https://doi.org/10.1007/Bf01515993

Mitchell P (1976) Possible molecular mechanisms of protonmotive function of cytochrome systems. J Theor Biol 62(2):327–367. https://doi.org/10.1016/0022-5193(76)90124-7

Moore KJ, Fillingame RH (2008) Structural interactions between transmembrane helices 4 and 5 of subunit a and the subunit c ring of *Escherichia coli* ATP synthase. J Biol Chem 283:31726–31735

Morais VA, Haddad D, Craessaerts K, De Bock P-J, Swerts J, Vilain S, Aerts L, Overbergh L, Grünewald A, Seibler P, Klein C, Gevaert K, Verstreken P, De Strooper B (2014) PINK1 loss-of-function mutations affect mitochondrial complex I activity via NdufA10 ubiquinone uncoupling. Science 344:203–207. https://doi.org/10.1126/science.1249161

Morales-Rios E, Montgomery MG, Leslie AGW, Walker JE (2015) Structure of ATP synthase from *Paracoccus denitrificans* determined by X-ray crystallography at 4.0 Å resolution. Proc Natl Acad Sci U S A. https://doi.org/10.1073/pnas.1517542112

Moreno-Lastres D, Fontanesi F, García-Consuegra I, Martín MA, Arenas J, Barrientos A, Ugalde C (2012) Mitochondrial complex I plays an essential role in human respirasome assembly. Cell Metab 15:324–335. https://doi.org/10.1016/j.cmet.2012.01.015

Muller FL, Liu YH, Van Remmen H (2004) Complex III releases superoxide to both sides of the inner mitochondrial membrane. J Biol Chem 279(47):49064–49073. https://doi.org/10.1074/jbc.M407715200

Muramoto K, Ohta K, Shinzawa-Itoh K, Kanda K, Taniguchi M, Nabekura H, Yamashita E, Tsukihara T, Yoshikawa S (2010) Bovine cytochrome c oxidase structures enable O reduction with minimization of reactive oxygens and provide a proton-pumping gate. Proc Natl Acad Sci U S A 107(17):7740–7745. https://doi.org/10.1073/pnas.0910410107

Murata T, Yamato I, Kakinuma Y, Leslie AGW, Walker JE (2005) Structure of the rotor of the V-type Na^+-ATPase from *Enterococcus hirae*. Science 308:654–658

Nakai M, Endo T, Hase T, Tanaka Y, Trumpower BL, Ishiwatari H, Asada A, Bogaki M, Matsubara H (1993) Acidic regions of cytochrome c are essential for ubiquinol-cytochrome c reductase activity in yeast cells lacking the acidic QCR6 protein. J Biochem 114(6):919–925

Noji H, Yasuda R, Yoshida M, Kinosita K (1997) Direct observation of the rotation of F_1-ATPase. Nature 386:299–302

Ogilvie I, Aggeler R, Capaldi RA (1997) Cross-linking of the δ subunit to one of the three α subunits has no effect on functioning, as expected if δ is a part of the stator that links the F_1 and F_0 parts of the *Escherichia coli* ATP synthase. J Biol Chem 272:16652–16656

Ohnishi T (1998) Iron-sulfur clusters/semiquinones in complex I. Biochim Biophys Acta 1364(2):186–206

Ohnishi T, Nakamaru-Ogiso E (2008) Were there any "misassignments" among iron-sulfur clusters N4, N5 and N6b in NADH-quinone oxidoreductase (complex I)? Biochim Biophys Acta 1777(7–8):703–710. https://doi.org/10.1016/j.bbabio.2008.04.032

Ohnishi T, Kawaguchi K, Hagihara B (1966) Preparation and some properties of yeast mitochondria. J Biol Chem 241(8):1797–1806

Ohnishi ST, Salerno JC, Ohnishi T (2010) Possible roles of two quinone molecules in direct and indirect proton pumps of bovine heart NADH-quinone oxidoreductase (complex I). Biochim Biophys Acta 1797(12):1891–1893. https://doi.org/10.1016/j.bbabio.2010.06.010

Osman C, Wilmes C, Tatsuta T, Langer T (2007) Prohibitins interact genetically with Atp23, a novel processing peptidase and chaperone for the F_1F_o-ATP synthase. Mol Biol Cell 18:627–635

Pagadala V, Vistain L, Symersky J, Mueller DM (2011) Characterization of the mitochondrial ATP synthase from yeast *Saccharomyces cerevisae*. J Bioenerg Biomembr 43:333–347

Page CC, Moser CC, Chen X, Dutton PL (1999) Natural engineering principles of electron tunnelling in biological oxidation-reduction. Nature 402(6757):47–52. https://doi.org/10.1038/46972

Parsons DF (1963) Negative staining of thinly spread cells and associated virus. J Cell Biol 16:620–626

Parsons WJ, Williams RS, Shelton JM, Luo YA, Kessler DJ, Richardson JA (1996) Developmental regulation of cytochrome oxidase subunit VIa isoforms in cardiac and skeletal muscle. Am J Physiol-Heart C 270(2):H567–H574

Paumard P, Vaillier J, Coulary B, Schaeffer J, Soubannier V, Mueller DM, Brethes D, di Rago J-P, Velours J (2002) The ATP synthase is involved in generating mitochondrial cristae morphology. EMBO J 21(3):221–230

Peters K, Belt K, Braun HP (2013) 3D gel map of *Arabidopsis* complex I. Front Plant Sci 4:153. https://doi.org/10.3389/fpls.2013.00153

Pitceathly RDS, Rahman S, Wedatilake Y, Polke JM, Cirak S, Foley AR, Sailer A, Hurles ME, Stalker J, Hargreaves I, Woodward CE, Sweeney MG, Muntoni F, Houlden H, UK10K Consortium, Taanman J-W, Hanna MG (2013) NDUFA4 mutations underlie dysfunction of a cytochrome c oxidase subunit linked to human neurological disease. Cell Rep 3(6):1795–1805. https://doi.org/10.1016/j.celrep.2013.05.005

Ploegman JH, Drent G, Kalk KH, Hol WG (1978) Structure of bovine liver rhodanese. I. Structure determination at 2.5 Å resolution and a comparison of the conformation and sequence of its two domains. J Mol Biol 123(4):557–594

Pogoryelov D, Yu J, Meier T, Vonck J, Dimroth P, Müller DJ (2005) The c_{15} ring of the *Spirulina platensis* F-ATP synthase: F_1/F_0 symmetry mismatch is not obligatory. EMBO Rep 6(11):1045–1052

Pogoryelov D, Yildiz Ö, Faraldo-Gómez JD, Meier T (2009) High-resolution structure of the rotor ring of a proton-dependent ATP synthase. Nat Struct Mol Biol 16(10):1068–1073. https://doi.org/10.1038/nsmb.1678

Pogoryelov D, Klyszejko AL, Krasnoselska G, Heller E-M, Leone V, Langer JD, Vonck J, Müller DJ, Faraldo-Gómez JD, Meier T (2012) Engineering rotor ring stoichiometries in ATP synthases. Proc Natl Acad Sci U S A 109:E1599–E1608

Popovic DM (2013) Current advances in research of cytochrome c oxidase. Amino Acids 45(5):1073–1087. https://doi.org/10.1007/s00726-013-1585-y

Preiss L, Yildiz Ö, Hicks DB, Krulwich TA, Meier T (2010) A new type of proton coordination in an F_1F_o-ATP synthase rotor ring. PLoS Biol 8(8):443

Preiss L, Klyszejko AL, Hicks DB, Liu J, Fackelmayer OJ, Yildiz Ö, Krulwich TA, Meier T (2013) The c-ring stoichiometry of ATP synthase is adapted to cell physiological requirements of alkaliphilic *Bacillus pseudofirmus* OF4. Proc Natl Acad Sci U S A 110:7874

Preiss L, Langer JD, Yildiz Ö, Eckhardt-Strelau L, Guillemont JEG, Koul A, Meier T (2015) Structure of the mycobacterial ATP synthase F_0 rotor ring in complex with the anti-TB drug bedaquiline. Sci Adv 1(4):e1500106. https://doi.org/10.1126/sciadv.1500106

Quarato G, Piccoli C, Scrima R, Capitanio N (2011) Variation of flux control coefficient of cytochrome c oxidase and of the other respiratory chain complexes at different values of protonmotive force occurs by a threshold mechanism. BBA-Bioenergetics 1807(9):1114–1124. https://doi.org/10.1016/j.bbabio.2011.04.001

Quinlan CL, Gerencser AA, Treberg JR, Brand MD (2011) The mechanism of superoxide production by the antimycin-inhibited mitochondrial Q-cycle. J Biol Chem 286(36):31361–31372. https://doi.org/10.1074/jbc.M111.267898

Rak M, Gokova S, Tzagoloff A (2011) Modular assembly of yeast mitochondrial ATP synthase. EMBO J 30:920–930. https://doi.org/10.1038/emboj.2010.364

Rak M, Benit P, Chretien D, Bouchereau J, Schiff M, El-Khoury R, Tzagoloff A, Rustin P (2016) Mitochondrial cytochrome c oxidase deficiency. Clin Sci 130(6):393–407. https://doi.org/10.1042/Cs20150707

Ramirez-Aguilar SJ, Keuthe M, Rocha M, Fedyaev VV, Kramp K, Gupta KJ, Rasmusson AG, Schulze WX, van Dongen JT (2011) The composition of plant mitochondrial supercomplexes changes with oxygen availability. J Biol Chem 286(50):43045–43053. https://doi.org/10.1074/jbc.M111.252544

Rasmussen T, Scheide D, Brors B, Kintscher L, Weiss H, Friedrich T (2001) Identification of two tetranuclear FeS clusters on the ferredoxin-type subunit of NADH:ubiquinone oxidoreductase (complex I). Biochemistry 40(20):6124–6131

Rees DM, Leslie AGW, Walker JE (2009) The structure of the membrane extrinsic region of bovine ATP synthase. Proc Natl Acad Sci U S A 106(51):21597–21601

Requejo R, Hurd TR, Costa NJ, Murphy MP (2010) Cysteine residues exposed on protein surfaces are the dominant intramitochondrial thiol and may protect against oxidative damage. FEBS J 277(6):1465–1480. https://doi.org/10.1111/j.1742-4658.2010.07576.x

Rich PR, Marechal A (2013) Functions of the hydrophilic channels in protonmotive cytochrome c oxidase. J R Soc Interface 10(86). https://doi.org/10.1098/rsif.2013.0183

Roberts PG, Hirst J (2012) The deactive form of respiratory complex I from mammalian mitochondria is a Na^+/H^+ antiporter. J Biol Chem 287(41):34743–34751. https://doi.org/10.1074/jbc.M112.384560

Rodenburg RJ (2016) Mitochondrial complex I-linked disease. Biochim Biophys Acta 1857(7):938–945. https://doi.org/10.1016/j.bbabio.2016.02.012

Roessler MM, King MS, Robinson AJ, Armstrong FA, Harmer J, Hirst J (2010) Direct assignment of EPR spectra to structurally defined iron-sulfur clusters in complex I by double electron-electron resonance. Proc Natl Acad Sci U S A 107(5):1930–1935. https://doi.org/10.1073/pnas.0908050107

Rottenberg H, Covian R, Trumpower BL (2009) Membrane potential greatly enhances superoxide generation by the cytochrome bc complex reconstituted into phospholipid vesicles. J Biol Chem 284(29):19203–19210. https://doi.org/10.1074/jbc.M109.017376

Rubinstein JL, Walker JE, Henderson R (2003) Structure of the mitochondrial ATP synthase by electron cryomicroscopy. EMBO J 22(23):6182–6192

Runswick MJ, Fearnley IM, Skehel JM, Walker JE (1991) Presence of an acyl carrier protein in NADH:ubiquinone oxidoreductase from bovine heart mitochondria. FEBS Lett 286(1–2):121–124

Salje J, Ludwig B, Richter OMH (2005) Is a third proton-conducting pathway operative in bacterial cytochrome c oxidase? Biochem Soc Trans 33:829–831

Sarewicz M, Borek A, Cieluch E, Swierczek M, Osyczka A (2010) Discrimination between two possible reaction sequences that create potential risk of generation of deleterious radicals by cytochrome bc_1: implications for the mechanism of superoxide production. BBA-Bioenergetics 1797(11):1820–1827. https://doi.org/10.1016/j.bbabio.2010.07.005

Sazanov LA, Hinchliffe P (2006) Structure of the hydrophilic domain of respiratory complex I from *Thermus thermophilus*. Science 311:1430–1436

Schäfer E, Seelert H, Reifschneider NH, Krause F, Dencher NA, Vonck J (2006) Architecture of active mammalian respiratory chain supercomplexes. J Biol Chem 281:15370–15375

Schäfer E, Dencher NA, Vonck J, Parcej DN (2007) Three-dimensional structure of the respiratory chain supercomplex $I_1III_2IV_1$ from bovine heart mitochondria. Biochemistry 44(46):12579–12585

Schägger H, Pfeiffer K (2000) Supercomplexes in the respiratory chain of yeast and mammalian mitochondria. EMBO J 19(8):1777–1783

Schägger H, Pfeiffer K (2001) The ratio of oxidative phosphorylation complexes I–V in bovine heart mitochondria and the composition of respiratory chain supercomplexes. J Biol Chem 276:37861–37867

Schägger H, Link TA, Engel WD, Von Jagow G (1986) Isolation of the eleven protein subunits of the bc complex from beef heart. Methods Enzymol 126:224–237

Schlerf A, Droste M, Winter M, Kadenbach B (1988) Characterization of 2 different genes (CDNA) for cytochrome c oxidase subunit Vla from heart and liver of the rat. EMBO J 7(8):2387–2391

Schönfeld P, Więckowski MR, Lebiedzińska M, Wojtczak L (2010) Mitochondrial fatty acid oxidation and oxidative stress: lack of reverse electron transfer-associated production of reactive oxygen species. Biochimica et Biophysica Acta (BBA)-Bioenergetics 1797(6):929–938

Schwem BE, Fillingame RH (2006) Cross-linking between helices within subunit *a* of *Escherichia coli* ATP synthase defines the transmembrane packing of a four-helix bundle. J Biol Chem 281:37861–37867

Seelert H, Poetsch A, Dencher NA, Engel A, Stahlberg H, Müller DJ (2000) Proton-powered turbine of a plant motor. Nature 405:418–419

Seelert H, Dani DN, Dante S, Hauß T, Krause F, Schäfer E, Frenzel M, Poetsch A, Rexroth S, Schwaßmann HJ, Suhai T, Vonck J, Dencher NA (2009) From protons to OXPHOS supercomplexes and Alzheimer's disease: structure–dynamics–function relationships of energy-transducing membranes. Biochim Biophys Acta – Bioenergetics 1787:657–671

Senes A, Engel DE, DeGrado WF (2004) Folding of helical membrane proteins: the role of polar, GxxxG-like and proline motifs. Curr Opin Struct Biol 14:465–479

Sharma V, Wikström M (2016) The role of the K-channel and the active-site tyrosine in the catalytic mechanism of cytochrome c oxidase. BBA-Bioenergetics 1857(8):1111–1115. https://doi.org/10.1016/j.bbabio.2016.02.008

Sharma V, Belevich G, Gamiz-Hernandez AP, Róg T, Vattulainen I, Verkhovskaya ML, Wikström M, Hummer G, Kaila VRI (2015) Redox-induced activation of the proton pump in the respiratory complex I. Proc Natl Acad Sci U S A 112(37):11571–11576. https://doi.org/10.1073/pnas.1503761112

Shimokata K, Katayama Y, Murayama H, Suematsu M, Tsukihara T, Muramoto K, Aoyama H, Yoshikawa S, Shimada H (2007) The proton pumping pathway of bovine heart cytochrome c oxidase. Proc Natl Acad Sci U S A 104(10):4200–4205. https://doi.org/10.1073/pnas.0611627104

Silman HI, Rieske JS, Lipton SH, Baum H (1967) A new protein component of complex 3 of mitochondrial electron transfer chain. J Biol Chem 242(21):4867–4875

Skippington E, Barkman TJ, Rice DW, Palmer JD (2015) Miniaturized mitogenome of the parasitic plant *Viscum scurruloideum* is extremely divergent and dynamic and has lost all nad genes. Proc Natl Acad Sci U S A 112(27):E3515–E3524. https://doi.org/10.1073/pnas.1504491112

Soberanes S, Urich D, Baker CM, Burgess Z, Chiarella SE, Bell EL, Ghio AJ, De Vizcaya-Ruiz A, Liu J, Ridge KM, Kamp DW, Chandel NS, Schumacker PT, Mutlu GM, Budinger GRS (2009) Mitochondrial ccomplex III-generated oxidants activate ASK1 and JNK to induce alveolar epithelial cell death following exposure to particulate matter air pollution. J Biol Chem 284(4):2176–2186. https://doi.org/10.1074/jbc.M808844200

Soubannier V, Vaillier J, Paumard P, Coulary B, Schaeffer J, Velours J (2002) In the absence of the first membrane-spanning segment of subunit 4(b), the yeast ATP synthase is functional but does not dimerize or oligomerize. J Biol Chem 277:10739–10745

Sousa JS, Mills DJ, Vonck J, Kühlbrandt W (2016) Functional asymmetry and electron flow in the bovine respirasome. eLife 5:e21290. https://doi.org/10.7554/eLife.21290

Spero MA, Aylward FO, Currie CR, Donohue TJ (2015) Phylogenomic analysis and predicted physiological role of the proton-translocating NADH:quinone oxidoreductase (complex I) across bacteria. mBio 6(2):e00389–e00315. https://doi.org/10.1128/mBio.00389-15

Stahlberg H, Müller DJ, Suda K, Fotiadis D, Engel A, Meier T, Matthey U, Dimroth P (2001) Bacterial Na^+-ATP synthase has an undecameric rotor. EMBO Rep 2(3):229–233

Steimle S, Schnick C, Burger EM, Nuber F, Kramer D, Dawitz H, Brander S, Matlosz B, Schafer J, Maurer K, Glessner U, Friedrich T (2015) Cysteine scanning reveals minor local rearrangements of the horizontal helix of respiratory complex I. Mol Microbiol 98(1):151–161. https://doi.org/10.1111/mmi.13112

Stock D, Leslie AG, Walker JE (1999) Molecular architecture of the rotary motor in ATP synthase. Science 286:1700–1705

Stoeckenius W (1963) Some observations of negatively stained mitochondria. J Cell Biol 17:443–454

St-Pierre J, Buckingham JA, Roebuck SJ, Brand MD (2002) Topology of superoxide production from different sites in the mitochondrial electron transport chain. J Biol Chem 277(47):44784–44790

Strauss M, Hofhaus G, Schröder RR, Kühlbrandt W (2008) Dimer ribbons of ATP synthase shape the inner mitochondrial membrane. EMBO J 27:1154–1160

Sun F, Huo X, Zhai Y, Wang A, Xu J, Su D, Bartlam M, Rao Z (2005) Crystal structure of mitochondrial respiratory membrane protein complex II. Cell 121(7):1043–1057. https://doi.org/10.1016/j.cell.2005.05.025

Szklarczyk R, Wanschers BF, Nabuurs SB, Nouws J, Nijtmans LG, Huynen MA (2011) NDUFB7 and NDUFA8 are located at the intermembrane surface of complex I. FEBS Lett 585(5):737–743. https://doi.org/10.1016/j.febslet.2011.01.046

Thomas D, Bron P, Weimann T, Dautant A, Giraud M-F, Paumard P, Salin B, Cavalier A, Velours J, Brèthes D (2008) Supramolecular organization of the yeast F_iF_o-ATP synthase. Biol Cell 100(10):591–601

Tormos KV, Anso E, Hamanaka RB, Eisenhart J, Joseph J, Kalyanaraman B, Chandel NS (2011) Mitochondrial complex III ROS regulate adipocyte differentiation. Cell Metab 14(4):537–544. https://doi.org/10.1016/j.cmet.2011.08.007

Trumpower BL, Gennis RB (1994) Energy transduction by cytochrome complexes in mitochondrial and bacterial respiration – the enzymology of coupling electron-transfer reactions to transmembrane proton translocation. Ann Rev Biochem 63:675–716. https://doi.org/10.1146/annurev.biochem.63.1.675

Tsukihara T, Aoyama H, Yamashita E, Tomizaki T, Yamaguchi H, Shinzawa-Itoh K, Nakashima R, Yaono R, Yoshikawa S (1995) Structures of metal sites of oxidized bovine heart cytochrome c oxidase at 2.8 Å. Science 269(5227):1069–1074. https://doi.org/10.1126/science.7652554

Tsukihara T, Aoyama H, Yamashita E, Tomizaki T, Yamaguchi H, Shinzawa-Itoh K, Nakashima R, Yaono R, Yoshikawa S (1996) The whole structure of the 13-subunit oxidized cytochrome c oxidase at 2.8 Å. Science 272:1136–1144

Tsukihara T, Shimokata K, Katayama Y, Shimada H, Muramoto K, Aoyama H, Mochizuki M, Shinzawa-Itoh K, Yamashita E, Yao M, Ishimura Y, Yoshikawa S (2003) The low-spin heme of cytochrome c oxidase as the driving element of the proton-pumping process. Proc Natl Acad Sci U S A 100:15304–15309

Turrens JF (2003) Mitochondrial formation of reactive oxygen species. J Physiol 552(Pt 2):335–344. https://doi.org/10.1113/jphysiol.2003.049478

Tzagoloff A, Barrientos A, Neupert W (2004) Atp10p assists assembly of Atp6p into the F_0 unit of the yeast mitochondrial ATPase. J Biol Chem 279:19775–19780

van Hellemond JJ, van der Klei A, van Weelden SW, Tielens AG (2003) Biochemical and evolutionary aspects of anaerobically functioning mitochondria. Philos Trans R Soc Lond Ser B Biol Sci 358(1429):205–213. https://doi.org/10.1098/rstb.2002.1182

van Lis R, Atteia A, Mendoza-Hernandez G, Gonzalez-Halphen D (2003) Identification of novel mitochondrial protein components of *Chlamydomonas reinhardtii*. A proteomic approach. Plant Physiol 132:318–330

van Lis R, Mendoza-Hernández G, Groth G, Atteia A (2007) New insights into the unique structure of the F_0F_1-ATP synthase from the chlamydomonad algae *Polytomella* sp. and *Chlamydomonas reinhardtii*. Plant Physiol 144:1190–1199

Varanasi L, Hosler JP (2012) Subunit III-depleted cytochrome c oxidase provides insight into the process of proton uptake by proteins. Biochim Biophys Acta 1817(4):545–551. https://doi.org/10.1016/j.bbabio.2011.10.001

Vempati UD, Han XL, Moraes CT (2009) Lack of cytochrome c in mouse fibroblasts disrupts assembly/stability of respiratory complexes I and IV. J Biol Chem 284(7):4383–4391. https://doi.org/10.1074/jbc.M805972200

Verkhovskaya ML, Belevich N, Euro L, Wikström M, Verkhovsky MI (2008) Real-time electron transfer in respiratory complex I. Proc Natl Acad Sci U S A 105(10):3763–3767. https://doi.org/10.1073/pnas.0711249105

Videira A (1998) Complex I from the fungus *Neurospora crassa*. Biochim Biophys Acta 1364(2):89–100

Vik SB, Antonio BJ (1994) Mechanism of proton translocation by F_iF_0 ATP synthases suggested by double mutants of the *a* subunit. J Biol Chem 269:30364–30369

Vik SB, Dao NN (1992) Prediction of transmembrane topology of F_0 proteins from *Escherichia coli* F_iF_0 ATP synthase using variational and hydrophobic membrane analyses. Biochim Biophys Acta 1140:199–207

Vinothkumar KR, Zhu J, Hirst J (2014) Architecture of mammalian respiratory complex I. Nature 515(7525):80–84. https://doi.org/10.1038/nature13686

Vinothkumar KR, Montgomery MG, Liu S, Walker JE (2016) Structure of the mitochondrial ATP synthase from *Pichia angusta* determined by electron cryo-microscopy. Proc Natl Acad Sci U S A 113:12709–12714. https://doi.org/10.1073/pnas.1615902113

Vonck J, Schäfer E (2009) Supramolecular organization of protein complexes in the mitochondrial inner membrane. Biochim Biophys Acta 1793(1):117–124

Vonck J, Krug von Nidda T, Meier T, Matthey U, Mills DJ, Kühlbrandt W, Dimroth P (2002) Molecular architecture of the undecameric rotor of a bacterial Na^+-ATP synthase. J Mol Biol 321(2):307–316

Vonck J, Pisa KY, Morgner N, Brutschy B, Müller V (2009) Three-dimensional structure of A_1A_0 ATP synthase from the hyperthermophilic archaeon *Pyrococcus furiosus* by electron microscopy. J Biol Chem 284(15):10110–10119

Vukotic M, Oeljeklaus S, Wiese S, Vögtle FN, Meisinger C, Meyer HE, Zieseniss A, Katschinski DM, Jans DC, Jakobs S, Warscheid B (2012) Rcf1 mediates cytochrome oxidase assembly and respirasome formation, revealing heterogeneity of the enzyme complex. Cell Metab 15(3):336–347

Walker JE (2013) The ATP synthase: the understood, the uncertain and the unknown. Biochem Soc Trans 41:1–16. https://doi.org/10.1042/BST20110773

Walker WH, Singer TP (1970) Identification of the covalently bound flavin of succinate dehydrogenase as 8α-(histidyl) flavin adenine dinucleotide. J Biol Chem 245:4224–4225

Wang R (2012) Physiological implications of hydrogen sulfide: a whiff exploration that blossomed. Physiol Rev 92(2):791–896. https://doi.org/10.1152/physrev.00017.2011

Watt IN, Montgomery MG, Runswick MJ, Leslie AGW, Walker JE (2010) Bioenergetic cost of making an adenosine triphosphate molecule in animal mitochondria. Proc Natl Acad Sci U S A 107:16823–16827

Weidner U, Geier S, Ptock A, Friedrich T, Leif H, Weiss H (1993) The gene locus of the proton-translocating NADH: ubiquinone oxidoreductase in *Escherichia coli*. Organization of the 14 genes and relationship between the derived proteins and subunits of mitochondrial complex I. J Mol Biol 233(1):109–122. https://doi.org/10.1006/jmbi.1993.1488

Weiss MC, Sousa FL, Mrnjavac N, Neukirchen S, Roettger M, Nelson-Sathi S, Martin WF (2016) The physiology and habitat of the last universal common ancestor. Nat Microbiol 1:16116. https://doi.org/10.1038/NMICROBIOL.2016.116

Whelan SP, Zuckerbraun BS (2013) Mitochondrial signaling: forwards, backwards, and in between. Oxid Med Cell Longev. https://doi.org/10.1155/2013/351613

Wikström MK (1977) Proton pump coupled to cytochrome c oxidase in mitochondria. Nature 266(5599):271–273

Wikström M, Sharma V, Kaila VRI, Hosler JP, Hummer G (2015) New perspectives on proton pumping in cellular respiration. Chem Rev 115(5):2196–2221. https://doi.org/10.1021/cr500448t

Wilkens S, Capaldi RA (1998) ATP synthase's second stalk comes into focus. Nature 393:29

Wirth C, Brandt U, Hunte C, Zickermann V (2016) Structure and function of mitochondrial complex I. Biochim Biophys Acta 1857(7):902–914. https://doi.org/10.1016/j.bbabio.2016.02.013

Xia D, Yu C-A, Kim H, Xia J, Kachurin AM, Zhang L, Yu L, Deisenhofer J (1997) Crystal structure of the cytochrome bc complex from bovine heart mitochondria. Science 281:64–71

Yagi T, Matsuno-Yagi A (2003) The proton-translocating NADH-quinone oxidoreductase in the respiratory chain: the secret unlocked. Biochemistry 42(8):2266–2274. https://doi.org/10.1021/bi027158b

Yakovlev G, Reda T, Hirst J (2007) Reevaluating the relationship between EPR spectra and enzyme structure for the iron sulfur clusters in NADH:quinone oxidoreductase. Proc Natl Acad Sci U S A 104(31):12720–12725. https://doi.org/10.1073/pnas.0705593104

Yang XH, Trumpower BL (1986) Purification of a three-subunit ubiquinol-cytochrome c oxidoreductase complex from Paracoccus denitrificans. J Biol Chem 261(26):12282–12289

Yang M, Trumpower BL (1994) Deletion of QCR6, the gene encoding subunit six of the mitochondrial cytochrome bc complex, blocks maturation of cytochrome c, and causes temperature-sensitive petite growth in Saccharomyces Cerevisiae. J Biol Chem 269(2):1270–1275

Yang W-L, Iacono L, Tang W-M, Chin K-V (1998) Novel function of the regulatory subunit of protein kinase A: regulation of cytochrome c oxidase activity and cytochrome c release. Biochemistry 37(40):14175–14180. https://doi.org/10.1021/bi981402a

Yankovskaya V, Horsefield R, Törnroth S, Luna-Chavez C, Miyoshi H, Léger C, Byrne B, Cecchini G, Iwata S (2003) Architecture of succinate dehydrogenase and reactive oxygen species generation. Science 299:700–704

Yong R, Searcy DG (2001) Sulfide oxidation coupled to ATP synthesis in chicken liver mitochondria. Comp Biochem Physiol B Biochem Mol Biol 129(1):129–137

Yoshikawa S, Shimada A (2015) Reaction mechanism of cytochrome c oxidase. Chem Rev 115(4):1936–1989. https://doi.org/10.1021/cr500266a

Zara V, Conte L, Trumpower BL (2009) Evidence that the assembly of the yeast cytochrome bc complex involves the formation of a large core structure in the inner mitochondrial membrane. FEBS J 276(7):1900–1914. https://doi.org/10.1111/j.1742-4658.2009.06916.x

Zeng X, Neupert W, Tzagoloff A (2007) The metallopeptidase encoded by ATP23 has a dual function in processing and assembly of subunit 6 of mitochondrial ATPase. Mol Biol Cell 18:617–623

Zeng X, Barros MH, Shulman T, Tzagoloff A (2008) ATP25, a new nuclear gene of Saccharomyces cerevisiae required for expression and assembly of the Atp9p subunit of mitochondrial ATPase. Mol Biol Cell 19:1366–1377

Zhang C, Allegretti M, Vonck J, Langer JD, Marcia M, Peng G, Michel H (2014) Production of a fully assembled and active form of *Aquifex aeolicus* F_1F_o ATP synthase in *Escherichia coli*. BBA – Gen Subj 1840(1):34–40. https://doi.org/10.1016/j.bbagen.2013.08.023

Zhao J, Benlekbir S, Rubinstein JL (2015) Electron cryomicroscopy observation of rotational states in a eukaryotic V-ATPase. Nature 521:241–245

Zhou A, Rohou A, Schep DG, Bason JV, Montgomery MG, Walker JE, Grigorieff N, Rubinstein JL (2015) Structure and conformational states of the bovine mitochondrial ATP synthase by cryo-EM. eLife 3:e10180. https://doi.org/10.7554/eLife.10180

Zhu J, Vinothkumar KR, Hirst J (2016) Structure of mammalian respiratory complex I. Nature 536(7616):354–358. https://doi.org/10.1038/nature19095

Zickermann V, Wirth C, Nasiri H, Siegmund K, Schwalbe H, Hunte C, Brandt U (2015) Mechanistic insight from the crystal structure of mitochondrial complex I. Science 347:44–49. https://doi.org/10.1126/science.1259859